Nanofluids with Enhanced Thermal Transport Properties

By

Zenghu Han

Submitted in Partial Fulfillment of the Requirements
for the degree of
Doctor of Philosophy

Department of Mechanical Engineering
University of Maryland at College Park
College Park, Maryland

ABSTRACT

Title of Dissertation: **Nanofluids with Enhanced Thermal Transport Properties**

Zenghu Han, Doctor of Philosophy, 2008

Directed By: Dr. Bao Yang, Assistant Professor
Department of Mechanical Engineering

Heat transfer fluids have inherently low thermal conductivity that greatly limits the heat exchange efficiency. While the effectiveness of extending surfaces and redesigning heat exchange equipments to increase the heat transfer rate has reached a limit, many research activities have been carried out attempting to improve the thermal transport properties of the fluids by adding more thermally conductive solids into liquids. Liquid dispersions of nanoparticles, which have been termed "nanofluids", exhibit substantially higher thermal conductivities than those of the corresponding base fluids.

In this study, new nanofluid systems have been developed by utilizing semiconductor nanorods, hybrid nanoparticles, phase-change liquid nanodroplets and phase-change metallic nanoparticles as the dispersed phases. A nanoemulsification technique has been developed and used to synthesize nanofluids. The thermal transport properties of nanofluids, including thermal conductivity, viscosity, heat capacity and heat transfer coefficient in convective environment were characterized and modeled. Obvious thermal conductivity increases have been observed in these nanofluid systems, e.g., 52% enhancement in thermal conductivity was found in water-in-FC72 nanofluids. This anomalous enhancement can not be well explained by the Effective Medium Theory. Theoretical Models based on Ordered Liquid Layering, Brownian motion and

Nanoparticle Aggregates theories are used to describe the thermal conductivity enhancement in nanofluids.

Since the heat capacity of heat transfer fluids is another important thermal transport property, phase-change nanodroplets and nanoparticles are thus used to synthesize phase-change nanofluids. Up to 126% and 20% increases in the effective heat capacity were experimentally found in water-in-FC72 nanoemulsions and indium-in-PAO nanofluids，respectively, due to the large amount of latent heat absorbed in phase transition from nanoparticles to nanodroplets and released in reverse transition.

The viscosity of nanofluids is increased as a result of the addition of nanoparticles, which can be described by the Einstein-Batchelor model. But due to the enhanced thermal conductivity of nanofluids, 15% increase in heat transfer coefficient of natural convection has been observed in water-in-FC72 nanofluids. The results show that nanofluids possess improved thermal transport properties and it has been experimentally proved that nanofluids have potential as next-generation advanced heat transfer fluids.

Nanofluids with Enhanced Thermal Transport Properties

By

Zenghu Han

Dissertation submitted to the Faculty of the Graduate School of the
University of Maryland, College Park, in partial fulfillment
of the requirements for the degree of
Doctor of Philosophy
2008

Advisory Committee:

Dr. Bao Yang, Chair/Advisor
Dr. Shapour Azarm
Dr. Tien-Mo Shih
Dr. Santiago Solares
Dr. Kenneth Yu

Dedication

To my wife Ye, my parents, my parents-in-law, my brother, my sister-in-law and my niece.

Acknowledgements

I would like to thank my advisor, Dr. Bao Yang for his guidance, support, and encouragement through the last four years. I would also like to thank Dr. Shapour Azarm, Dr. Tien-Mo Shih, Dr. Santiago Solares, and Dr. Kenneth Yu for serving on my dissertation committee, reviewing my dissertation and giving me valuable suggestions.

I would like to thank Dr. Dan Janiak and Dr. Von Cresce for helping me conduct the DSC experiments and Dr. Yi Qi for aiding me during TEM imaging.

Table of Contents

Dedication ..... **ii**
Acknowledgements ..... **iii**
Table of Contents ..... **iv**
List of Tables ..... **vi**
List of Figures ..... **vii**
Nomenclature ..... **xii**
1 Introduction **1**
1.1 Brief History of Nanofluids 1
1.2 Motivation of Improving Thermal Conductivity of Fluids 6
1.3 Rationales behind the Nanofluids 10
1.4 Objective of Present Research 15
1.4.1 Physical Mechanisms behind Thermal Conductivity Enhancement 15
1.4.2 Mass Production Method of Nanofluids 16
1.4.3 Nanofluid Systems Based on Per-fluorocarbons 17
1.4.4 Phase-Change Nanofluids 18
2 Literature Review **20**
2.1 Synthesis of Nanofluids 20
2.2 Heat Transfer in Nanofluids 25
2.2.1 Thermal Conduction in Nanofluids 25
2.2.2 Thermal Convection in Nanofluids 33
2.2.3 Pool Boiling in Nanofluids 35
2.2.4 Theoretical Models of the Thermal Transport in Nanofluids 36
2.3 Viscosity 39
2.4 Applications of Nanofluid 43
2.5 Summary 46
3 Experimental Methods **48**
3.1 Synthesis Approach 48
3.2 Characterization of Nanofluid Systems 53
3.2.1 Determination of Elemental Compositions 54
3.2.2 Investigation of Particle Size and Geometry 54
3.2.3 Microstructure Characterization 55
3.2.4 Mobility of Nanoparticles 55
3.2.5 Stability of Nanofluids 56
3.2.6 Measurement of Viscosity 57
3.2.7 Heat Capacity Measurement and Phase Change Characterization 57
3.2.8 Thermal Conductivity Measurement 58
4 Thermal Conductivity of Nanorods-in-oil Nanofluids **63**
4.1 Introduction 63
4.2 Synthesis of Bi_2Te_3 Nanorods 64
4.3 Preparation of Nanorods-in-Oil Nanofluids 66
4.4 Thermal Conductivity Measurement 67
4.5 Temperature Dependence of Thermal Conductivity Enhancement 69
4.6 Discussion 70
4.7 Summary 74
5 Application of Hybrid Urchin-Like Nanoparticles **75**

5.1 Introduction 75
5.2 Synthesis of Urchin-like Nanoparticles 77
5.3 Preparation of Nanofluids 79
5.4 Diffusion Mobility of Urchin-like Nanoparticles 80
5.5 Thermal Conductivity Measurement of Nanofluids 82
5.6 Discussion 84
5.7 Summary 86
6 Phase Change Water-in-FC72 Nanofluids 87
6.1 Introduction 87
6.2 Synthesis of Water-in-FC72 Nanofluids 89
6.3 Measurement of Diffusion Mobility of Water Nanodroplets 91
6.4 Thermal Conductivity Measurements 93
6.5 Viscosity of Water-in-FC72 Nanofluids 97
6.6 Heat Capacity of Water-in-FC72 Nanofluids 99
6.7 Phase Change Behavior of Water-in-FC72 Nanofluids 101
6.8 Natural Convective Heat Transfer in Nanofluids 104
6.9 Summary 106
7 Phase-Change Indium-in-PAO Nanofluids 107
7.1 Introduction 107
7.2 Synthesis of Indium Nanoparticles 109
7.3 Thermal Conductivity Measurement 114
7.4 Heat Capacity of Phase-Change Nanofluids 115
7.5 Phase Change Behavior of indium-in-PAO nanofluids 116
7.6 Viscosity of Indium-in-PAO Nanofluids 119
7.7 Summary 121
8 Modeling Thermal Transport in Nanofluids 123
8.1 Introduction 123
8.2 Density, Heat Capacity and Dynamic Viscosity of Nanofluids 123
8.3 Thermal Conductivity Enhancement 123
8.3.1 Effective Medium Theory 124
8.3.2 Brownian motion of Nanoparticles 127
8.3.3 Other Mechanisms 133
9 Conclusions, Major Contributions and Future Directions 137
9.1 Conclusions of Experimental and Modeling Work 137
9.2 Major Contributions 142
9.3 Future Directions 145
9.4 Relevant Publications and Patents 148
Appendix 150
Bibliography 170

List of Tables

Table 1-1 Thermophysical properties of liquid-metal coolants……..8

Table 1-2 Thermal conductivity of common solids and liquids……...….12

Table 2-1 Summary of maximum measured thermal conductivity enhancement for nanofluids containing metal oxide nanoparticles. The base fluids used are water, ethylene glycol and mineral oils……...27

Table 2-2 Summary of maximum measured thermal conductivity enhancement for nanofluids containing metallic nanoparticles. The base fluids used are water, ethylene glycol and mineral oils……...29

Table 2-3 Summary of maximum measured thermal conductivity enhancement for nanofluids containing carbon nanotubes. The base fluids used are water, ethylene glycol and mineral oils……..30

Table 6-1 Diameters of encapsulated water nanodroplets in nanoemulsions of different volumetric fractions of water. The diameter of water droplets decreases with increasing water loading, the reason lies in that more surfactant are used for more concentrated nanoemulsions.……...93

Table 7-1 Thermophysical properties of materials used for the synthesis of phase-change metallic nanoparticles-in-PAO nanofluids……...……107

List of Figures

Figure 1-1 Enhancement in thermal conductivity of nanofluids as a function of particle loading in terms of volumetric fraction, as documented in literature ……...10

Figure 2-1 Two-step method for nanofluids production……...22

Figure 2-2 Schematic diagram of nanofluid production system designed for direct evaporation of materials into low-vapor-pressure liquids…….....24

Figure 3-1 Experimental set-up of the one-step nanoemulsification method: (a) For water in oil nanoemulsions; (b) For LMP metals or alloys in oil nanoemulsions …….....51

Figure 3-2 Water-in-FC72 nanofluid. When a laser beam passes through the nanofluid, the Tyndall effect (i.e. a light beam can be seen when viewed from the side) is observed…….52

Figure 3-3 As-prepared nanofluids by using the nanoemulsification method at room temperature. From left to right are: gallium, Field's Metal, Wood's metal and indium nanoparticles in PAO nanofluids……...52

Figure 3-4 TEM bright field images of metal and alloy nanoparticles. (a) gallium; (b) Field's metal; (c) Wood's metal, and (d) indium……...53

Figure 3-5 Experimental setup of 3ω-wire technique for thermal conductivity measurement of liquid …….....59

Figure 4-1 TEM BF image of Bi_2Te_3 nanorods produced by the sonochemical technique. The insert at top right corner is the electron diffraction pattern of the prepared Bi_2Te_3 nanorods. Image taken by a JEOL 4000FX transmission electron microscope……66

Figure 4-2 Measured amplitude of the temperature oscillation in the metal wire immersed in the pure hexadecane oil as a function of the frequency of the drive current……68

Figure 4-3 Comparison of the thermal conductivity of the pure hexadecane oil measured by the 3ω-wire technique to the literature data……..68

Figure 4-4 Thermal conductivity enhancement $\Delta k / k_o$ as a function of temperature in nanofluids consisting of Bi_2Te_3 nanorods and hexadecane oil. The prediction by the effective medium theory is shown for comparison……....70

Figure 4-5 Normalized Brownian diffusivity D_B, calculated from Eqs. 4-2 and 4-3, and normalized thermal conductivity of nanofluids k_{eff}, estimated from the effective medium theory, vs. the particle aspect ratio. Both D_B and k_{eff} are normalized to the values for spherical nanoparticles. In the calculation, the diameter of Bi_2Te_3 nanoparticles is 20nm, and the volume fraction is 0.8%.....73

Figure 5-1 Nanoparticles of different geometries with different aspect ratios. a) Spherical Au nanoparticles (aspect ratio ~1); (b) Carbon Nanotubes, (aspect ratio >100).....75

Figure 5-2 A schematic illustration of carbon tubes-on-spheres nanoparticles……76

Figure 5-3 Synthesis processes of hybrid nanoparticles. Hybrid nanoparticles were synthesized in Dr. Zachariah's group……77

Figure 5-4 TEM image of a sample urchin-like nanoparticle produced by the aerosol method. Numerous carbon nanotubes are attached to the spherical, alumina/iron oxide nanoparticles. Image taken by a JEOL 2010 High-Resolution Transmission Electron Microscope (HRTEM)……...78

Figure 5-5 Illustration of well-dispersed urchin-like nanoparticles in PAO. This figure shows that nanoparticles are in Brownian motion and can easily get in touch with the help of extending-out carbon nanotubes ……...80

Figure 5-6 Correlation function of the scattered light vs. delay time for the nanofluid consisting of urchin-like particles and poly-alpha-olefin (PAO). Measurements taken by a Photocor-Complex DLS instrument……..81

Figure 5-7 Measured amplitude of the temperature oscillation in the metal wire immersed in poly-alpha-olefin (PAO) with and without urchin-like particles as a function of frequency of the drive current. The test temperature is 25^{o}C……83

Figure 5-8 Temperature dependence of the thermal conductivity enhancement of nanofluids with urchin-like particles at 0.1 and 0.2 vol% concentrations. Thermal conductivity enhancement in the nanofluids is normalized by the thermal conductivity of the base fluids at each specified temperature. Linear fits to the data are shown as a guide to the eye……84

Figure 5-9 Performance comparison of particles with various morphologies, e.g., spheres, carbon nanotubes (CNTs), and hybrid sphere-CNTs particles (urchin-like), in nanofluids …….85

Figure 6-1 Water-in-FC72 nanoemulsion fluid (Bottle A) and pure FC72 (Bottle B). Liquids in both bottles are transparent. When a laser beam is passed through Bottles A and B, the Tyndall effect (i.e. a light beam can be seen when viewed from the side) is observed only in Bottle A. Pictures taken by a Canon PowerShot digital camera……...90

Figure 6-2 (a) Correlation function of the scattered light for the water-in-FC72 nanoemulsion fluids; (b) the curve for 6 vol% water-in-FC72 is fitted with the inelastic light scattering model. Measurements taken by a Photocor-Complex DLS instrument……..92

Figure 6-3 Measured amplitude of the temperature oscillation in the metal wire immersed in the FC72 with and without water nanodroplets as a function of frequency of the drive current. Volume fraction of nanoemulsion fluid is 12%. ……..94

Figure 6-4 Thermal conductivity of FC72 is seen to be improved by up to 52% through emulsifying 12 vol% (or 7.1wt%) water into FC72…….....95

Figure 6-5 Brief summary of thermal conductivity enhancement in stable suspensions of nanoparticles in fluids. Early experimental studies are limited to solid nanoparticles, such as metal and oxide……..97

Figure 6-6 Viscosity of water-in-FC72 nanoemulsions measured at different volumetric fractions of water nanodroplets. The measurements were conducted at room temperature on a Brookfield viscometer……99

Figure 6-7 DSC cyclic curves of FC-72 and nanoemulsions. The heat capacity of fluids can be derived from these curves……100

Figure 6-8 DSC measured and calculated heat capacities of water-in-FC72 nanoemulsion. The heat capacities of nanoemulsions are also calculated according to the rule of mixture (ROM)……..101

Figure 6-9 DSC cyclic curves of water-in-FC72 nanoemulsions for different water loading. Exothermal peaks are observed at -20 ℃, corresponding to the freezing of water nanodroplets, while endothermal peaks are observed at 0 ℃, corresponding to the melting of water nanoparticles……..103

Figure 6-10 Natural convective heat transfer curves for pure FC72 and the water-in-FC72 nanoemulsion fluids. Note the bulk temperature of FC72 is 24 ^{o}C while the boiling point of FC 72 is 56 ^{o}C……104

Figure 7-1 Dynamic viscosity of PAO, water and toluene as a function of temperature. Much higher viscosity index is found in PAO 2Cst than water and toluene……...110

Figure 7-2 Experimental set-up of the nanoemulsion preparation.....112

Figure 7-3 Schematic illustrating the formation of molten metal-in-oil nanoemulsion. (a) PAO and molten metals are in the reaction vessel. These two liquids are immiscible and phase separate; (b) the polymer surfactant is soluble in PAO and preferentially adsorbs at the interface. One end shows affinity to metallic liquids and the other end extends to the solvent to impart solubility; (c) the mixture is stirred using a magnetic stirrer and the bulk molten metal breaks into microscale droplets; (d) the microscale emulsion is exposed to high-intensity ultrasonication till nanoemulsion is formed…….....112

Figure 7-4 TEM BF image of as-prepared indium nanoparticles …….……113

Figure 7-5 Thermal conductivity of the pure PAO and indium-in-PAO nanofluid (left x-axis) and relative conductivity of the nanofluid (right x-axis) vs. temperature ……..115

Figure 7-6 DSC curves of PAO, PAO-based nanofluid containing indium nanoparticles and bulk indium……...117

Figure 7-7 Dynamic viscosity of PAO and nanofluid at different temperatures. The coefficient *B* used in the modified Einstein equation is estimated with LSM as 13.6…121

Figure 8-1 Experimental data and EMT values of the thermal conductivity enhancement in water-in-FC72 nanofluids ……...126

Figure 8-2 Thermal conductivity of the pure PAO and indium-in-PAO nanofluid (left x-axis) and relative conductivity of the nanofluid (right x-axis) vs. temperature. The relative thermal conductivity estimated from the HJ Model (solid line) is also shown for comparison. A temperature-independent interfacial resistivity is used in this calculation……127

Figure 8-3 Comparison of the thermal conductivity enhancement predicted by a theoretical model and the experimental data. The theoretical models include the contributions from both thermal conduction and Brownian motion……132

Figure 8-4 Thermal conductivity enhancements as a function of nanoparticle radius with consideration of the effect of ordered layers of liquid molecule on the surface of nanoparticles……135

Figure A-1 Schematic cross-sectional structure of a nanoparticle and the interfacial nanolayer of liquid molecules……..157

Figure A-2 Formation of nanoparticle clusters/aggregates…….166

Nomenclature

Acronyms and Abbreviations:

AC	Alternating Current
BF	Bright Field (a TEM imaging technique)
CHF	Critical Heat Flux
CNTs	Carbon Nanotubes
- DWCNTs	Double-Walled Carbon Nanotubes
- MWCNTs	Multi-Walled Carbon Nanotubes
- SWCNTs	Single-Walled Carbon Nanotubes
DC	Direct Current
DI	De-Ionized
DLS	Dynamic Light Scattering
DSC	Differential Scanning Calorimetry
ED	Electron Diffraction
EDS (or EDX)	X-ray Energy Dispersive Spectroscopy
EMT	Effective Medium Theory
EG	Ethylene Glycol
FC	Fluorocarbons
HC	Hamilton-Crosser model
HJ	Hasselman-Johnson model
HTFs	Heat Transfer Fluids
LMP	Low Melting Point
PAO	Polyalphaolefin
PCMs	Phase-Change Materials
- MCPCMs	Microencapsulated Phase Change Materials
ROM	Rule of Mixture
RPM	Round Per Minute
SSA	Specific Surface Area
TEM	Transmission Electron Microscopy
- FE-TEM	Field-Emission TEM

- HRTEM	High Resolution TEM
XRD	X-Ray Diffraction

Symbols:

a	Coefficient
b	Coefficient
B	Correlation coefficient in Einstein-Batchelor model
c	Coeeficient
C	Constant
C_p	Heat capacity, kJ/kg
C_{rt}	Temperature coefficient of resistance, $^{o}K^{-1}$ (K means Kelvin)
d_p	Nanoparticle diameter, m
d_f	Fractal dimension of the aggregates
d_{mol}	Molecular diameter, m
D	Diameter, m
D_B	Brownian diffusivity, m^2/s
D_{trans}	Translational diffusivity, m^2/s
f	Friction coefficient, $N.s/m^2$
F	Force, N
G	Interfacial thermal conductance, W/K
G_T	Temperature gradient, K/m
H_f	Heat of fusion, kJ/kg
h	Convective heat transfer coefficient, $W/m^2.K$
I	Electrical current, A
k	Thermal conductivity, W/m.K
k_B	Boltzmann constant, $m^2\ kg\ s^{-2}\ K^{-1}$
K	Shape factor
l	Mean free path, m
L	Length, m

m	Mass, kg
n	Empirical shape factor
n_p	Number of particles
n_r	Refractive index
Nu	Nusselt number
P	Electrical power, W
Pe_r	Peclet number
Pe_t	Modified Peclet number
P_r	Prandtl number
q	Wave vector, m^{-1}
r	Radius, m
$\mathbf{r}$	Radius, vector
r_p	Radius of nanoparticles
r_a	Radius of gyration of aggregates, m
R_a	Rayleigh number
R_{bd}	Boundary thermal resistance, K/W
R_E	Electrical resistance, Ω
Re	Reynolds number
R_h	Hydrodynamic radius, m
R_k	Kapitza resistance, K/W
t	Time, s
T	Temperature, K
T_m	Melting temperature, K
u	Velocity of random motion, m/s
U	Velocity, m/s
V	Voltage, V
Vol	Volume, m^3

Greek Letters:

α	Thermal conductivity ratio

α_f	Thermal diffusivity of fluids, m^2/s
β	Aspect ratio of nanoparticles
ε	Constant
ξ	Ratio of the thickness
ζ	Equatorial semi-axis of the ellipsoid, m
ρ	Density, kg/m^3
ϕ	Volume fraction
Γ	Linewidth, m
λ	Wavelength, m
Ψ	Sphericity of the particle
φ	Phase shift
γ	Velocity gradient, s^{-1}
$\dot{\gamma}$	Shear rate, s^{-1}
δ	Standard deviation
σ	Interfacial energy, J/m^2
τ	Time, s
μ	Dynamic viscosity, Pa.s
μ_B	Brownian mobility, s/kg
ν	Kinematic viscosity, m^2/s
ω	Frequency, Hz
η	Constant

Supscripts:

b	Bulk
α, - α	Exponents

Subscripts:

0	Initial or reference value
a	Aggregates
bd	Boundary
B	Brownian Motion

c	Cluster
cp	Composite particles
convec	Convection
droplet	Nanodroplet
D	Average over the diameter
DC	Direct current
eff	Effective
E	Electrical
EMT	Effective Media Theory
f	Base fluid
L	Liquid
m	Melting
mol	Molecule
M	Matrix
nf	Nanofluid
np	Nanoparticles
p	Nanoparticle
r	Reduced
rot	Rotational
s	Surface
S	Solid
trans	Translational
V	Vapor
ω(1ω,2ω,3ω)	Frequency (Signal with frequency at *1ω,2ω,3ω)*

1 Introduction

1.1 Brief History of Nanofluids

Heat transfer fluids (HTFs) have many industrial and civil applications, including in transport, energy supply, air-conditioning and electronic cooling, etc. Traditional HTFs, such as water, oils, glycols and fluorocarbons, however, have inherently poor heat transfer performance due to their low thermal conductivities. Research and development activities are being carried out to improve the heat transport properties of fluids. Solid metallic materials, such as silver, copper and iron, and non-metallic materials, such as alumina, CuO, SiC and carbon nanotubes, have much higher thermal conductivities than HTFs. It is thus an innovative idea trying to enhance the thermal conductivity by adding solid particles into HTFs since Maxwell initiated it in 1881 (Maxwell 1873). At the very beginning, solid particles of micrometer, even millimeter magnitudes were blended into the base fluids to make suspensions or slurries. However, large solid particles cause troublesome problems, such as abrasion of the surface, clogging the microchannels, eroding the pipeline and increasing the pressure drop, which substantially limits the practical applications. Actually, liquid suspension was primarily a theoretical treatment only of some theoretical interest, and subsequent studies by other researchers achieved minor success. The large size of the particles and the difficulty in production of small particles were limiting factors.

The situation changed when S.U.S. Choi and J. Eastman in Argonne National Laboratory revisited this field with their nanoscale metallic particle and carbon nanotube suspensions (Choi and Eastman 1995; Eastman et al. 1996). Choi and Eastman have tried

to suspend various metal and metal oxides nanoparticles in several different fluids (Choi 1998; Choi et al. 2001; Chon et al. 2005; Chon et al. 2006; Eastman et al. 2001; Eastman et al. 1999; Eastman et al. 2004), and the results are promising, however, many things remain elusive about these suspensions of nano-structured materials, which have been termed "nanofluids" by Choi and Eastman.

Generally, nanofluids are formed by dispersing nanometer-sized particles (1-100 nm) or droplets into HTFs. Nanoparticles have unique properties, such as large surface area to volume ratio, dimension-dependent physical properties, and lower kinetic energy, which can be exploited by the nanofluids. At the same time, the large surface area make nanoparticles better and more stably dispersed in base fluids. Compared with micro-fluids or milli-fluids, nanofluids stay more stable, so nanofluids are promising for practical applications without causing problems mentioned above. Nanofluids well keep the fluidic properties of the base fluids, behave like pure liquids and incur little penalty in pressure drop due to the fact that the dispersed phase (nanoparticles) are extremely tiny, which can be very stably suspended in fluids with or even without the help of surfactants (Xuan and Li 2003). A most attractive characteristic of nanofluids is that even by the addition of small amount of nanoparticle, they show anomalous enhancement in thermal conductivity over 10 times more than the theoretically predicted. Eastman et al (Eastman et al. 2001) reported a 40% thermal conductivity increase in ethylene glycol by adding only 0.3 vol.% of copper nanoparticles with a diameter smaller than 10 nm. Experiments on convection heat transfer of nanofluids were conducted by several research groups (Buongiorno 2006; Chein and Huang 2005; Etemad et al. 2006; Kim et al. 2004a; Said and Agarwal 2005; Xuan and Li 2003). The experimental results showed significant improvements in heat

transfer rates of nanofluids. Meanwhile, the thermal conductivity enhancement of nanofluids show a temperature-dependent characteristic – increase of enhancement with rising temperature, which makes the nanofluids more suitable for applications at elevated temperatures (Das et al. 2003c; Yang and Han 2006a). Another interesting phenomenon of nanofluids is that even extremely low concentration of small nanoparticle will dramatically increase the critical heat flux (CHF) in a pool boiling system (Das et al. 2003a; Wen and Ding 2005b; You et al. 2003). The improved thermal transport properties of nanofluids would improve the efficiency of heat exchanging, reduce the size of the systems, save pump power, reduce operational cost and provide much greater safety margins. Better properties of nanofluids may be obtained if higher-quality and more monodispersed nanoparticles can be synthesized. Meanwhile, nanofluids with the low volume fraction of the suspended nanoparticles incur almost no extra penalty of pump power (i.e., the viscosity increase is small.).

However, the research work on nanofluids is only at its infant stage. More work is necessary for an in-depth understanding of the anomalous thermal conductivity jump and the enhancement in the convective heat transfer coefficient in nanofluids. Some of the current theoretical models attribute the increasing thermal conductivity to the high conductivity of solids. But Chen (Chen 1996; Chen et al. 2004) argued that when the particle size is smaller than the mean free path of heat-carriers (electrons, phonons, or molecules), the heat carrier transport is ballistic or non-local and Fourier's law is not applicable. In fact, thermal conductivity decreases rapidly with decreasing particle size. Very limited data have indicated an inverse dependency of nanofluids' thermal conductivity on the particle size -- with decreasing particle size, the effective thermal

conductivity of nanofluids tends to increase, which apparently contradicts the phenomenological size-dependent thermal conductivity of nanoparticles, and thus an investigation of the effects of particle's thermal conductivity on the thermal behavior of nanofluids is imperative. At the same time, with decreasing particle size, the interfacial area between particles and the base fluid increases dramatically so that the interfacial resistance (Kapitza resistance) should be carefully taken into consideration. There has not been a systematic experimental investigation of size dependent conductivity reported. An investigation of the effects of different particle sizes on thermal conductivity enhancement is necessary before good-performance nanofluids can be synthesized. On the other hand, the large interface areas between the nanoparticles and the base fluids increase the heat transfer rate, so nanosheets, nanorods, and nanowires, which have large surface areas, perhaps are favorable to more significantly increase the thermal conductivity of nanofluids.

Many mechanisms have been proposed to describe the anomalous thermal conductivity increase in nanofluids. Among these models the famous Hamilton-Crosser (HC) model was based on the Maxwell's model, and both of them only take into consideration of the volume fraction and the geometry of particles (Hamilton and Crosser 1962a; Hamilton and Crosser 1962b). HC model gives a good description of systems with micrometer or larger-size particles, but fails to predict the measured thermal conductivity of nanofluids. Recently, Keblinski et al (Keblinski et al. 2005; Keblinski et al. 2002) presented four possible mechanisms in nanofluids which may contribute to the thermal conduction: (1) Brownian motion of nanoparticles; (2) Liquid layering at liquid/particle interface; (3) Ballistic nature of heat transport in nanoparticles; (4) Nanoparticle

clustering in nanofluids. It turns out that, Brownian motion of nanoparticles is too slow to directly transport a significant amount of heat through a nanofluid, however, it could have an important indirect role to produce a convection-like micro-environment around the nanoparticles and particle clustering to increase the heat transfer; the presence of an ordered interfacial liquid molecule layer seems to be not solely responsible for the anomalous increase of thermal conductivity, especially this mechanism works well only when the particle size is smaller than 10nm; nanoparticle clustering have both positive and negative effects on the increase of the thermal conductivity. Although these possible mechanisms can explain the thermal behavior of nanofluids partially, more convincing and comprehensive experimental and theoretical studies are needed in search of new nanofluids with better thermal performance.

Most research work on nanofluids is trying to increase the thermal conductivity, and other important thermal transport properties, heat capacity and viscosity, have been paid less attention to. Actually, functional thermal fluids, including emulsions and suspensions have been a new class of heat transfer fluids with improved thermal transport properties (Bai and Lu 2003; Chen et al. 2006; Inaba 2000; Inaba et al. 2007). One of the main advantages of these functional thermal fluids is that they can be specially designed to optimally fulfill particular objectives, such as enhanced thermal conductivity, a higher thermal energy storage capacity, a higher heat transfer coefficients, a higher critical heat flux, a better temperature stabilization, and less pressure drop, etc. The use of phase change materials (PCMs) as dispersed phases in continuous phases (base fluids) attracts much attention – by taking advantages of phase change latent heat of PCMs, the effective heat capacity of the fluids is boosted while the fluidic properties of the fluids still remain.

The most commonly used PCMs are water, low-melting point metals, salt hydrates, fatty acids, esters, polyethylene glycols and paraffins. Microencapsulated PCMs provide a portable heat storage system: by coating a microscopic sized PCM with a protective coating, the particles can be suspended within a continuous phase such as engine oil. With the use of nanoparticles of PCMs with high thermal conductivity, the heat capacity of nanofluids is expected to be improved as well as the thermal conductivity.

1.2 Motivation of Improving Thermal Conductivity of Fluids

Recent years have eye-witnessed a blossom in the development of electronics, communications, and auto-computing industries, and this trend is indisputably continuing in this century. Cooling of mechanical, electrical and electronic components has become a problem in today's fast-growing technologies. The heat required to be rejected is continually increasing due to trends toward faster speeds and smaller volumes for microelectronic devices, more power output for engines, and brighter beams for optical devices. Though all three modes of heat transfer can be used for cooling, the utilization of fluids by taking the advantage of the large heat flux of convection and boiling is one of the most common and effective way. Heat transfer fluids have found many industrial and civil applications, including in automotive, aerospace, energy supply, air-conditioning and electronic cooling, etc. However, the low thermal conductivity of the heat transfer fluids is a limiting factor in the design of the cooling systems. The increasing power but decreasing size of the equipments calls for innovative cooling technologies and now the thermal management has become one of the top technical challenges and a primary concern of component design. There are two ways to meet the cooling requirements:

designing new cooling devices, such as increasing the surface by fins, microchannels, integrated spot cooling and miniaturized cryodevices, and improving the heat transfer capability of the fluids (Duncan and Peterson 1994; Eastman et al. 2004). The effectiveness of updating the design of cooling devices as a conventional method to increase the heat transfer rate, however, has reached a limit (Eastman et al. 2004). With the increasing demand for machines and devices to operate efficiently, the seeking for new heat transfer fluids with higher thermal conductivity and more effective cooling capacity is an emergency now. The research and development work are being carried out to improve the heat transport properties of conventional heat transfer fluids (Das et al. 2006).

Liquid metals are thermally conductive and their heat transfer characteristics have been attracting much interest. Liquid metals are used as heat transfer fluids in specialized branches of engineering involving very high heat fluxes (Miner and Ghoshal 2004). As an example, in nuclear engineering, there is the requirement to obtain high rates of heat extraction from reactors. Also liquid metal is used in gas turbine, where the need for effective blade-cooling systems remains as pressing as ever in order to achieve the greatest thermodynamic advantage. Liquid metals usually have very high thermal conductivity, which mark them off from other conventional HTFs, i.e., water, oils and glycols. In Table 1-1, thermophysical properties of liquid metals are shown.

Liquid mercury has been proposed as the working fluid in cooling devices like heat pipes for the heat rejection systems or the radiation panels of spacecraft. Moreover, liquid mercury is sometimes used as the coolant for nuclear reactors; however, because of its

high density, a lot more energy is required to circulate liquid mercury as coolant (Fleitman and Weeks 1971).

Table 1-1 Thermophysical properties of liquid metals

Liquid Metal	Melting Point (^oC)	Density (kg/m^3)	Thermal Conductivity (W/m.K)	Dynamic Viscosity (mPa.s)
Mercury	-38.8	13.534	8.3	1.526 (300 K)
Sodium	97.7	0.968	142	0.7 (400 K)
Galinstan	-19	6.441	16.5	2.4 (300 K)

It should be noted that liquid mercury is toxic and corrosive to other metals, and mercury is incompatible with metal oxides. But actually, metals exposed to air tend to oxidize and then these oxides react with Hg to form mercuric oxide. Also, as a coolant, the price of liquid mercury is high.

Sodium is an important liquid metal coolant. It can be used as the heat transfer fluid in some types of nuclear reactors (Liquid Metal Fast Breeder Reactor) and inside the hollow valves of high-performance internal combustion engines (Vissers et al. 1974). Sodium does not corrode steel to any significant degree and is compatible with many nuclear fuels. However, it ignites spontaneously on contact with air and is violently reactive with water, so it must be stored and used in an inert environment.

Galinstan is a newly developed liquid-metal coolant, which is a eutectic alloy of gallium, indium, and tin. It is already in liquid state at below room temperature. Due to its low toxicity, it has found many applications as a non-toxic replacement of liquid mercury or sodium-potassium alloy (NaK) (Mohseni and Baird 2007).

However, galinstan tends to wet and adhere to many materials just like gallium, which limits its use compared to mercury. Surfaces need to be coated with gallium oxide

so the metal does not stick to them. The high cost and the aggressive properties of galinstan are major obstacles for its use.

It seems that liquid metal coolants appear as very suitable heat-transfer media only in some special applications, and in most engineering components, conventional heat transfer fluids are more suitable and the improvement of their thermal conductivity is thus important and necessary.

Maxwell's idea of enhancing the thermal conductivity is to add more thermally conductive solid particles into fluids. Initially, the idea of Maxwell was a theoretical treatment, and subsequent studies by other researchers achieved little success (Hamilton and Crosser 1962b; Wasp et al. 1977). The reason lies in that the large size of the particles was a limiting factor to increase the thermal conductivity and the techniques for preparing tiny particles at that time were a restraint. In 1990s, S.U.S. Choi and J. Eastman in Argonne National Labs made nanofluids with nanometer-scaled metallic particle and carbon nanotubes suspensions in ethylene glycol and oils, respectively (Choi et al. 2001; Eastman et al. 2001) and the results are really exciting and inspiring according to the measurements of these fluids (Choi and Eastman 1995; Eastman et al. 1996; Eastman et al. 1999). Figure 1-1 is a summary of documented data in literature showing the enhancement in thermal conductivity of nanofluids. It can be seen from Figure 1.1 that the particle loading of nanofluids is usually from 0.1% to 10%, and the thermal conductivity enhancement has already been 10% to 80% or even more. The carbon nanotubes are more effective than spherical nanoparticles, and an enhancement of up to 160% has been achieved by adding 1 vol.% carbon nanotubes into engine oils (Choi et al.

2001; Eastman et al. 2001; Eastman et al. 1999; Xie et al. 2003; Xie et al. 2001; Xie et al. 2002).

The anomalously enhanced thermal conductivity of nanofluids is not only of academic interest, but it makes nanofluids potential candidates for nanotechnology-based cooling applications.

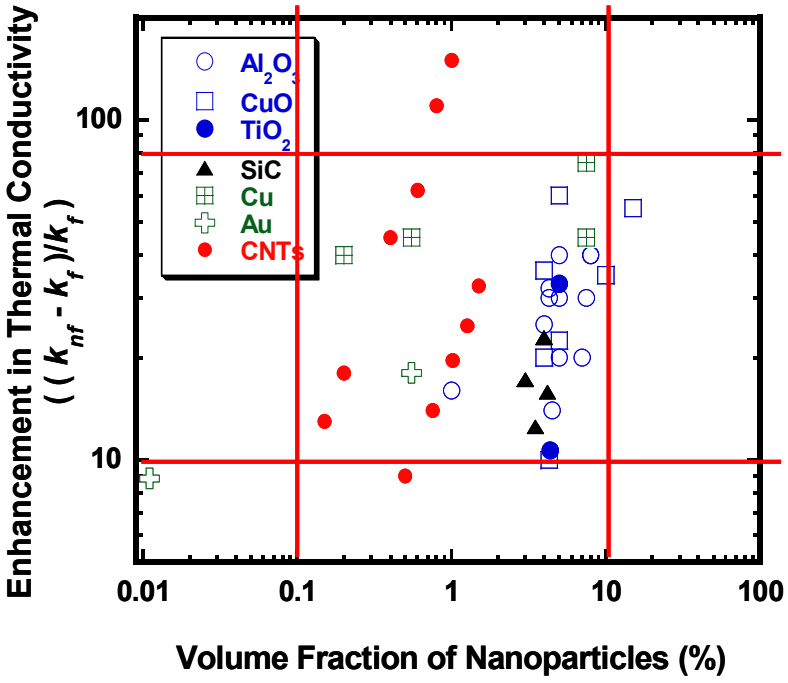

Figure 1-1 Enhancement in thermal conductivity of nanofluids as a function of particle loading in terms of volumetric fraction, as documented in literature (Choi and Eastman 1995; Choi et al. 2001; Eastman 1998; Eastman et al. 2001; Patel et al. 2003; Wu et al. 2005; Xie et al. 2003; Xie et al. 2001; Xie et al. 2002)

1.3 Rationales behind the Nanofluids

Since solid materials have much higher thermal conductivities than fluids, as shown in Table 1-2, it is then a straightforward logic to increase the thermal conductivity of

fluids by adding solids. However, if solid particles of micrometer, even millimeter magnitudes are added into the base fluids to make slurries, the increase in thermal conductivity of the slurries is insignificant even at high particle loading. Meanwhile, large particles cause many troublesome problems:

a) Large particles are easy to settle out from the base fluids, especially in low-speed circulation, not only losing the enhancement in thermal conductivity, but forming a sediment layer at the surface, increasing the thermal resistance and impairing the heat transfer capacity of the fluids;

b) The large size of the particles or the agglomerates of these particles causes severe clogging problems, especially at low circulation rate of fluids or in microchannels;

c) Large particles and the agglomerates in fluid flows carry too much momentum and kinetic energy, which may cause damage to the surface;

d) The erosion of the pipelines by the coarse and hard particles increases rapidly when the speed the circulation increases;

e) Noticeable conductivity enhancement is based on high particle concentration, which leads to apparent increase in viscosity. The pressure drop in fluids (slurries) goes up considerably due to the increase of viscosity.

Table 1-2 Thermal conductivities of common solids and liquids

Materials		Thermal Conductivity (W/m-K)	Viscosity at 25℃ (mPa.s)
Carbon	Diamond	2300	
	Carbon Nanotubes	~2000	
	Graphite	110-190	
Metallic Materials	Silver	429	
	Copper	401	
	Aluminum	237	
Non-Metallic Materials	Silicon	148	
	Silicon Carbide	120	
	Alumina	40	
Heat Transfer Fluids	Water	0.613	0.89
	Ethylene Glycol	0.253	16.6
	Engine Oil	0.145	~20
	FC-72	0.057	0.64

Due to these disadvantages of the liquid suspension of large particles, the method of enhancing the thermal conductivity by adding solid particles is not a preferred one until the emergence of nanofluids. Modern material process and synthesis technologies provide us an opportunity to explore the dimensional bottoms of materials. A variety of nanostructured materials has been produced possessing quite different mechanical,

optical, thermal and electrical properties from the corresponding bulk materials. Several outstanding features of nanoparticles, such as the small sizes, large specific surface area, less particle momentum, and high mobility make nanoparticles perfect candidates as the dispersed phases in liquid suspensions. As a junction of conventional thermal science and modern nanotechnology, now nanofluids have show potential as advanced heat transfer fluids with enhanced thermal transport properties (Zhao and Lu 2002).

Well-dispersed and stable nanofluids are formed after properly dispersing nanoparticles into base fluids and the resulting nanofluids are expected to exhibit several beneficial features:

a) **Greatly improved heat conduction.** Nanofluids demonstrate higher thermal conductivities than the base fluid due to several factors. The large surface area of nanoparticles per unit volume allows for more heat transfer between solids particles and base fluids. Another advantage is that the high mobility of the nanoparticles due to the tininess, which may introduce micro-convection of fluids to further stimulate heat transfer. The experimental enhancement in thermal conductivity has been reported to be much greater than that predicted by considering solely the contribution of high thermal conductivity of solids. Furthermore, it has been reported the thermal conductivity enhancement in nanofluids increases significantly with rising temperature, which also indicates a contribution of Brownian motion(Evans et al. 2006; Prasher et al. 2005; Prasher et al. 2006a).

b) **High stability of nanofluids.** Because the nanoparticles are small, the particles are stably staying in the liquid phases for months or even years without

sedimentation. Brownian motion (the random thermally driven movement of particles suspended in a fluid) can increase the stability of the suspension.

c) **Elimination of clogging.** Nanoparticles are only composed of hundreds or thousands of atoms, about 1 ~ 100 nm in diameter and are well-dispersed in nanofluids, so that they will not causing any clogging problem. Nanofluids can therefore be used in microchannels, which can further promote the heat transfer rate by combining enhanced thermal conductivity of fluids and increased heat transfer area.

d) **Reduction of erosion.** Nanoparticles are very small and do not carry so much momentum as their micro- or macro- counterparts, and thus the momentum and the kinetic energy which they will impart to solid surfaces is small. Consequently the erosion of components, such as pipelines, pumps and heat exchangers, will be greatly reduced. Furthermore it has been reported that nanoparticles dispersed in liquid phases reduce friction and decrease wear.

e) **Smaller press drop and reduction in pump power.** Due to the large specific surface area, nanoparticles have demonstrated high effectiveness to enhance the thermal conductivity of fluids. It is expected that much smaller concentrations of nanoparticles is required to achieve similar enhancements in larger particle suspensions. Less material is needed so that the viscosity increase is smaller, and the pumping power required is also reduced. Meanwhile, the pump power must goes up by tenfold in order to increase the heat transfer of conventional fluids by a factor of two, but if the thermal conductivity of fluids is enhanced

three times, the heat transfer rate has already doubled. Thus, a large increase in thermal conductivity of fluids can save lots of pumping power.

1.4 Objective of Present Research

The objectives of this research are as follows: 1) find the physical mechanisms behind the thermal conductivity enhancement of nanofluids through the investigation of the effects of nanoparticle properties, and the effectiveness of hybrid tubes-on-spheres nanoparticles; 2) develop a new mass production method of nanofluids; 3) synthesize new nanofluid systems based on per-fluorocarbons (e.g., FC72), and 4) develop a new class of phase-change nanofluids to simultaneously improve both the thermal conductivity and the heat capacity.

1.4.1 Physical Mechanisms behind Thermal Conductivity Enhancement

a) The influence of nanoparticle properties

Nanofluids have been extensively investigated (Choi et al. 2001; Eastman et al. 2001; Patel et al. 2003; Prasher et al. 2005; Xie et al. 2002; You et al. 2003), however, the temperature dependence of thermophysical properties of nanofluids has less been studied as most of experimental data to date on nanofluids were obtained at room temperature. In this section, the temperature-dependent enhancement of thermal conductivity is investigated in Bi_2Te_3-in-hexadecane nanofluids. The effects of the particle aspect ratio (the ratio of length to diameter) and the change of particle thermal conductivity on thermal transport in nanofluids will be discussed.

b) The effectiveness and the application of hybrid tubes-on-spheres nanoparticles in nanofluids

Previous studies on nanofluids have focused on spherical nanoparticles or carbon nanotubes (CNTs) (Chang et al. 2004; Ren et al. 2005; Sanchez-Ramirez et al. 2006; Wang et al. 1999; Wen and Ding 2004b; Wu et al. 2005; Xie et al. 2003; Xie et al. 2001). CNTs are very effective to increase the thermal conductivity of fluids attributable to their high thermal conductivity and high aspect ratio (Assael et al. 2004; Choi et al. 2001; Xie et al. 2003; Yang et al. 2006); however, CNTs are easy to be entangled and agglomerate due to their long length and low diffusive mobility in base fluids. Stable suspensions of CNTs are not easy to be made and usually the CNTs settle out from the liquid phases soon, causing erosion and clogging problems (Assael et al. 2005; Marquis and Chibante 2005). New hybrid tubes-on-spheres nanoparticles have been proposed for the applications in nanofluids to promote the heat transport in nanofluids containing such hybrid nanoparticles. The urchin-like nanoparticles can improve the diffusive mobility and the colloidal stability of nanotubes, while they are as effective as CNTs on enhancing the thermal conductivity.

1.4.2 Mass Production Method of Nanofluids

Two nanofluid production methods have been developed as documented in literature. The first one is a two-step method. In this process, nanoparticles are prepared as the first step and then as the second step, the prepared nanoparticles are dispersed into base fluids with mechanical agitation (stirring)

or ultrasonication method (Bourlinos et al. 2006; Chang et al. 2005; Ding et al. 2006; Hwang et al. 2006). The nanofluids are homogenized with or without surfactants depending on the interface properties of between nanoparticles and base fluids. This method is mainly limited by the availability of nanoparticles.

The second one is a one-step process, which has been developed in ANL. By direct evaporating metallic materials into low-vapor-pressure liquids, nanoparticles are simultaneously made and dispersed into base fluids to make nanofluids. It is a good method for producing nanofluids of metallic nanoparticles in low-vapor-pressure base fluids.

However, these two methods are not suitable for mass production and there still remains a question regarding the ability to effectively mass-produce nanofluids. In this section, a mass production method of nanofluids will be developed based on a nanoemulsification technique.

1.4.3 Nanofluid Systems Based on Per-fluorocarbons

Water, glycols and mineral oils based nanofluids have been produced and extensively characterized showing improved thermal conductivity. Fluorocarbons (FC) are important heat transfer fluids (Bar-Cohen 1997; Kim et al. 2006b; Mudawar 1992), but the drawback of FC-72 is also outstanding – the thermal conductivity of FC72 is very low. At room temperature, the thermal conductivity of FC72 is only 0.057 W/m.K, only one tenth of the thermal conductivity of water (0.58 W/m.K).

In this section, FC-72 based nanofluids are proposed in an attempt to increase the thermal conductivity. Moreover, due to its low boiling point and stability, FC72 is a perfect candidate for pool boiling in electronic cooling applications (Golobiac and Ferjancic 2000; Liu et al. 2001; Rainey and You 2000). It has been reported that the addition of small amount of nanoparticles to fluids has significant influence on the boiling process (Bang and Heung Chang 2005; Das et al. 2003a; Das et al. 2003b; Wen and Ding 2005b; You et al. 2003). The critical heat flux is drastically enhanced by up to 200% in water suspension of alumina when the concentration of nanoparticles is only 0.05 g/L (~0.125 vol.%) (You et al. 2003). However, FC-72 is one of the most hydrophobic and oleophobic materials ever invented, the preparation of stable FC72 based nanofluids is not a trivial work. For different nanoparticles, different fluorinated amphiphilic surfactants are used, which can be well dissolved in FC72 to impart the solubility to nanoparticles.

1.4.4 Phase-Change Nanofluids

Heat transfer fluids are suffering from not only low thermal conductivity, but also low heat capacity. Though common nanofluids have enhanced thermal conductivity, the addition of solid nanoparticles will not increase the heat capacity. A new class of phase-change nanofluids with improved thermal conductivity and heat capacity is then proposed, which are synthesized by dispersing thermally conductive phase-changeable nanoparticles into base fluids. The high thermal conductivity of solid nanoparticles will increase the thermal conductivity of fluids just as common nanofluids. At the same time,

the phase change process of nanoparticles is reversible, large amount of latent heat will be absorbed or released during the melting-freezing process, and the heat storage capacity of the nanofluids can thus be increased.

2 Literature Review

Nanoparticles have great potential to more effectively improve the thermal transport properties of HTFs than micrometer and millimeter sized particles. This is mainly due to the tininess of nanoparticles or other nanostructures, which not only improves the stability and the applicability of liquid suspensions, but also increases the specific surface area (SSA) and the diffusion mobility of Brownian motion of nanoparticles. Furthermore, the tininess of nanoparticles can provide nanofluids a potential to be used in miniaturized electronic cooling and microchannels, where larger particles would either clog the channels or settle out from the carrying fluids quickly. In this chapter, experimental and theoretical efforts on synthesis process, experimental measurements of thermal conductivity, heat capacity, viscosity and heat transfer rates in convective and pool boiling environments, and detailed proposed theories for explaining the experimental results will be reviewed and discussed.

2.1 Synthesis of Nanofluids

A large variety of combinations of nanostructures and heat transfer fluids can be used to synthesize stable nanofluids with improved thermal transport properties. Nanostructures made from metals, oxides, carbides and carbon nanotubes can be dispersed into HTFs, such as water, ethylene glycol, hydrocarbons and fluorocarbons with or without the presence of stabilizing agents. In most experimental studies, nanofluids are synthesized in a two-step process (Assael et al. 2004; Bang and Heung Chang 2005; Choi 1998; Hwang et al. 2006; Kim et al. 2006a; Kim et al. 2004a; Ma et al. 2006; Maiga et al. 2004), which is the first and the most classic synthesis method of

nanofluids, as shown in Figure 2-1. In the first step, nanoparticles are prepared by mechanical comminuting, chemical reaction, vapor condensation or decomposition of organic complex (Agostiano et al. 2000; Ahmadi et al. 1996; Gesenhues 1999; Guo et al. 2000; Jiang et al. 1999; Suenaga et al. 1997; Talapin et al. 2002; Wegner et al. 2002). Then it is followed by the second step in which the as-produced nanoparticles are dispersed into base HTFs with mechanical agitation (stirring) or ultrasonication (Hwang et al. 2008; Li et al. 2008). Nanofluids are homogenized using or not using surfactants depending on the properties of interfaces between nanoparticles and base fluids. The main advantage of this two-step synthesis method is that it produces nanoparticles under clean conditions, without undesirable surface coatings and other contaminants (Lee et al. 1999). The major problem is that agglomeration of nanoparticles may occur. When finely divided solid nanostructures are immersed in liquids, they often do not form a stable dispersion. Many of the particles aggregate together in forms of clumps. Though these particles can be easily re-dispersed in liquids by mechanical dispersion, they soon clump together again to form large aggregates that will settle out of the suspension quickly. Uniform dispersions can be significantly stabilized by steric barriers surrounding the nanoparticles to form a coating layer that is sterically bulky, for example, polymeric surfactant. When absorbed on the surfaces of solid particle, the surfactant molecules can produce a barrier to prevent aggregation of nanoparticles and impart solubility to particles in base fluids, so that the prepared nanofluids can sustain the stability without visible precipitation for months or even years. Oxide nanoparticles are firstly used for nanofluids, mainly because they are easy to produce, chemically stable and easy to be dispersed into water due to their surface hydrophilicity.

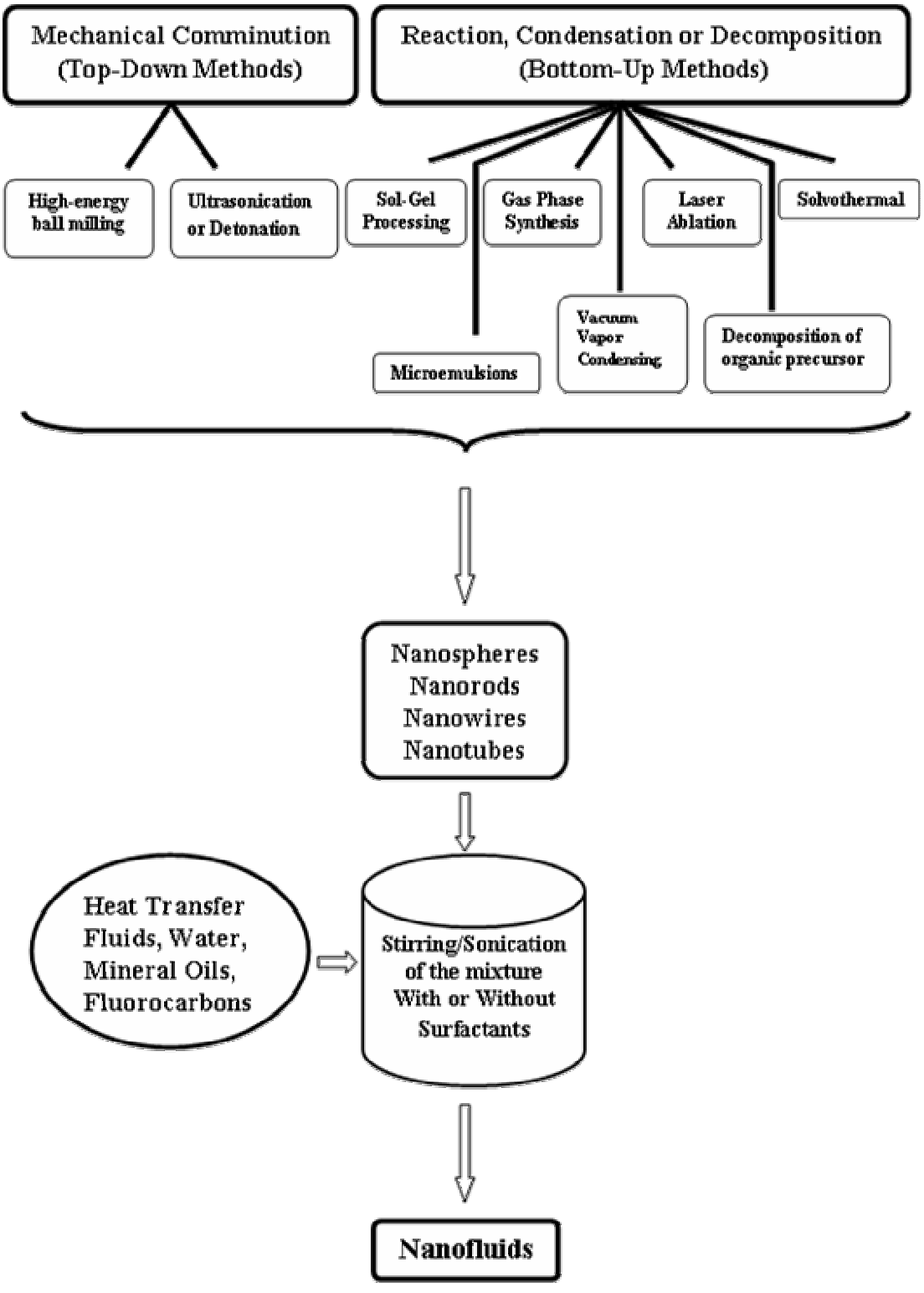

Figure 2-1 Two-step method for nanofluids production

Agglomeration is greatly reduced in a one-step method by combining together the synthesis process and the subsequent dispersing process into a single step. This one-step approach can be traced back to Yatsuya et al.(Yatsuya et al. 1978), and later it was improved by Wagener et al. (Wagener and Gunther 1999) and Eastman et al.(Eastman et al. 1996). This one-step method employs a direct evaporation condensation (DEC) technique, which is a modified inert gas-condensation (IGC) process that has been used in ANL (Eastman 1998; Eastman et al. 1996; Eastman et al. 2001). The schematic of this method is shown in Figure 2-2. There are four steps in the process in this one-step process,

1. A cylinder containing a heat transfer fluid such as water or ethylene glycol is rotated so that a thin film of the fluid is constantly being transported over the top of the chamber;
2. A piece of the metallic material as the source of nanoparticle is evaporated by heating on a crucible;
3. Evaporated particles contact the fluid overhead and condense as nanoparticles;
4. The fluid is cooled at the base of the chamber to prevent any unwanted evaporation of the fluid.

The presence of surfactants in the carrying liquid can further suppress the agglomeration of nanoparticles. The main advantages of this process are: 1) it enables producing nanoparticles without undesirable and less conductive oxide layers, which increase the thermal resistance between the particles and liquids; 2) the size of the produced nanoparticle is as small as <10 nm and the size distribution of particle is in a

narrow range; 3) the nanoparticle yield is high due to the high evaporation rate; 4) the agglomeration of nanoparticles is substantially reduced and the nanofluids are very stable. However, this method has limitations that the base fluids must have a low vapor pressure (usually below 1 torr), and oxidation may occur at the surface of pure metallic particles. High liquid vapor pressures of base fluids may lead to apparent aggregation of nanoparticles.

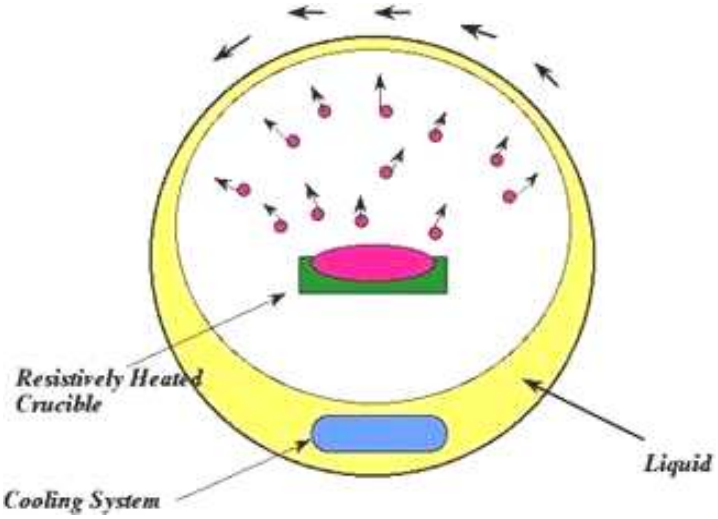

Figure 2-2 Schematic diagram of nanofluid production system designed for direct evaporation of materials into low-vapor-pressure liquids (Eastman et al. 2001)

Another method of nanofluid synthesis is the laser ablation method which has been used to produce alumina nanofluids (Tran and Soong 2007). Pure chemical synthesis is also an option which has been used by Pratel to prepare gold and silver nanoparticle nanofluids (Patel et al. 2003). Zhu et al also use a one-step pure chemical synthesis method to prepare nanofluids of Cu nanoparticles dispersed in ethylene glycol (Zhu et al. 2004).

Generally, there are mainly four concerns about the synthesis of nanofluids, 1) dispersability of nanoparticles, 2) stability of nanoparticles in base fluids, 3) chemical compatibility of nanoparticles and base fluids, and 4) thermal stability of nanofluids. These four rules can be used as the guidelines for the development of new synthesis methods of nanofluids.

2.2 Heat Transfer in Nanofluids

As is well known, there are three modes of thermal energy transport, which are conduction, convection and radiation. However, seldom there is only one mode in a heat transfers process, though one of these three modes may dominate in a particular transfer process or phenomenon. In this section, the thermal transport in nanofluid systems will be discussed in three categories -- conduction, convection and pool boiling.

2.2.1 Thermal Conduction in Nanofluids

Dispersions of oxide nanoparticles in water are the first batch of nanofluids that have been investigated. In 1993, Masuda et al. (Masuda et al. 1993) dispersed Al_2O_3 nanoparticles of 13 nm in diameter into water with a volume fraction up to 4.3%, and obtained an enhancement in thermal conductivity of 30%. Eastman et al. (Eastman et al. 1996) also reported an enhancement of 30% in thermal conductivity in water suspensions of Al_2O_3 nanoparticles with an average diameter is 33 nm, at a volume fraction of 5%. Wang et al. (Wang et al. 2003b) studied the effects of synthesis process on the thermal conductivity of water based nanofluids containing Al_2O_3 nanoparticles. They found the dispersion techniques have no obvious effect on the measured thermal conductivity enhancements, while the addition of polymeric surfactants would decrease the thermal

conductivity. The reason is that although the addition of surfactants makes nanoparticles better dispersed, polymer molecules coating onto the surface of nanoparticles actually increase the interfacial thermal resistance.

Besides Al_2O_3, CuO is another extensively investigated oxide due to its higher thermal conductivity and easy availability. Eastman et al. (Eastman et al. 1996) studied the thermal conductivity enhancement of water dispersions of 36nm CuO nanoparticles, and found the enhancement increase is linearly proportional to the particle concentration. The thermal conductivity enhancement was measured as approximately 60% at a CuO nanoparticle concentration of 5 vol.%, significantly higher than the 30% enhancement measured in Al_2O_3-in-water nanofluids at the same concentration. This is due to the fact that CuO has a higher intrinsic thermal conductivity than that of Al_2O_3. Lee et al. (Lee et al. 1999) also obtained similar results with their nanofluids of CuO particles in both water and ethylene glycol. They found greater enhancements in CuO nanofluids than those in Al_2O_3 nanofluids.

TiO_2 nanoparticles have also been used in nanofluids. Murshed at al. (Murshed et al. 2005) measured the thermal conductivity of aqueous nanofluids containing both spherical and cylindrical TiO_2 nanoparticles. He found that nanofluids containing 15 nm spherical nanoparticles showed slightly lower enhancements than those containing 40 nm by 10 nm nanorods. As high as 33% enhancement was achieved in nanofluids containing 5 vol.% of TiO_2 cylindrical nanorods,, much higher than that predicted by HC model. Pak and Cho (Pak and Cho 1998) dispersed 27nm TiO_2 nanoparticles into water to make nanofluids. The thermal conductivity enhancement was measured to be 10.7% at a TiO_2 concentration of 4.35%, much lower than the 32% enhancement of Al_2O_3 nanofluids at

the same concentration of solid particles. The reason is that thermal conductivity of Al_2O_3 is higher than that of TiO_2. The maximum measured thermal conductivity enhancement for nanofluids containing metal oxide nanoparticles has been summarized in Table 2-1.

Table 2-1 Summary of maximum measured thermal conductivity enhancement for nanofluids containing metal oxide nanoparticles. The base fluids used are water, ethylene glycol and mineral oils

Reference	Base fluid	Nanoparticles and Diameter	Maximum Concentration (vol.%)	Maximum Enhancement in k (%)
Masuda (Masuda et al. 1993)	Water	Al_2O_3, 13 nm	4.3	30
Eastman (Eastman et al. 1996)	Water	Al_2O_3, 33 nm	5	30
Pak (Pak and Cho 1998)	Water	Al_2O_3, 13 nm	4.3	32
Wang (Wang et al. 1999)	Water	Al_2O_3, 28 nm	4.5	14
Wang (Wang et al. 1999)	Ethylene Glycol	Al_2O_3, 28 nm	8	40
Wang (Wang et al. 1999)	Pump Oil	Al_2O_3, 28 nm	7	20
Wang (Wang et al. 1999)	Engine Oil	Al_2O_3, 28 nm	7.5	30
Lee (Lee et al. 1999)	Water	Al_2O_3, 24.4 nm	4.3	10
Lee (Lee et al. 1999)	Ethylene Glycol	Al_2O_3, 24.4 nm	5	20
Das (Das et al. 2003c)	Water	Al_2O_3, 38 nm	4	25
Xie (Xie 2002)	Water	Al_2O_3, 60 nm	5	20
Xie (Xie 2002)	Ethylene Glycol	Al_2O_3, 60 nm	5	30
Xie (Xie 2002)	Pump Oil	Al_2O_3, 60 nm	5	40
Prasher (Prasher et al. 2005)	Water	Al_2O_3, 10 nm	0.5	100
Krishnamurthy (Krishnamurthy et al. 2006)	Water	Al_2O_3, 20 nm	1	16
Eastman (Eastman et al. 1996)	Water	CuO, 36 nm	5	60
Lee (Lee et al. 1999)	Water	CuO, 18.6 nm	4.3	10
Lee (Lee et al. 1999)	Ethylene Glycol	CuO, 18.6 nm	4	20
Wang (Wang et al. 1999)	Water	CuO, 23 nm	10	35
Wang (Wang et al. 1999)	Ethylene Glycol	CuO, 23 nm	15	55
Liu (Liu et al. 2006)	Ethylene Glycol	CuO, 25 nm	5	22.4
Das (Das et al. 2003c)	Water	CuO, 28.6 nm	4	36
Pak (Pak and Cho 1998)	Water	TiO_2, 27 nm	4.35	10.7
Murshed (Murshed et al. 2005)	Water	TiO_2, 15 nm	5	33

Metallic nanoparticles have much higher thermal conductivity than oxides, therefore theoretically much lower concentrations of metallic nanoparticles is needed in order to achieve the same level of thermal conductivity enhancement, or at the same concentration of nanoparticles, much higher enhancement can be obtained than that in those oxide nanofluids. Though not so many studies were conducted on nanofluids containing metallic nanoparticles as those on nanofluids containing oxides, the results have already shown more encouraging results, for example, up to 45% enhancement in thermal conductivity has been observed through the addition of less than 0.055 vol.% of 35 nm Cu particles into pump oil (Eastman et al. 1996). Eastman et al.(Eastman et al. 2001) also found 40% thermal conductivity enhancement in EG containing less than 0.3 vol.% Cu nanoparticles. Xuan et al. (Xuan and Li 2000) prepared nanofluids by directly mixing Cu nanopowders with water and oils. The nanofluids they measured were much more concentrated than those measured by Eastman et al., however, the thermal conductivity enhancement is comparable. At a Cu nanoparticle concentration of 7.5 vol.%, they were able to obtain 75% and 45% enhancements in water and transformer oil based nanofluids, respectively.

Nanofluids containing gold and silver nanoparticles have also been produced and measured (Patel et al. 2003). The enhancement in the thermal conductivity has been observed to increase as temperature rises. At a temperature of 60ºC, the enhancement in thermal conductivity was found to be 8.8% in toluene nanofluids at a Au nanoparticle concentration of 0.011vol.%. Though Ag has a higher thermal conductivity than gold (429 W/m·K for Ag and 317 W/m·K for Au), Ag nanofluids exhibit smaller thermal conductivity enhancement than the Au nanofluids. The reason lies in that Ag

nanoparticles dispersed in water was an order of magnitude larger than gold nanoparticles dispersed in water and toluene. Hong et al. (Hong et al. 2006; Hong et al. 2005) dispersed 10 nm Fe nanoparticles into ethylene glycol and measured the thermal conductivity enhancement in order to study the effects of both ultrasonication time and storage time. An enhancement in thermal conductivity of approximate 18% was found at a concentration of 0.55 vol.%. It is much lower compared to the results of Eastman obtained in Cu nanofluids, and it is due the lower thermal conductivity of Fe. The maximum measured thermal conductivity enhancement for nanofluids containing metallic nanoparticles has been summarized in Table 2-2.

Table 2-2 Summary of maximum measured thermal conductivity enhancement for nanofluids containing metallic nanoparticles. The base fluids used are water, ethylene glycol and mineral oils

Reference	Base fluid	Nanoparticles and Diameter	Maximum Concentration (vol.%)	Maximum Enhancement in k (%)
Eastman (Eastman et al. 1996)	Pump Oil	Cu, 35 nm	0.055	45
Xuan (Xuan and Li 2000)	Water	Cu, 100 nm	7.5	75
Xuan (Xuan and Li 2000)	Transformer Oil	Cu, 100 nm	7.5	45
Eastman (Eastman et al. 2001)	Ethylene Glycol	Cu, 10 nm	0.2	40
Patel (Patel et al. 2003)	Toluene	Au, 15 nm	0.011	8.8
Patel (Patel et al. 2003)	Water	Au, 15 nm	0.00026	8.3
Patel (Patel et al. 2003)	Water	Ag, 70 nm	0.001	4.5
Hong (Hong et al. 2006; Hong et al. 2005)	Ethylene Glycol	Fe, 10 nm	0.55	18

The greatest thermal conductivity enhancement of nanofluids so far was observed in carbon nanotubes in PAO nanofluids (Choi et al. 2001). A thermal conductivity enhancement of up to 160% has been observed at a CNTs loading of 1 vol.%. The enhancement of thermal conductivity increases as a function of MWCNTs loading in a

strong nonlinear way, indicating that the interaction between individual tubes plays an important role in thermal transport. Theoretical and experimental research has already disclosed that CNTs have longitudinal thermal conductivities of more than 3000 W/m·K (Berber et al. 2000; Che et al. 2000; Ruoff and Lorents 1995), close to that of diamond and over an order of magnitude higher than that of oxides and metals. Combining with their low density (~0.2 g/cm^3), high aspect ratio and easy availability, CNTs seem to be attractive candidates used in nanofluid applications. Actually, CNTs have been used for decades in composites to increase the thermal conductivity of solid materials. For example, Biercuk et al. (Biercuk et al. 2002) reported a 70% thermal conductivity enhancement in their industrial epoxy by adding 1 wt % unpurified SWCNTs and they attributed this abnormal rise to the high thermal conductivity and the high aspect ratio of CNTs.

Table 2-3 Summary of maximum measured thermal conductivity enhancement for nanofluids containing carbon nanotubes. The base fluids used are water, ethylene glycol and mineral oils

Reference	Base fluid	CNT type	Maximum Concentration (vol.%)	Maximum Enhancement in k (%)
Choi (Choi et al. 2001)	PAO	MWCNTs	1	160
Xie (Xie et al. 2003)	Water	MWCNTs	1	6
Xie (Xie et al. 2003)	Ethylene Glycol	MWCNTs	1	12
Xie (Xie et al. 2003)	Decene	MWCNTs	1	20
Wen (Wen and Ding 2004b)	Water	MWCNTs	0.84	21
Yang (Yang et al. 2006)	PAO	MWCNTs	0.35	200
Assael (Assael et al. 2004; Assael et al. 2005)	Water	DWCNTs	1	8
Assael (Assael et al. 2004; Assael et al. 2005)	Water	MWCNTs	0.6	34
Liu (Liu et al. 2005)	Synthetic oil	MWCNTs	2	30
Liu (Liu et al. 2005)	Ethylene Glycol	MWCNTs	1	12.4

Some other researchers also studied nanofluids containing CNTs, based on oils, glycols or water; however, they have not found comparably extraordinary results as those of Choi's. The maximum measured thermal conductivity enhancement for nanofluids containing CNTs has been summarized in Table 2-3.

Even carbides have been used to synthesize nanofluids. Xie et al. (Xie et al. 2002) dispersed spherical SiC particles with an average diameter of 26 nm (SiC-26) and cylindrical SiC particles with an average diameter of 600 nm (SiC-600) into distilled water (DI-H_2O) and ethylene glycol (EG) separately at volume fractions up to 4.2 vol.%. For SiC-26 in DI-H_2O suspension, the thermal conductivity can be increased by about 15.8% at a volume fraction of 4.2%. For SiC-600 in DI-H_2O, the thermal conductivity can be increased by 22.9% at a volume fraction of 4%. It seems that the high aspect ratio of nanoparticles is conducive to the heat transfer in nanofluids, though this behavior needs to be explained.

According to research articles, it seems that particle materials, particle size, operating temperature, the thermal conductivity or even the pH value of aqueous base fluids have impact on the thermal conductivity enhancement in nanofluids. Das et al. (Das et al. 2003a; Das et al. 2003c) were the first group who studied the temperature dependence of thermal conductivity enhancement in nanofluids. By dispersing Al_2O_3 nanoparticles with a mean diameter of 38 nm in water, they made nanofluids with concentrations from 1 to 4 vol.% and then they measured the thermal conductivity of these nanofluids at varying temperatures from 21 ºC to 51 ºC. They found that as the temperature rose, the enhancement in thermal conductivity was also linearly increased depending on the concentration of nanoparticles. Xie et al. (Xie 2002) even reported that

the pH value of the base fluid as well as the nanoparticle size affected the thermal conductivity enhancement of Al_2O_3 in water, ethylene glycol, and pump oil nanofluids. It seems that the thermal conductivity enhancement decreases with increasing pH value and as the thermal conductivity of the base fluid increases, the enhancement decreases. Prasher et al. (Prasher et al. 2006b) found a maximum enhancement of 100% at 85 ºC for 10 nm Al_2O_3 nanoparticles in water at a concentration of only 0.5 vol.%, much higher than the results reported by other researchers and they attributed this surprising results to the small size of Al_2O_3 nanoparticles and the higher measurement temperatures. Another very interesting study was carried out by Patel et al. (Patel et al. 2003) by suspending naked and polymer monolayer-coated gold and silver nanoparticles of 10 to 20 nm in water and toluene. At extremely low concentrations of below 0.011% for gold and 0.001% for silver, they were able to demonstrate a 3% to 10% thermal conductivity enhancement and a strong temperature dependence of such enhancements as well.

Li and Peterson (Li and Peterson 2006) blended CuO and Al_2O_3 nanoparticles with area weighted diameters of 29 nm and 36 nm into distilled water at different volume fractions from 2% to 10%. Thermal transport properties were measured at temperatures from 27.5 ^oC to 34.7 ^oC. Their results showed that the thermal conductivity of nanoparticles, particle size, volume fraction and the temperature all had a significant impact on the effective thermal conductivity of the as-prepared nanofluids. At 34 ^oC, water suspension of 6 vol.% CuO nanoparticles showed enhanced thermal conductivity which is 1.52 times that of pure distilled water, while suspension of 10 vol.% Al_2O_3 nanoparticles increased the thermal conductivity by a factor of 1.3. Based on their results,

they suggested the thermal conductivity enhancement in nanofluid could be described by the following equation for Al_2O_3-in-water,

$$\frac{k_{EMT} - k_f}{k_f} = 0.764481\phi + 0.018688867T - 0.462147175 \quad (2\text{-}1)$$

or the following one for CuO-in-water,

$$\frac{k_{EMT} - k_f}{k_f} = 3.76108\phi + 0.017924T - 0.30734 \quad (2\text{-}2)$$

where T is the operating temperature.

Kumar's group (Kumar et al. 2004) has developed a comprehensive theoretical model to account for the thermal conductivity enhancement in nanofluids. The strong temperature dependence was modeled by taking the particle size, concentration and temperature into consideration. Theoretical predictions with their model agreed with the experimental data on thermal conductivity measurements of nanofluids.

2.2.2 Thermal Convection in Nanofluids

It should be noted that the enhancement in thermal conductivity alone is not sufficient to prove that nanofluids have improved thermal transport properties and the performance of nanofluids in convective environments is a stronger evidence to evaluate the nanofluids. Convection tests of nanofluid were firstly conducted in turbulent forced convective conditions. Eastman et al. (Eastman et al. 1996) reported a >15% increase in heat transfer coefficient in 0.9 vol.% CuO-in-water nanofluids compared to that of pure water without nanoparticles. More recently, Xuan and Li (Xuan and Li 2000; Xuan and Roetzel 2000) prepared water based nanofluids containing Cu nanoparticles and

measured the convective heat transfer coefficient. It was found that the addition of small amount (< 2 vol.%) of nanoparticles greatly improves the convective heat transfer in water within a Reynolds number range between 10,000 and 25,000. The Nusselt number of nanofluids containing 2 vol.% Cu nanoparticles shows a >39% increase compared to that of pure DI water. Further more, the Nusselt number of water-based nanofluids increases with the increasing particle loading and Reynolds number. The Dittus-Boelter correlation fails to describe the heat transfer coefficient of nanofluids. However, increased viscosity of nanofluids may have negative effect on convective heat transfer, for example, Pak and Cho (Pak and Cho 1998) found the convective heat transfer coefficient of water-based nanofluids containing 3 vol.% Al_2O_3 and TiO_2 was reduced by 12% compared to that of pure water.

Wen and Ding (Wen and Ding 2004a) investigated the laminar heat transfer at the entrance region of alumina-in-water nanofluids flowing through a tube. The viscosity of the nanofluid was estimated according to Einstein's formula. For nanofluids that contained 1.6 vol.% nanoparticles, the heat transfer coefficient was found to be enhanced by 41%. Similar to the Dittus-Boelter correlation in turbulent flows, the classical Shah correlation (thermal entry length solutions for the circular tube and parallel plates) fails to predict the convective heat transfer of nanofluids. Ding and Wen (Wen and Ding 2005a; Wen et al. 2005) investigated the convective heat transfer of CNTs nanofluids in the laminar flow region at a constant wall heat flux. The thermal conductivity of CNTs nanofluids increases with increasing CNTs loading and temperature.

Natural convection of nanofluids was less investigated compared to forced convection and pool boiling. However, it has begun to attract attention due to the

potential applications of nanofluids in MEMS cooling and electronic cooling. Due to the increased viscosity, natural convection in nanofluids usually shows a decreased heat transfer coefficient (Putra et al. 2003). However, Khanafer at al. (Khanafer et al. 2003) showed enhancement of heat transfer coefficient of natural convection in nanofluids containing Cu nanoparticles. The reason is due to the enhanced thermal dispersion effect by random motion of nanoparticles, and as Xuan and Roetzel (Xuan and Roetzel 2000) have pointed out, thermal dispersion was a major mechanism of heat transfer in flowing nanofluid, similar to the thermal conductivity enhancement of "static" nanofluids.

2.2.3 Pool Boiling in Nanofluids

Inspired by the thermal conductivity enhancement in nanofluids, Das et al.(Das et al. 2003a; Das et al. 2003b) conducted an experimental study of pool boiling of Al_2O_3-in-water nanofluids on a horizontal tube with large diameter (20mm). They showed a deterioration of the pool boiling performance of nanofluids with increasing particle loading and attributed this deterioration of the pool boiling not to the change of fluid properties, but to the change of tube surface characteristics by nanoparticles trapped on the rough surface. You et al. (You et al. 2003) found an unprecedented three-fold increase in Critical Heat Flux (CHF) in Al_2O_3 nanofluids over pure water at a mass fraction of nanoparticle as low as 10^{-5}. Compared to the boiling in pure water, the average size of bubbles increased while the frequency of bubbles decreased significantly. Vassallo et al. (Vassallo et al. 2004) confirmed You's results in nanofluids containing SiO_2. Two to three-fold increases in CHF was observed. Similar results have been observed by Bang and Chang in water based alumina nanofluids. Later on, Bang and Chang (Bang et al. 2005a; Bang et al. 2005b; Bang and Heung Chang 2005) obtained

similar results from their pool boiling studies in Al_2O_3-in-water nanofluids. A 200% increase in CHF was observed on the measured pool boiling curves of nanofluids.

Pool boiling characteristics of nanofluids have so far been extensively investigated and it turns out that the addition of a small amount of nanoparticles to fluids is an effective way to dramatically increase the CHF. Studies of CHF of pool boiling in nanofluids have established that,

1. Significant CHF enhancement up to 200% has been found in nanofluids containing different nanoparticles, such as silicon, aluminum and titanium oxides;
2. Significant CHF enhancements occur even at extremely low nanoparticle loading, typically less than 1 vol %;
3. Nanoparticles settle out from the nanofluids to form a porous layer on the surface during nucleate boiling.

The change of CHF has been argued to be due to a possible surface coating mechanism that may change the nucleation site density (Arik et al. 2007; Bang et al. 2005a).

2.2.4 Theoretical Models of the Thermal Transport in Nanofluids

Since Choi and Eastman found the so-called "anomalous" increase in thermal conductivity of nanofluids, efforts have been made to seek the causes and mechanisms behind. Many propositions, including the Brownian motion of nanoparticles, the ordered interfacial layering of liquid molecules, clustering of nanoparticles, have been tested. The traditional Effective Medium Theory (EMT) used to explain the thermal conductivity enhancement of slurries and liquid suspensions was derived by Maxwell. Maxwell

assumed a very dilute suspension of spherical particles by neglecting the interactions between particles and then he solved Laplace equations for the temperature field beyond the particles in two equivalent ways: 1) Assume a large sphere containing all the spherical particles with an effective thermal conductivity k_{eff} embedded in the base fluid with thermal conductivity k_f ; or 2) assume all the spherical particles with a thermal conductivity k_p embedded in the base fluid with a thermal conductivity k_f. He then was able to get two equivalent equations and by equating these two equations, Maxwell obtained the effective thermal conductivity of the suspension. Maxwell's model was adopted by Hamilton and Crosser and later these EMT theories were modified by including the effects of particle shape, particle distribution, high particle concentrations, contact resistance and particle interactions (Granqvist and Hunderi 1978; Hasselman and Johnson 1987; Jeffrey 1973; Rayleigh 1892; Xue 2000). However, Maxwell's theory and modified EMT theories fail to predict the thermal conductivity of nanofluids, as well as the dependence of thermal conductivity enhancement on the interface between the particles and liquid, the size of the particles and the temperature, while all these factors have been considered to be important factors by Putra , Das and Ding et al.(Das et al. 2003c; Ding et al. 2006; Putra et al. 2003). The Maxwell and Hamilton-Crosser models assume a diffusive heat transfer in both the nanoparticles and the base fluids, and they did not take nanoparticles motions and interactions into account. A more detailed, atomic-level understanding of the mechanisms is necessary, as well as versatile models that can accurately predict the behavior of nanofluids.

Keblinski et al. (Keblinski et al. 2005; Keblinski et al. 2002) proposed four possible mechanisms for the thermal conductivity enhancement in nanofluids: 1) ordered layering

of the liquid molecules at the liquid/nanoparticle interface, 2) Brownian motion of nanoparticles, 3) the effects of clustering of nanoparticles, and 4) the nature of heat transport in nanoparticles. It has been known that liquid molecules in the proximity to a solid surface form layered structure. Because they are in an intermediate physical state between solids and liquids, the ordered liquid layers are expected to have a higher thermal conductivity than the bulk liquid. Based on these theories, in 2003, Yu and Choi (Yu et al. 1999a; Yu et al. 1999b; Yu and Choi 2003) modified the Maxwell equation by including the effect of the ordered liquid layers for the description of thermal conductivity of nanofluids. This theory can also be used for nanofluids containing nonspherical particles. Yu and Choi also derived an equation to predict the effective thermal conductivity for nanometer-scaled ellipsoid or shell-in-water nanofluids based on modified Hamilton-Crosser equation (Yu and Choi 2004).

Due to their tininess, Brownian motion of these nanoparticles has been considered as a potential factor of the enhanced thermal conductivity. Wang et al. (Wang et al. 2003a; Wang et al. 2003b) already attributed the enhancement to particle motion, surface action and electro-kinetic effects. Xuan (Xuan and Li 2003; Xuan et al. 2003) modified the Maxwell equation according to this Brownian motion assumption. Jang and Choi (Jang and Choi 2004) developed another dynamic model and took into account the micro-convection induced by the random motion of nanoparticles. By considering the Brownian motion of nanoparticles as a correction factor, Prasher (Prasher et al. 2005; Prasher et al. 2006a) developed a modified Maxwell equation to include both the motion of particles and the contact resistance at the surface of nanoparticles.

In nanofluids, though they are well dispersed, nanoparticles usually form structures of loosely bounded clusters or aggregates. These structures act like local percolation structures, providing a short path for heat transfer, and may contribute to the effective thermal conductivity enhancement of nanofluids. Wang et al. (Wang et al. 2003a) investigated the effect of nanoparticle aggregation and introduced a cluster radius distribution function *n(r),* so that he could develop a modified Maxwell equation to model the thermal conductivity of Al_2O_3-in-water nanofluids. Prasher et al. (Prasher et al. 2006b) argued that the aggregation of nanoparticles could play an important role in the pure thermal conduction phenomenon of nanofluids. Based on these models, it seems that nanoparticle clusters and aggregates structures in nanofluids contribute to the thermal transport; however, large clusters tend to settle out from the base fluids and therefore decrease the thermal conductivity enhancement.

2.3 Viscosity

Viscosity of nanofluids is less investigated than thermal conductivity, however, the rheological properties of liquid suspensions had been studied since Einstein (Einstein 1906). The viscosity of a liquid suspension of hard spheres can be predicted according to the Einstein equation as,

$$\mu_{nf} = \mu_f (1 + 2.5\phi) \tag{2-3}$$

where μ_f is the viscosity of base fluids and ϕ is the volume fraction of solid dispersed particles. This equation holds only the suspension is dilute, i.e., the volume fraction of solid particles ϕ is not more than 0.03, when the interactions between solid particles are negligible. With increasing particle concentration, the flow around one particle begins to

be affected by other particles in neighborhood and the assumption does not hold any more. Solid particles then experience hydrodynamic interactions and the viscosity is not only linearly dependent on the particle concentration ϕ but also on some higher orders ϕ^2, ϕ^3, ….This effect of hydrodynamic interactions on viscosity of suspensions was studied by Batchelor (Batchelor 1976; Batchelor 1977), and he concluded that the coefficient of the second-order term was 6.2, that is,

$$\mu_{nf} = \mu_f (1 + 2.5\phi + 6.2\phi^2 + ...) \tag{2-4}$$

This equation enables the calculation of the viscosity of suspensions at a particle concentration up to 10 vol.%.

Pak and Cho (Pak and Cho 1998) firstly measured the viscosity of their Al_2O_3-in-water nanofluids as a function of shear rate and concentration. The Al_2O_3 nanoparticles have a average diameter of 13 nm and the concentration is up to 10 vol.%. It is observed that nanofluids show a Newtonian behavior, i.e., the viscosity is independent of the shear rate and the maximum viscosity of nanofluids is up to 300 times higher than that of the base fluid. The measured viscosities of nanofluids are in far excess of those predicted by Batchelor equation. Wang et al. (Wang et al. 1999) only observed a 90% increase in viscosity in same Al_2O_3 in water nanofluids with similar concentrations and particle dimensions. Though Wang et al. measured the viscosity of Al_2O_3 nanofluids and did not find any non-Newtonian effect, many nanofluid systems show non-Newtonian behavior, unlike the corresponding base fluids. Das et al. (Das et al. 2003a) measured the viscosity of water based nanofluids containing Al_2O_3 nanoparticles and they observed slightly change in viscosity as the shear rate increased and exhibited Newtonian behavior. They also investigated the temperature dependence of the viscosity and found similar to that of

base fluids. The maximum viscosity of nanofluids was found in nanofluid at highest particle loading and lowest temperature. Kwak and Kim (Kwak and Kim 2005) dispsered 12 nm CuO nanoparticles into EG and conducted viscosity measurements. They found as the concentration increased, the viscosity of nanofluids changed from Newtonian to shear thinning. For nanofluids with a CuO concentration of 1 vol.%, the viscosity decreases by two orders of magnitude as the shear rate increases from 0.01 sec-1 to 1000 sec-1. Kulkarni et al (Kulkarni et al. 2006) observed the same shear thinning behavior in their Cuo-in-water nanofluids. As for carbon nanotubes nanofluids, Ding et al (Ding et al. 2006) dispersed MWCNTs in water and found similar results in these nanofluids to those of spherical nanoparticle suspensions. In fact, the shear thinning behavior of CNTs nanofluids was more drastic than that of spherical nanoparticle nanofluids. Davis et al. (Davis et al. 2004) found similar shear thinning in the viscosity of CNTs nanofluids and when they measured the viscosity of nanofluids as a function of the CNTs concentration, they found a local maximum value and a local minimum minimum. This phenomenon was explained by the phase behaviors of the Brownian rigid rods in nanofluids. At the beginning, as the volume fraction of CNTs increases, the nanofluids transit from a dilute regime in which the nanotubes do not interact with each other to a liquid crystal phase. That is, as the concentration of carbon nanotubes increases, interactions between nanotubes begin to constraint the motion of tubes, causing an increase in viscosity. Further increase in concentration leads the nanofluid system to transit from biphasic system to a solely liquid crystal system, and this occurs between the local maximum and the local minimum of viscosities. However, if the concentration continues to increase, the viscosity will increase rapidly from the local minimum point.

Though Einstein-Batchelor correlation is a well developed model that has been extensively accepted for calculating the viscosity of a liquid suspension for the concentration up to 10 vol.%, there are other accurate correlations which includes the temperature dependence of the nanofluid viscosity. For example, White (White 1991) correlation,

$$\ln \frac{\mu_{nf}}{\mu_0} \approx a + b\left(\frac{T_0}{T}\right) + c\left(\frac{T_0}{T}\right)^2 \tag{2-5}$$

where μ_{nf} is the viscosity of nanofluids, T is the operating temperature, μ_0 and T_0 are reference values, while a, b, and c are dimensionless coefficients which can be derived by fitting the experimental data.

This model has been used by Kulkarni et al. (Kulkarni et al. 2006)to fit their experimental results and good agreement was found. A more robust correlation has been used by Kulkarni that did not require the coefficients to be estimated through fitting experimental data, but instead to be calculated according to the concentration of solid particles. The more robust correlation is given as,

$$\ln \mu_{nf} = a\left(\frac{1}{T}\right) - b \tag{2-6}$$

$$a = 20587\phi^2 + 15857\phi + 1078.3$$
$$b = -107.12\phi^2 + 53.548\phi + 2.8715$$

In addition to these semi-empirical mathematical correlations, Phelan et al. (Phelan et al. 2005) are making efforts to model the rheological properties of nanofluids and describe the importance in terms of designing new nanofluids. They adopted a Brownian dynamics simulation method to model the viscosity of water and EG based nanofluids

containing 28 nm Al_2O_3 nanoparticles and compared their data to the experimental data. Their simulation is in good agreement with the experimental results. The simulation also predicts that for nanofluids containing Al_2O_3 nanoparticles with an average diameter of less than 30nm, the enhancement in thermal conductivity is greater than the enhancement in viscosity. If the diameter of the dispersed nanoparticles is further reduced, greater enhancement in thermal conductivity can be realized.

2.4 Applications of Nanofluid

Nanofluids have experimentally and theoretically been shown to possess improved heat transport properties and higher energy efficiency in a variety of thermal exchange systems for different industrial applications, such as transportation, electronic cooling, military, nuclear energy, and space, etc.

As for transportation, mixture of ethylene glycol and water is almost a universally used vehicle coolant due to its lowered freezing point for anti-freezing as well as the elevated boiling point. However, thermal conductivity of ethylene glycol is relatively low compared to that of water. At the same time, engine oils are even much worse heat transfer fluids than ethylene glycol in thermal transport performance. The addition of nanoparticles and nanotubes to these coolants to form nanofluids can increase the thermal conductivity, and has the potential to improve the heat exchange rates and fuel efficiency. The improvements can be used to reduce the size of cooling systems or remove more heat from the vehicle engine exhaust by keeping the same cooling system. Tzeng (Tzeng et al. 2005) has conducted research to study the effects of nanofluids in the cooling of automatic transmission. In his research, CuO (4.4 wt %) and Al_2O_3 (4.4 wt %)

nanoparticles and antifoam agents were dispersed into transmission fluid and then the transmission fluid was used in a real-time four wheel automatic transmission. The results showed that by using nanofluids, more heat was removed from the transmission system and the automatic transmission can be kept at lower temperature distribution at both high and low rotating speeds. Gosselin and Da Silva (Gosselin and Silva 2004) carried out an investigation on the optimization of particle loading in attempt to maximize the thermal transport performance of nanofluids with appropriate constraint conditions. They found that when the particle loading was low, the improvement of heat transfer rate is small, while more nanoparticles were added, the increase in viscosity led to large shear stresses and then larger pumping power is necessary. However, we can still maximize the heat transfer rate with a constant pumping power by setting an appropriate particle loading.

Power dissipation of IC and microelectronic components has dramatically increased recently. Better thermal management and cooling fluids with improved thermal transport properties are needed. Nanofluids have been considered as the working fluid in heat pipes for electronic cooling applications (Tsai et al. 2004). In a most recent study, Ma et al investigated the effect of nanofluids on the heat transport capability of an oscillating heat pipe. A nanofluid at a nanoparticle loading of 1vol% have show to be capable to reduce the temperature difference between the evaporator and the condenser from 40.9 ^{o}C to 24.3 ^{o}C. Chein and Huang (Chein and Huang 2005) numerically tested the performance of nanofluids as coolants in silicon microchannels. The nanofluids they used were water suspensions of Cu nanoparticles at various particle loadings. They found the performance of the microchannel heat sink was greatly improved due to the increased thermal conductivity and thermal dispersion effects, as well as that the presence of nanoparticles

in water did not cause too much pressure drop due to the small volume fraction of solid particles.

Military equipments dissipate large amounts of heat and consequently require and high-heat-flux cooling solutions having high cooling capacity up to the tens of MW/m^2. Nanofluids have the capability to provide the required cooling capacity in such applications as well as in other military systems, including no limitation military vehicles, submarines and high-power lasers. Nanofluids for military applications sometimes involve multifunctional nanofluids by adding thermal storage materials (PCMs) or energy harvesting materials through chemical reactions. The past two decades have witnessed the performance of IC chips increase exponentially and millions or even more transistors are squeezed onto a tiny chip. More heat needs to be removed per unit area dissipated by the electronic components. Koo and Kleinstreuer (Koo and Kleinstreuer 2005) had numerically investigated the heat transfer of micro heat sinks using two types of nanofluids, i.e., CuO nanoparticles in water and ethylene glycol. You at al. (You et al. 2003) and Vassalo at al. (Vassallo et al. 2004)reported drastic increase in the critical heat flux (CHF) in pool boiling of nanofluids compared to base fluids. This characteristic of nanofluids may be used in electronic cooling for space applications.

Besides the applications in cooling and thermal management, nanofluid technology can be used to better oils and lubricants. Recent nanofluid research demonstrates the potential of adding nanoparticles into lubricants to improve the tribological properties, such as load-carrying capacity, wear resistance and friction reduction between the mechanical components in motion. It has been verified by experimental results that the addition of surface-modified nanoparticles can be easily dispersed into lubricants to form

stable nanofluids and are effective in reducing friction and improving load-carrying capacity.

More research work is still needed for the production, the experimental measurements and the mechanism understanding of nanofluids. The challenge in production of nanofluids is to develop new methods to cost-effectively mass produce nanofluids at an industrial-scale for commercial applications. In ideal case, a method that does not need vacuum system and show capabilities to provide continuous fluid feed and nanofluid extraction is the potential candidate.

2.5 Summary

More than ever before, cooling is one of the most pressing challenges of many technologies nowadays. Many efforts have been made trying to disperse nanoparticles into HTFs to make nanofluids with enhanced thermal transport properties. Nanoparticles of oxides and metals, carbon nanotubes and other nanostructures have been used. Thermal conductivity, heat transfer coefficient in convective environments, and viscosity of many nanofluids have been investigated. Experimental and theoretical studies have shown that if prepared properly, nanofluids have attracting characteristics that make them ideal for cooling systems. Their improved thermal transport properties allows for the dissipation of more thermal energy even by using less coolant. Engine oils, automatic transmission fluids, fluorocarbons, and other synthetic heat transfer fluids all possess poor heat transfer capabilities and so they could benefit from the high thermal conductivity offered by nanofluid techniques.

Effective Medium Theories are successful for characterizing the thermal conduction behaviors in liquid suspensions. Experiments on nanofluids, however, show conflicting behavior such as increasing thermal conductivity with decreasing nanoparticle size, saturation at higher volume fractions, and lack of correlation to the intrinsic thermal conductivity of the nanoparticles, and a relatively large thermal conductivity enhancement at low volume fractions. New mechanisms should be proposed to explain the thermal conductivity enhancement of nanofluids. Comprehensive theoretical models involving the effects of various factors, such as concentration, particle size, particle geometry, temperature, interactions of nanoparticles, etc., are necessary to describe the thermal conduction in nanofluids.

Heat storage capacity of HTFs is also an important property for better cooling performance. Conventional HTFs suffer not only from low thermal conductivity, but from low heat storage capacity. Nanoparticles that undergo phase transition can be used for the synthesis of novel nanofluids with improved both thermal conductivity and heat capacity. Due to the addition of solid particles, the viscosity of nanofluids is obviously increased. It seems important to control the viscosity of nanofluids by adding appropriate amount of nanoparticles with small diameters and by using effective nanofluid synthesis techniques.

Nanofluids are currently expensive, partly due to the difficulty in manufacturing nanofluids. Development of new synthesis methods is necessary to make nanofluids more affordable before they will see widespread applications.

3 Experimental Methods

3.1 Synthesis Approach

Nanofluids are synthesized by suspending nanoparticles, usually 1-100 nm in diameter, in conventional HTFs. The material of nanoparticles can be metals, non-metals and oxides possessing high thermal conductivities. Traditionally, nanofluids are prepared by dispersing pre-synthesized nanoparticles into fluids, and if necessary, an appropriate amount of surfactants is added to keep nanoparticles stable in the fluids. The range of potentially applicable combinations of nanoparticles and base HTFs is substantially extensive – metal, nonmetal nanoparticles and CNTs can be dispersed into water, glycols, oils and fluorocarbons. For the purpose of synthesizing stable nanofluids consisting of certain nanoparticles and a given fluid, methods for nanoparticle production, dispersion and nanofluid synthesis have been developed.

As has been reported in literature, nanoparticles, colloids and nanostructured catalyst have already been prepared with sonochemical method in liquid phases (Suslick et al. 1991; Suslick et al. 1996; Suslick and Nyborg 1990; Zhu et al. 2000). The sonochemical effects used in sonochemical synthesis method originates from the cavitation phenomenon, which is the process of formation, growth and collapse of microbubbles in a liquid when a large negative pressure is applied. The consequence of the collapse of these microbubbles is the release of intense local energy and then the development of hot spots in the liquid phases, which possess high temperature of about 5000 ℃, high pressure of over 1000 atm, and cooling rates in excess of 10^{10} K s^{-1}. These

hotspots provide unique microenvironments for chemical reactions. Nanoparticles of CdSe, Bi_2Te_3, Ag_2Te, PbSe, ZnS, as well as Fe_2O_3 ferrofliuds, have been reported to be produced successfully with sonochemical methods (Suslick 1991; Suslick and Price 1999).

At the same time, high-intensity emulsification methods can be used to disperse one liquid (dispersed phase) into another immiscible liquid (as continuous phase) to form nano-scaled droplets with the help of surfactants (Asua 2002; Xu et al. 2004). The sonochemical effects can break up the larger micro-scaled droplets to form much smaller nanometer-scaled droplets. Though they are thermodynamically metastable, nanodroplets can persist for several months or even years because they are well coated with surfactant molecules, which can prevent the coalescence of these nanodroplets (Tiarks et al. 2001). The dispersed phases, such as water, low-melting point alloys and metals, are essentially insoluble in the continuous phase, i.e., FC72 and PAOs, so a proper surfactant is needed. The insolubility of the dispersed phases in the base fluids can suppress the Ostawald ripening. The continuous phase contains excessive surfactants and when the droplets are ruptured by high-intensity shear, new surface areas of the formed nanodroplets are enabled to be coated by the excessive surfactant molecules in the continuous phase. High-intensity shear is a necessary in order to rupture the premixed microscale droplets into nanodroplets. The shear stress level must reach the Laplace pressure of nanodroplets, usually tens of atmospheric pressures.

Based on the high-intensity ultrasonication, we have recently developed a novel method for mass producing nanofluids by directly emulsifying low-melting-point metals into synthetic oils, i.e., polyalphaolefin (PAOs) (purchased from Chevron Philips

Chemicals Company LLC), and emulsifying water into fluorocarbons, such as FC-72 and FC-77 at the temperatures above the melting points of these metals and water. By employing proper surfactants, quality and stable nanofluids can be prepared via this one-step direct-emulsification method. The sonochemical effects are used as a source of high-intensity shear in the nanoemulsification method to produce nanodroplets in tens of nanometers. The nanodroplets undergo a phase transition and turn into solid nanoparticles when being cooled off to below their freezing points. The nanoparticles or nanodroplets of metals, alloys or water in the nanofluids are about 20~30 nm in diameter. The nanofluids keep stable and no precipitation was observed after the decreasing of temperatures to below the melting points of nanoparticles. Experimental set-up for this new mass production method of nanofluids is shown in Figure 3-1.

Nanofluid systems of different base fluid-nanoparticle combinations, such as water-in-FC72 nanofluids, PAO (synthetic engine oil) -based nanofluids containing gallium, Field's metal, Wood's metal and indium nanoparticles, and water-in-PAO nanofluids have been successfully prepared with this new mass production method. Some pictures of these nanofluids are shown in Figure 3-2 and Figure 3-3. TEM bright field (BF) images showing the as-prepared LMP metallic nanoparticles are given in Figure 3-4. Metallic nanoparticles are mostly spherical as shown in TEM BF images, due to the large surface tension of liquid metals. Liquid metallic nanodroplets tend to shrink and minimize the surface area in order to minimize the surface energy.

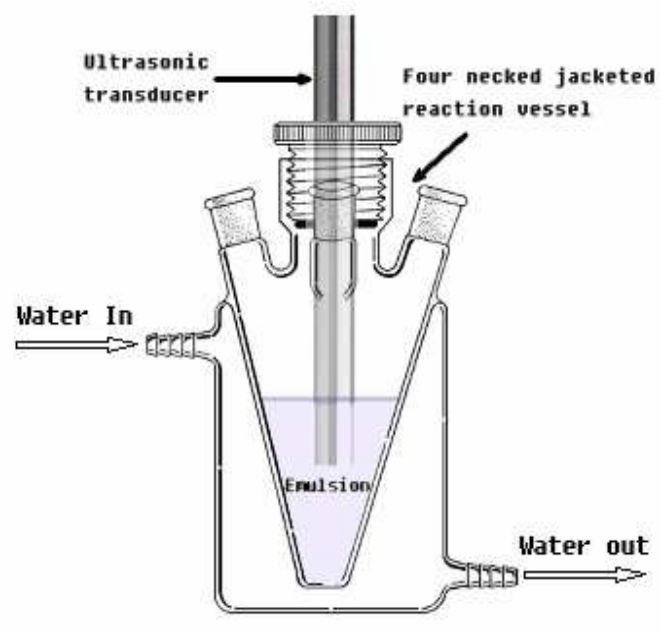

(a)

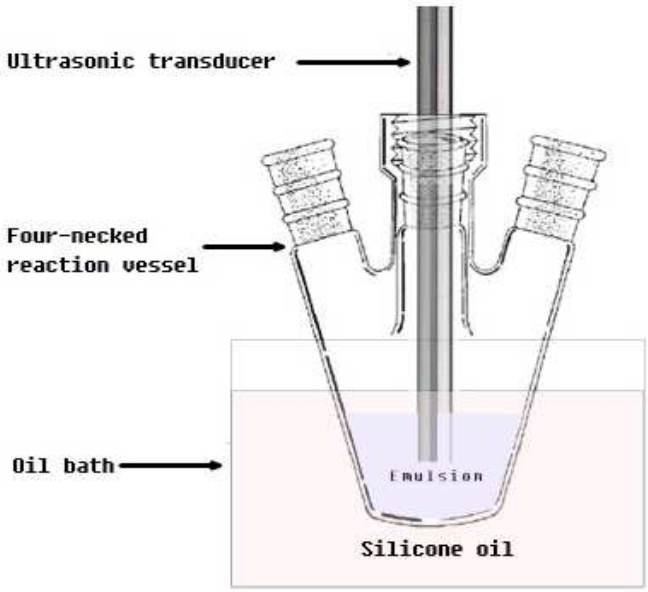

(b)

Figure 3-1 Experimental set-up of the one-step nanoemulsification method: (a) For water in oil nanoemulsions; (b) For LMP metals or alloys in oil nanoemulsions

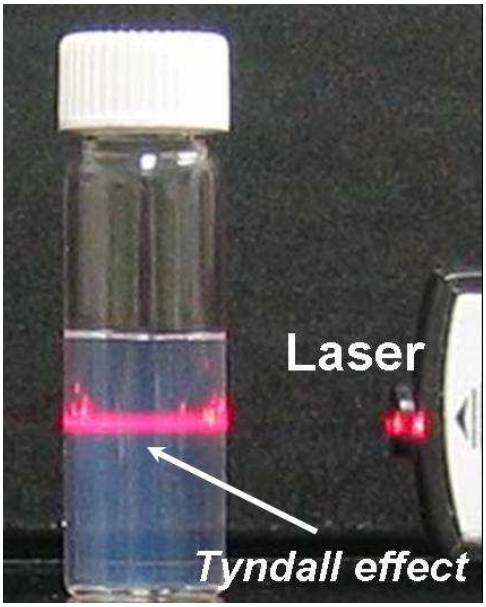

Figure 3-2 Water-in-FC72 nanofluid. When a laser beam passes through the nanofluid, the Tyndall effect (i.e. a light beam can be seen when viewed from the side) is observed

Figure 3-3 As-prepared nanofluids by using the nanoemulsification method at room temperature. From left to right are: gallium, Field's Metal, Wood's metal and indium nanoparticles in PAO nanofluids

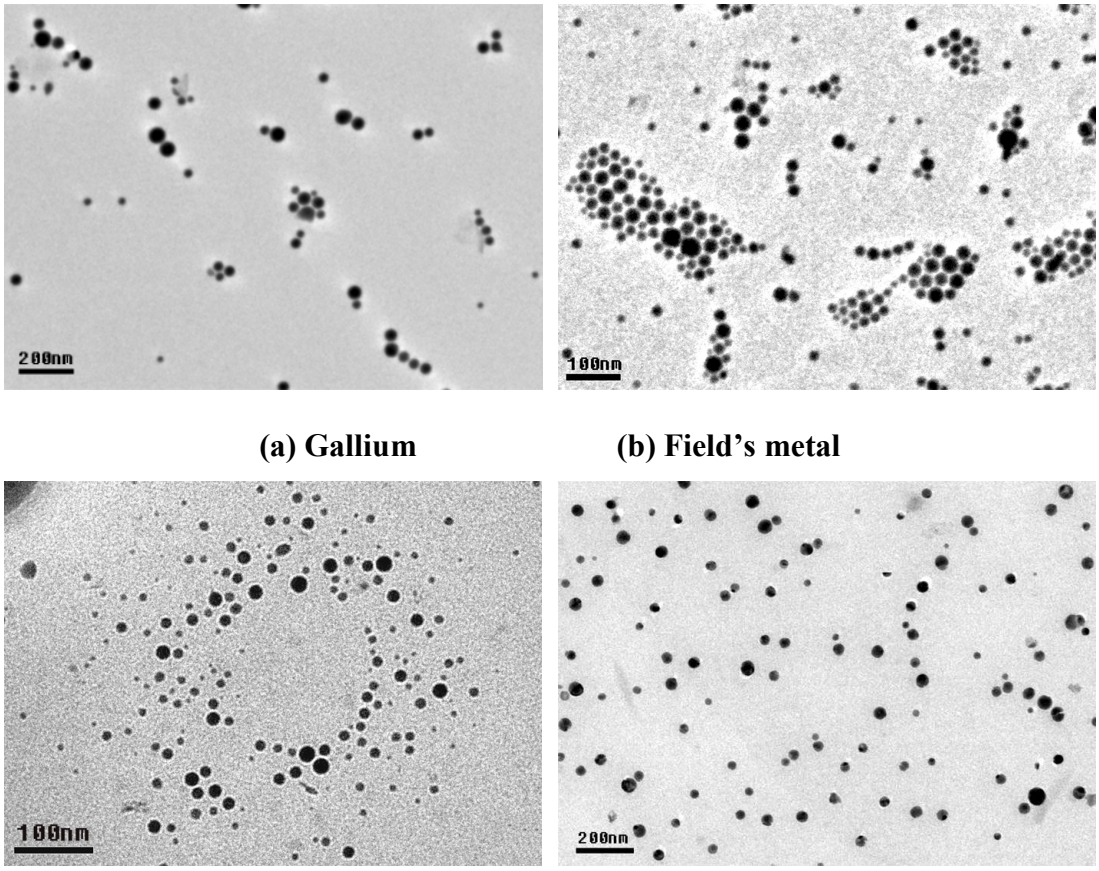

(a) Gallium **(b) Field's metal**

(c) Wood's Metal **(d) Indium**

Figure 3-4 TEM BF images of metallic nanoparticles. (a) gallium; (b) Field's metal; (c) Wood's metal, and (d) indium

3.2 Characterization of Nanofluid Systems

Characterization of nanofluid systems is composed of characterization of nanoparticles and characterization of nanofluids, since thermal transport properties of most conventional heat transfer fluids are already well known and do not need to be measured. The characterization of nanoparticles includes investigation of elemental compositions, determination of particle size and geometry, and characterization of particle microstructures. The characterization of nanofluids include investigation of nanofluid stability, measurement of mobility of nanoparticles in base fluids, measurement

of thermal conductivity, heat capacity and heat transfer coefficients, and measurement of viscosity. The chemical and the physical properties of nanoparticles and nanofluids are very important information for deepening the understanding of the mechanisms behind the anomalous increase in thermal conductivity of nanofluids, and, these properties are going to be used to evaluate the performance of the nanofluids as well as the potential applications of nanofluids.

3.2.1 Determination of Elemental Compositions

Elemental compositions of nanoparticles are determined by Energy dispersive X-ray spectroscopy (abbreviation: EDS or EDX). EDS is an analytical tool used mainly for characterization of chemical compositions of materials. The fundamental principle of EDS is that each element in the periodic table possesses a unique electronic structure and when a material is bombarded by accelerating incident electrons, the response of each element to these electromagnetic waves, for example, the wavelength of output characteristic X-rays, are unique. The information of characteristic X-rays thus can be used for chemical analysis. The quantity of surface coating materials and the extent of oxidation of nanoparticles can also be determined by EDS.

3.2.2 Investigation of Particle Size and Geometry

Transmission electron microscopy (TEM) is a straightforward method to observe the dimensions and geometry of nanoparticles. The main limitation of TEM observation of nanoparticles is that the viewing field of TEM is relatively small, which potentially raise the possibility that the region to be analyzed may not be

characteristic of the whole sample. Several (more than 6) different places are observed and averaged information is obtained and analyzed in order to overcome this drawback.

3.2.3 Microstructure Characterization

X-ray diffraction (XRD) and electron diffraction (ED) are two analytical techniques revealing information about the crystallographic structure. The reason for microstructure characterization is that the thermal conductivity is sensitive to the microstructure of materials. For nanoparticles having same elemental compositions but different microstructures, there is much difference in thermal conductivities. For example, single crystals have higher thermal conductivity than polycrystalline and amorphous materials.

3.2.4 Mobility of Nanoparticles

Dynamic light scattering (DLS) technique is used to measure the mobility of nanoparticles in nanofluids. Actually, dynamic light scattering can be used to determine the size distributions of these small particles in solution, which is called "hydrodynamic radius". A proper amount of surfactant maybe added when the nanoparticles are dispersed into base fluids and the surfactant molecules are tightly bound at the surface of nanoparticles, the "hydrodynamic radius" measured by DLS are different from the results of TEM. Theoretical results have been reported that the anomalous enhancement in thermal conductivity of nanofluids is attributed to Brownian motion. A Photocor-FC dynamic light scattering instrument with a laser light source having wavelength at 633 nm was used for the measurements at room

temperature. The scattering angle is 90°. The measured correlation function G(τ) is found to be related to the delay time τ as (Goldburg 1999; Yudin et al. 1997),

$$G(\tau) = \varepsilon * \exp(-\Gamma \tau) \tag{3-1}$$

where ε is a constant, Γ is the linewidth, which is proportional to the diffusion coefficient D_B of the droplets,

$$\Gamma = 2D_B q^2 \tag{3-2}$$

where the wave vector, $q = (4\pi n_r / \lambda)\sin\left(\frac{\theta}{2}\right)$, n_r the refractive index of the solvent, λ the laser wavelength and θ the scattering angle.

The linewidth Γ can be obtained by fitting the original data of DLS measurement, then the diffusion coefficient D_B is calculated according the above equation. The mean radius of interior water droplets can be obtained from the Stokes-Einstein equation,

$$r_p = \frac{k_B T}{6\pi\mu_f D_B} \tag{3-3}$$

where k_B is Boltzmann's constant, T is the temperature, and μ_f is the shear viscosity of the solvent.

3.2.5 Stability of Nanofluids

Although the stability of nanofluid is very important in order for practical application, the data of is limited on estimating the stability of nanofluids. UV–vis spectrophotometry has been used to quantitatively determine the colloidal stability of the dispersions (Jiang et al. 2003). Another method for the estimation of the stability

of nanofluids is to measure the volume of sediment vs. the sediment time. In this research, the stability of nanofluids is investigated through visual check. A vial of nanofluid sample is mounted onto a horizontal and stable surface; after a pre-set period of time, the liquid is carefully decanted, and the volume of the sediment is estimated. Due to the advanced dispersion technique used in preparation process and the addition of steric or ionic surfactants, nanofluids can keep stable for months without visible sediment.

3.2.6 Measurement of Viscosity

The viscosity of nanofluids is an important indication to evaluate the thermal transport properties of the nanofluids. In this dissertation, the viscosity of nanofluids will be measured with a Brookfield DV-I prime viscometer. Viscosity of nanofluids of different particle loadings is measured at different temperatures. Moreover, the viscosity of nanofluids is measured at different rotor RPMs to investigate if the nanofluids are Newtonian or non-Newtonian fluids.

3.2.7 Heat Capacity Measurement and Phase Change Characterization

Differential scanning calorimetry (DSC) is a powerful tool to measure the heat capacity of nanofluids. The difference in the amount of heat flow required for heating up a sample pan and reference pan are measured as a function of temperature. During the whole process, the sample and reference pans are maintained at nearly the same temperature throughout the experiment. The heat capacity of the reference pan is already known. By measuring the difference in heat flow, the heat capacity of the sample is obtained. If there are phase transitions happened in the sample pan, more or

less heat will need to flow to it than the reference to maintain both at the same temperature, so endothermal or exothermal peaks are shown on the DSC curves, corresponding to melting or freezing, respectively. The phase transition temperatures and latent heats are determined according to the DSC curves.

3.2.8 Thermal Conductivity Measurement

Hot-wire method is a transient dynamic technique for simultaneously measuring the thermal conductivity and the thermal diffusivity of materials. HTW is based on the measurement of the time-dependent temperature rise in a heat source, i.e. a hot wire, which has already been immersed in the fluid to be tested. The hot wire serves simultaneously as an electrical resistance heater and a resistance thermometer (Andersson and Backstrom 1976; Gross and Song 1996; Nagasaka and Nagashima 1981). The hot wires are fabricated extremely small in diameter (several to tens of microns) to approximate a simple one dimensional transient line-source of heat in an infinite medium as closely as possible in order to minimize the necessity of making corrections for the actual geometry. The hot wire temperature rise reaches usually up to 10ºC and the influence of convection on measurement is not negligible.

The 3ω-wire method was employed to measure the thermal conductivity of liquids. Most of the published thermal conductivity data on the nanofluids were obtained using the hot-wire method, which measures the temperature response of the metal wire in the time domain. The 3ω-wire method is actually a combination of the 3ω method and the hot-wire method. Similar to the hot-wire method, a metal wire with a length of L and a radius of r is suspended in a liquid acts as both a heater and a

thermometer, as shown in Figure 3-5. A sinusoidal AC current at frequency ω is passed through the metal wire (Borca-Tasciuc 2000),

$$I(t) = I_0 \cos(\omega t) \tag{3-4}$$

where I_0 is the amplitude of the sinusoidal AC current. The AC current acts as heating, which is a superposition of a DC source and a 2ω modulated heating source,

$$P(t) = I_0 R_E \cos^2(\omega t) = \left(\frac{I_0^2 R_E}{2}\right)_{DC} + \left(\frac{I_0^2 R_E \cos(2\omega t)}{2}\right)_{2\omega} \tag{3-5}$$

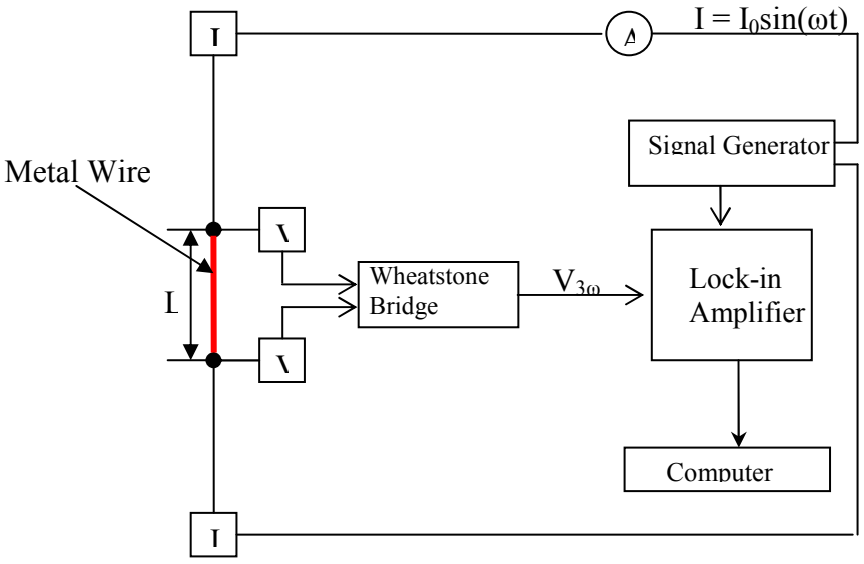

Figure 3-5 Experimental setup of 3ω-wire technique for thermal conductivity measurement of liquid

where R_E is the resistance of the metal wire under the experimental conditions, and it is a function of temperature. The corresponding temperature rise in the sample to be

measured is similar to the heat generation and is also a superposition of a DC component and a 2ω AC component,

$$T(t) = T_{DC} + T_{2\omega}\cos(2\omega t + \varphi) \tag{3-6}$$

where $T_{2\omega}$ is the amplitude of the AC temperature rise and φ is the phase shift induced by heating the thermal mass of the sample. The resistance of the wire depends on the temperature and there is a 2ω AC component in the resistance of the wire,

$$\begin{aligned} R_E(t) &= R_{E0}\left\{1 + C_{rt}\left[T_{DC} + T_{2\omega}\cos(2\omega t + \varphi)\right]\right\} \\ &= R_{E0}\left(1 + C_{rt}T_{DC}\right)_{DC} + \left(R_{E0}C_{rt}T_{2\omega}\cos(2\omega t + \varphi)\right)_{2\omega} \end{aligned} \tag{3-7}$$

in which $\boldsymbol{C_{rt}}$ is the temperature coefficient of resistance (TCR) for the metallic wire, $\boldsymbol{R_0}$ is the reference heater resistance at a reference temperature $\boldsymbol{T_0}$, and usually it is the bulk temperature of sample. The voltage across the metallic wire can be derived as,

$$\begin{aligned} V(t) = I(t)R_E(t) &= \left(I_0 R_{E0}\left(1 + C_{rt}T_{DC}\right)\cos(\omega t)\right)_{power} + \\ &\left(\frac{I_0 R_{E0} C_{rt} T_{2\omega}}{2}\cos(3\omega t + \varphi)\right)_{3\omega} + \left(\frac{I_0 R_{E0} C_{rt} T_{2\omega}}{2}\cos(\omega t + \varphi)\right)_{1\omega} \end{aligned} \tag{3-8}$$

In the above equation, the voltage across the wire contains the voltage drop due to the DC resistance of the wire at 1ω, and two new components proportional to the temperature rise in the wire at 3ω and 1ω. The 3ω voltage component

$V_{3\omega} = \left(\frac{I_0 R_{E0} C_{rt} T_{2\omega}}{2} \cos(3\omega t + \varphi) \right)_{3\omega}$ can be extracted by using a lock-in amplifier and then used to deduce the temperature rise amplitude at 2ω,

$$T_{2\omega} = \frac{2V_{3\omega}}{I_0 R_{E0} C_{rt}} \tag{3-9}$$

The frequency dependent temperature rise $T_{2\omega}$ is obtained by changing the frequency of the sinusoidal AC current at a constant applied voltage $V_{1\omega}$.

At the same time, the frequency dependent temperature rise $T_{2\omega}$ can be approximated as (Cahill 1990),

$$T_{2\omega} = \frac{P}{2\pi L k_f} \left[0.5 \ln\left(\frac{\alpha_f}{r^2} \right) - 0.5 \ln \omega + \eta \right] - i\left(\frac{P}{\pi L k_f} \right) = \frac{P}{\pi L k_f} f_{linear}(\ln \omega) \tag{3-10}$$

α_f is the thermal diffusivity and k_f is the thermal conductivity of the fluids. The temperature rise at frequency 2ω in the metal wire can be deduced by the voltage component at frequency 3ω as shown in equation (3-9) and the thermal conductivity of the liquid, *k*, is then determined by the slope of the 2ω temperature rise of the metal wire with respect to the frequency ω,

$$k_f = -\frac{P}{4\pi L} \left(\frac{\partial T_{2\omega}}{\partial \ln \omega} \right)^{-1} \tag{3-11}$$

where P is the applied electric power, ω is the frequency of the applied electric current, L is the length of the metal wire, and $T_{2\omega}$ is the amplitude of temperature oscillation at frequency 2ω in the metal wire.

The 3ω-wire method has several advantages over the traditional hot-wire transient method, such as: 1) the temperature oscillation can be kept small enough (below 1K, compared to about 5K for the hot-wire method) within the test liquid to retain constant liquid properties, 2) the background noises, such as temperature variation, have much less influence on the measurements due to the use of the lock-in technique. These advantages make the ω-wire method ideally suited for measuring the temperature dependent thermal conductivity of fluids.

4 Thermal Conductivity of Nanorods-in-oil Nanofluids

4.1 Introduction

Extensive studies have been conducted to investigate thermal transport properties of nanofluids in the past decade, and the improvement in thermal properties has been observed in many nanofluid systems. However, the temperature dependence of thermal properties has much less studied. Recently, two papers from the same group have reported two to four-fold increase in the thermal conductivity enhancement over a temperature range of 20-50^{o}C in nanofluids containing spherical oxide or metal nanoparticles (Das et al. 2003c; Patel et al. 2003). The observed strong temperature dependence of thermal conductivity enhancement was attributed to the Brownian motion of nanoparticles. But it remains to be undiscovered if this temperature-dependent behavior occurs in nanofluid containing non-spherical nanoparticles and if the particle Brownian motion plays a similar dominant role.

This chapter details the preparation and the thermal transport property measurements of Bi_2Te_3 nanorods-in-oil nanofluids. The thermal conductivity of nanofluids based on hexadecane oil containing Bi_2Te_3 nanorods has been measured over the temperature range from 20 ^{o}C to 50 ^{o}C. The Bi_2Te_3 nanorods with average diameter of 20 nm and average length of 170 nm were synthesized using the sonochemical technique, and then were dispersed into the hexadecane oil to form stable nanofluids. The 3ω-wire method was used to measure the thermal conductivity of the nanofluids in order to investigate the temperature dependence of thermal conductivity of the nanofluids. The thermal conductivity enhancement in the nanofluids containing Bi_2Te_3 nanorods has been

experimentally found to decrease with increasing temperature, about 6.1% at 20^{o}C and 3.9% at 50 ^{o}C, in contrast to the previous observation in nanofluids containing spherical metal or oxide nanoparticles. The contrary trend is attributable mainly to the large particle aspect ratio of nanorods and the decreasing thermal conductivity of Bi_2Te_3 nanorods as temperature rises. When the nanoparticle aspect ratio increases, the diffusive-conduction-based mechanism is expected to dominate the thermal conductivity enhancement of nanofluids.

4.2 Synthesis of Bi_2Te_3 Nanorods

The Bi_2Te_3 nanorods are prepared using the sonochemical method. In order to prepare Bi_2Te_3 nanorods, bismuth nitrate ($Bi(NO_3)_3$) and sodium tellurite ($NaTeO_3$) are used as precursors at a stoichiometric ratio of 2:3, while EDTA is added to the solution in order to control the growth, the size and the geometry of Bi_2Te_3 nanocrystals. At room temperature, bismuth nitrate and sodium tellurite are dissolved into DI water in the presence of EDTA to form a 200 ml mixture in which the concentrations of bismuth nitrate and sodium tellurite are 0.10mol/L and 0.15mol/L, respectively. The concentration of EDTA varies in different batches in order to get Bi_2Te_3 nanorods with different diameters and lengths. The PH value of the mixture is adjusted to around 10 by using NaOH solution. Then 12 ml hydrazine ($N_2H_4.H_2O$) is added into the mixture as reducing agent. Finally, the mixture is poured into a three-necked flask and is exposed to ultrasonic irradiation using a Ti horn (VCX 750, Sonics & Materials, Inc.), which is directly immersed into the solution by the depth of 3-5 cm. The power density of the Ti horn is 75W/cm^2 (adjustable) while the frequency is 20 KHz (fixed). The sealed flask is partly immersed in a circulating cooling water bath attempting to maintain the temperature of

the solution at ambient temperature. The solution is purged with Ar flow to remove the oxygen to prevent the nanocrystals from being oxidized. After being exposed to high-intensity ultrasonication for 10 minutes, black precipitate can be observed. The reaction steps and the formation process of Bi_2Te_3 nanocrystals in the sonochemical reduction can be summarized as,

$$N_2H_4 \cdot H_2O \leftrightarrow N_2H_5^+ + OH^-$$

$$N_2H_5^+ \leftrightarrow N_2 + 5H^+ + 4e^-$$

$$Bi^{3+} + 3e^- \rightarrow Bi$$

$$TeO_3^{2-} + 6H^+ + 4e^- \rightarrow Te + 3H_2O$$

$$2Bi + 3Te \rightarrow Bi_2Te_3 \downarrow$$

After 1 hour of ultrasonication, the reaction is stopped, and the resultant precipitate is filtered, separated and washed with DI water and ethanol for several times. The powder is collected and dried in vacuum oven at around 50℃. The TEM specimen is prepared by re-dispersing the nanoparticles to form a dilute suspension in ethanol and placing a drop of such suspension atop a carbon-coated copper grid.

Figure 4-1 shows the TEM BF image and electron diffraction (ED) patterns of Bi_2Te_3 nanorods. Bi_2Te_3 nanorods have a crystalline structure as determined by the ED patterns. The average diameter of Bi_2Te_3 nanorods is about 20 nm and the average length is about 170 nm, as shown in Figure 4-1.

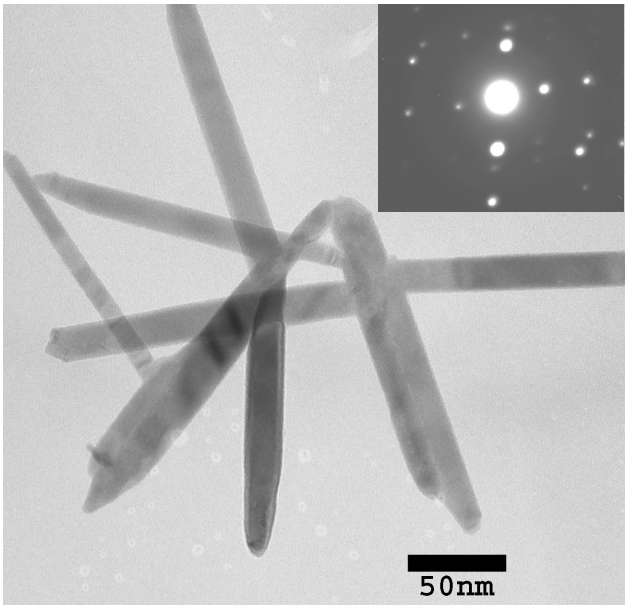

Figure 4-1 TEM BF image of Bi_2Te_3 nanorods produced with the sonochemical technique. The insert at top right corner is the electron diffraction pattern of the prepared Bi_2Te_3 nanorods. Image taken by a JEOL 4000FX transmission electron microscope

4.3 Preparation of Nanorods-in-Oil Nanofluids

The synthesis of Bi_2Te_3 nanorods using the sonochemical technique is only the first step. In the second step of nanofluid preparation, the Bi_2Te_3 nanorods are dispersed into the hexadecane oil with sonication to form stable nanofluids. In order to make the polar nanorods soluble in non-polar solvent to form stable colloids, nanorods should be coated with organic capping agents. The capping agents prevent the nanorods from agglomerating and coagulating. Oleic acid is then used as the capping agent in order to stabilize nanorods in hexadecane. Oleic acid has the formula of $CH_3(CH_2)_7CH=CH(CH_2)_7COOH$, in which the carboxyl can bind tightly onto the surface

of nanorods, while the carbon backbone extends to the solvent to make the coated nanorods soluble in the base fluid. A small amount of oleic acid is enough to improve the dispersion behavior, for example, in this experiment the concentration of oleic acid is 0.5 vol. %. The volume fraction of the Bi_2Te_3 particles in the nanofluids is 0.8%.

4.4 Thermal Conductivity Measurement

Most of previous studies on nanofluids focus on spherical nanoparticles (the ratio of the major axis to the minor axis, i.e. aspect ratio, =1) and long fibers such as carbon nanotubes or nanowires (aspect ratio 100~∞). It is thus expected that the nanofluids containing nanorods with moderate aspect ratio may exhibit different behaviors. The temperature dependence of thermal conductivity of nanofluids is evaluated in this experiment. The 3ω-wire method is used to measure the thermal conductivity of liquids. The thermal conductivity of the nanofluid, k_{nf}, is determined by the slope of the 2ω temperature rise of the metal wire, as shown in Figure 4-2,

$$k_{nf} = -\frac{P}{4\pi L}\left(\frac{\partial T_{2\omega}}{\partial \ln \omega}\right)^{-1} \qquad (4\text{-}1)$$

where P is the applied electric power, ω the frequency of the applied electric current, L the length of the metal wire, and $T_{2\omega}$ the amplitude of temperature oscillation at frequency 2ω in the metal wire.

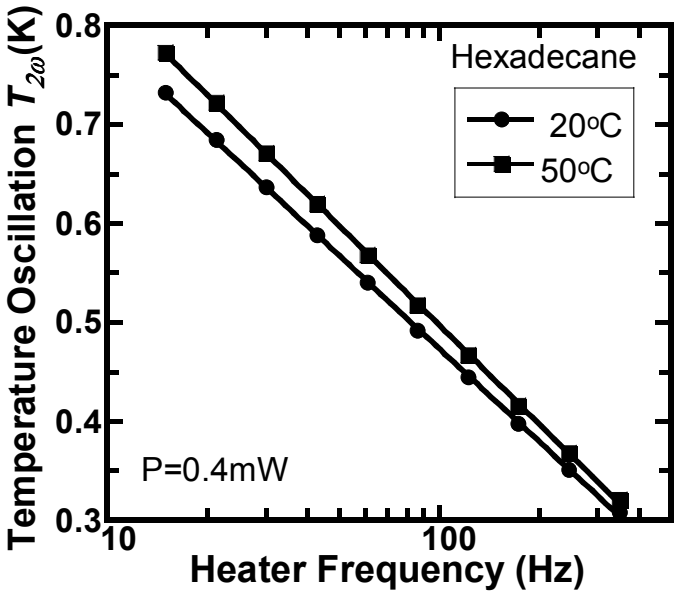

(a)

Figure 4-2 Measured amplitude of the temperature oscillation in the metal wire immersed in the pure hexadecane oil as a function of the frequency of the drive current

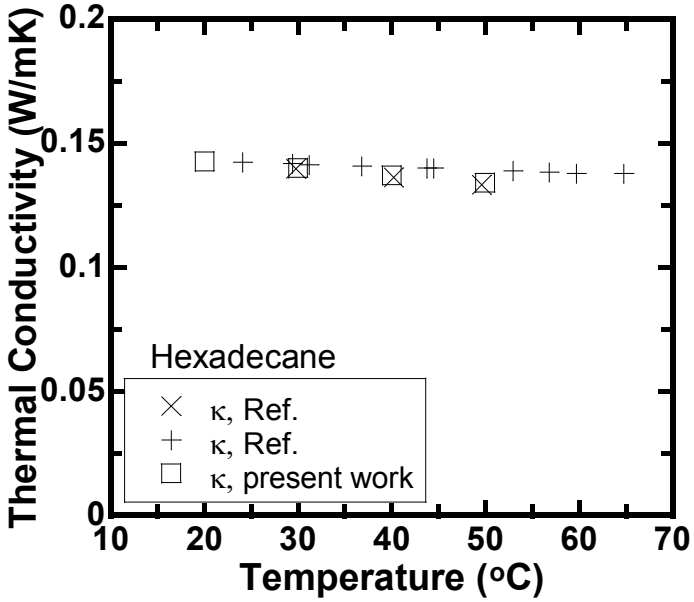

(b)

Figure 4-3 Comparison of the thermal conductivity of the pure hexadecane oil measured by the 3ω-wire technique to the literature data

Calibration experiments were performed for oil, fluorocarbon and water in order to guarantee the accuracy of measurements. Literature values of thermal conductivity of these three liquids were reproduced within an error of <1%. In the pure hexadecane oil, for example, the 2ω temperature oscillation of the metal wire vs the frequency is measured and plotted in Figure 4-3. The thermal conductivity of the hexadecane oil can be obtained using Eq.4-1, and the results are listed in Figure 4-3. It can be found that the measured data are in very good agreement with the literature data.

4.5 Temperature Dependence of Thermal Conductivity Enhancement

The thermal conductivity has been measured in the hexadecane oil with and without Bi_2Te_3 nanorods over a temperature range from 20°C to 50°C using the 3ω-wire method. The obtained thermal conductivity enhancement, as well as the prediction from the effective medium theory, is plotted in Figure 4.4. The thermal conductivity of this nanofluid was experimentally found to be 0.151W/mK at 20°C and 0.139W/mK at 50°C. The measured thermal conductivity enhancement decreases with increasing temperature, about 6.1% at 20°C and 3.9% at 50°C. The effective medium theory predicts a similar trend but slightly smaller values, which takes into account the effects of the particle thermal conductivity, but not the particle Brownian motion. The thermal conductivity of Bi_2Te_3 goes as $T^{-\alpha}$ (where α is 1.68~1.95 depending on the doping (Nolas et al. 2001)) in the moderate temperature range, possibly resulting in the observed trend of the thermal conductivity enhancement over the temperature range shown in Figure 4-4.

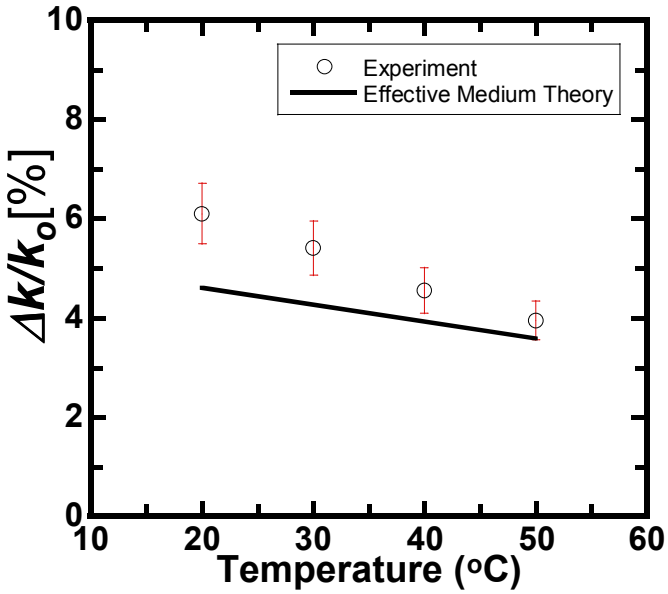

Figure 4-4 Thermal conductivity enhancement, $\Delta k / k_0$ as a function of temperature in nanofluids consisting of Bi_2Te_3 nanorods and hexadecane oil. The prediction by the effective medium theory is shown for comparison

4.6 Discussion

The trend of the temperature dependence of thermal conductivity measured in nanofluids in this study, however, is contrary to those observed by Das et al. in the nanofluids consisting of spherical metal or oxide nanoparticles dispersed in water (Das et al. 2003c; Patel et al. 2003). Das et al. measured the thermal conductivity of oxide nanofluids over a temperature range from 20 to 50 ^{o}C. They found the thermal conductivity enhancement increases rapidly with increasing temperature, and almost three fold increase, i.e., from 10% to 30%, in thermal conductivity has been observed in their alumina and CuO nanofluids. Lee et al. (Lee et al. 1999) obtained the similar results in Al_2O_3 and CuO nanofluids. Later on Pratel et al. (Patel et al. 2003) confirmed Lee's

results. Furthermore, Chon et al. (Chon et al. 2005) not only confirmed the temperature dependence, they also found the inverse particle-size dependence of the thermal conductivity enhancement in nanofluids by using water-based nanofluids containing alumina nanoparticles of three different sizes. All these findings indicate that the nanoparticle motion in nanofluids plays an important role in the thermal conductivity enhancement. The contrary trends observed in our Bi_2Te_3 nanofluids could be due to the difference in the particle aspect ratio, which should have important effects on both the particle Brownian motion and the diffusive heat conduction, as discussed below.

Nanoparticles in motion may act as "heat boats" to directly transport energy or as "stirrers" to induce convection to enhance the effective thermal conductivity in nanofluids. The Brownian motion can be characterized by the Brownian diffusivity D_B, which is given by for a prolate ellipsoid (Hunter 2001),

$$D_B = k_B T \Big/ 6\pi\mu_f \zeta K \tag{4-2}$$

where k_B is the Boltzmann constant, T the temperature in Kelvin, μ_f the dynamic viscosity of the liquid, ζ the equatorial semi-axis of the ellipsoid, and K is the shape factor of the particle. For the motion along the polar axis of the particle, the shape factor K is defined as

$$K = \frac{\frac{4}{3}(\beta^2 - 1)}{\frac{(2\beta^2 - 1)}{\sqrt{(\beta^2 - 1)}} In[\beta + \sqrt{(\beta^2 - 1)}] - \beta} \tag{4-3}$$

where β is the aspect ratio, i.e. the ratio of the major axis to the minor axis of the particle. The Brownian diffusivity D_B vs. the particle aspect ratio β is plotted in Figure 4-5 (Left

ordinate for D_B). As seen in this figure, the particle Brownian diffusivity D_B decreases monotonically with increasing β and is 0 when β approaches infinity. If the Brownian motion is the dominant mechanism, the thermal conductivity enhancement would increase with increasing temperature due to the temperature dependence of the Brownian diffusivity D_B. The nanofluids containing spherical metal or oxide nanoparticles in Das's studies are apparently in the Brownian-motion-dominant regime.

If the particle motion is ignored in nanofluids, heat is transported by the diffusive conduction. In this case, the effective thermal conductivity of nanofluids can be predicted by the effective medium theory. Figure 4.5 shows the thermal conductivity of nanofluids k_{eff} (right ordinate) vs. the particle aspect ratio β predicted by the effective medium theory. On contrary to the effects of the particle Brownian motion in nanofluids, the diffusive conduction benefits from the increased aspect ratio of nanoparticles. Although the long fibers are less mobile in nanofluids due to the drag force, they can promote heat transfer by providing rapid, longer heat flow paths. The Bi_2Te_3 nanorods used in our studies have an average aspect ratio of about 8.5. The calculation shown in Figure 4-5 combined with the experimental data indicates that the conduction-based mechanism should be primarily responsible for the thermal conductivity enhancement in nanofluids containing such nanorods. The higher-than-predicted thermal conductivity enhancement, shown in Figure 4-4, also implies the contribution from other mechanisms, such as the particle Brownian motion.

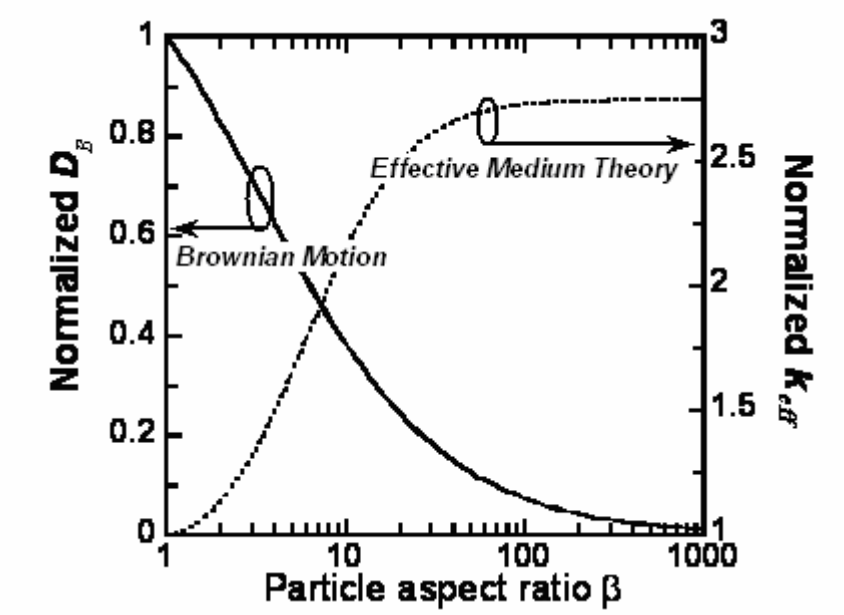

Figure 4-5 Normalized Brownian diffusivity D_B, calculated from Eqs. 4-2 and 4-3, and normalized effective thermal conductivity of nanofluids k_{eff}, estimated from the effective medium theory, vs. the particle aspect ratio β. Both D_B and k_{eff} are normalized to the values for spherical nanoparticles. In the calculation, the diameter of Bi_2Te_3 nanorods is 20nm, and the volume fraction is 0.8%

Based on the aforementioned analysis, the thermal conductivity enhancement should be attributed to the combined effects of the particle Brownian motion and the diffusive heat conduction. The Brownian motion would play a dominant role in thermal conductivity enhancement in nanofluids containing spherical nanoparticles (β=1). As β increases, the diffusive-conduction-based mechanism will gradually take over the dominance of the Brownian motion. One can imagine that there might exist an optimum particle aspect ratio for maximal combined effects of the Brownian motion and the diffusive heat conduction on the thermal conductivity enhancement in nanofluids. With

very few exceptions, previous studies on nanofluids have been confined to spherical particles ($\beta = 1$) and long fibers ($\beta = 100 \sim \infty$). A more comprehensive study is needed to explore the effects of particle shape on the heat transport in nanofluids.

4.7 Summary

In summary, the temperature dependence of thermal conductivity in oil-based nanofluids containing Bi_2Te_3 nanorods has been investigated. The analysis of the experimental data suggests that the dominant mechanism in thermal conductivity enhancement in nanofluids strongly depends on the particle aspect ratio. The effects of the Brownian motion could be predominant for spherical nanoparticle based nanofluids while the diffusive heat conduction mechanism will gradually take over the dominance as β increases.

5 Application of Hybrid Urchin-Like Nanoparticles

5.1 Introduction

Nanofluids have shown particular potential for enhancing the thermal transport in liquids and are a promising candidate as the next generation of advanced coolants for thermal management in cooling of microelectronics and optoelectronics (Masuda et al. 1993). Particularly over the past five years, various nanofluids have been studied to examine the thermal conductivity enhancement (Das et al. 2003a; Eastman 1998; Xie et al. 2003). However, these studies have been confined to spherical nanoparticles, or carbon nanotubes. The geometries of these nanostructures are shown in Figure 5-1 (a and b). So far the effectiveness of particle morphologies on heat transfer in nanofluids has been far less investigated.

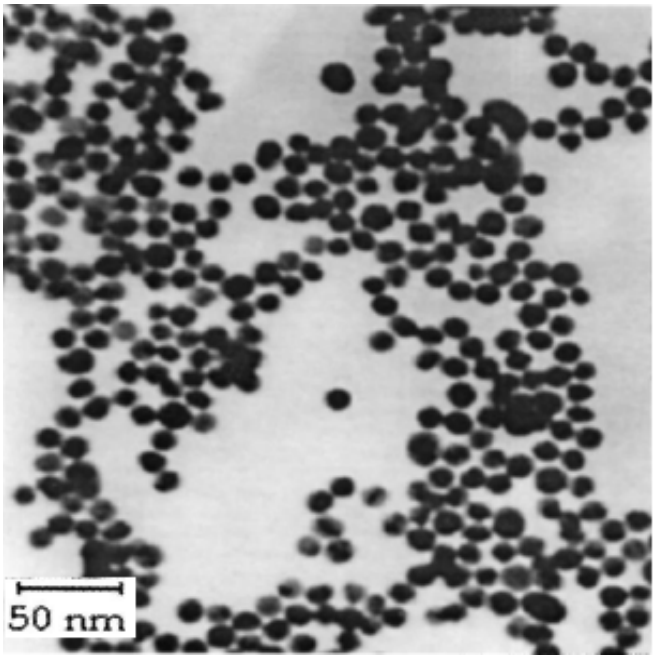

(a) Au nanoparticles in nanofluids (Patel et al. 2003)

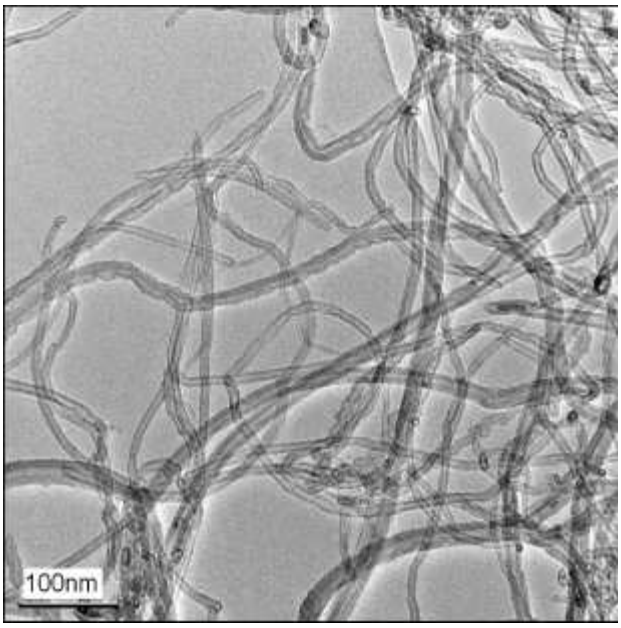

(b) Carbon nanotubes in nanofluids (Wen and Ding 2004b)

Figure 5-1 Nanoparticles of different geometries with different aspect ratios. a) Spherical Au nanoparticles (aspect ratio ~1); (b) Carbon Nanotubes, (aspect ratio >100)

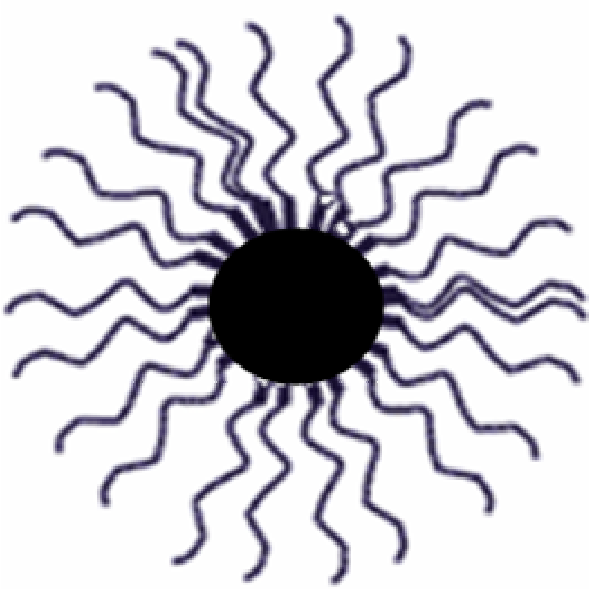

Figure 5-2 A schematic illustration of carbon tubes-on-spheres nanoparticles

In this chapter, a novel type of hybrid tubes-on-spheres nanoparticles, which are formed by attaching carbon nanotubes onto alumina-iron oxide nanospheres, are used to synthesize nanofluids to promote the heat transport in PAO base. A schemeatic of the urchin-like nanoparticles is shown in Figure 5-2. Within such hybrid nanoparticles, heat is expected to transport rapidly from one carbon nanotube to another through the centric alumina/iron sphere and thus leading to less thermal contact resistance between CNTs compared to common CNTs, which has been used in nanofluids. CNTs have extremely high longitudinal thermal conductivity (>3000 W/m.K), but the thermal resistance between CNTs and the fluid has limited their performance in nanofluids. Besides, the oxide spheres are expected to act as Brownian motion centers in the fluid, further enhance heat transfer and improve the stability of nanofluids.

5.2 Synthesis of Urchin-like Nanoparticles

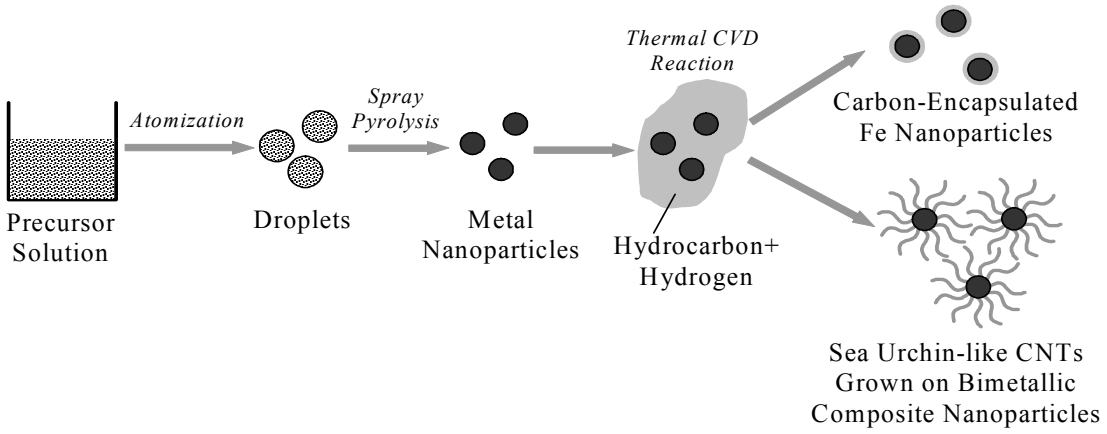

Figure 5-3 Synthesis process of urchin-like hybrid nanoparticles. Hybrid nanoparticles were synthesized in Dr. Zachariah's group

The hybrid sphere/CNT urchin-like nanoparticles are synthesized by spray pyrolysis followed by catalytic growth of CNTs, as shown in Figure 5-3 (Kim et al. 2002;

Kim et al. 2004b; Kim et al. 2005). Briefly, an aqueous precursor solution of $Fe(NO_3)_3$ and $Al(NO_3)_3$ with a mixing ratio of 1:1 is prepared to reach a total concentration of 3 wt%. The concentration of bimetallic composite is 3 wt%. The bimetallic composite nanoparticles of iron and aluminum are formed from thermal decomposition of aerosol droplets generated with a nebulizer operated with nitrogen carrier gas. After passing through a silica-gel dryer to remove water, the bimetallic composite aerosol particles are mixed with hydrogen at the entrance of the first tube furnace operating at ~1000 ^{o}C for pyrolytic conversion of the metal nitrate to the crystalline oxide composite aerosols. The spherical, oxide composite aerosol nanoparticles are then introduced into the second tube furnace (residence time ~3 sec), and are catalytically reacted with acetylene and hydrogen at 750 ^{o}C, which leads to the growth of CNTs on the surface of the bimetallic composite

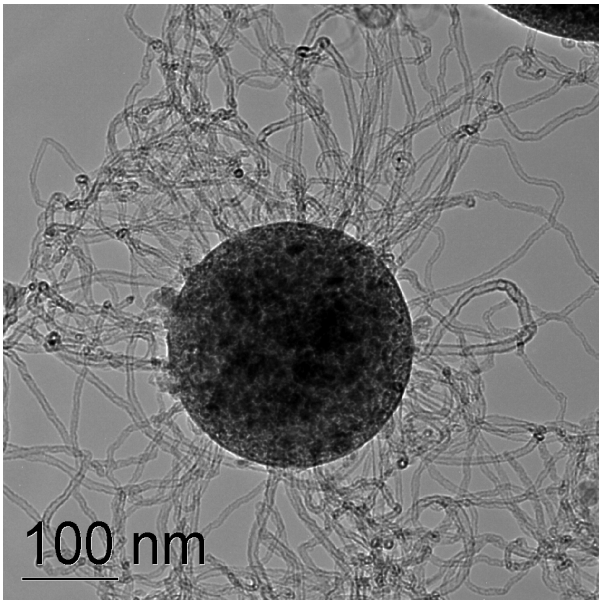

Figure 5-4 TEM image of a sample urchin-like nanoparticle produced by the aerosol method. Numerous carbon nanotubes are attached to the spherical, alumina/iron oxide nanoparticles. Image taken by a JEOL 2010 High-Resolution Transmission Electron Microscope (HRTEM)

nanoparticles (Kim et al. 2005). The final resulting hybrid sphere/CNTs particles are collected on a membrane filter, washed and dried in vacuum. The detailed structure of one hybrid sphere/CNT particle is shown in the TEM BF image (Shown in Figure 5-4), in which it can be seen that numerous CNTs are attached to the spherical, alumina-iron oxide composite nanoparticle of 250 nm diameter. The central, bimetallic particles are poly-dispersed with broad size ranging from 10 nm to 300 nm while the attached CNTs range from 300 nm to 500 nm in length. More than 10 TEM images were taken and the volume-weighted average diameter of the center spheres is estimated to be about 150nm, determined from the size distribution in TEM BF images.

5.3 Preparation of Nanofluids

The collected urchin-like nanoparticles are dispersed into poly-alpha-olefin (PAO) oil with sufficient exposure to ultrasonic radiation. A small amount of surfactant (about 1.5 wt %), Span-80, is added to the base fluid in order to obtain stable, well-dispersed and homogeneous nanofluids with minimum agglomeration. Span-80 was purchased from Sigma-Aldrich and used as is. No significant enhancement in thermal conductivity was observed in the PAO only containing the same amount of Span-80 but without nanoparticles. The head of Span-80 molecules will tightly bind to the surface of hybrid nanoparticles while the tail extends to the solvent to impart solubility to the nanoparticles so that the nanoparticles can be stably suspended in base fluids (PAO), as shown in Figure 5-5.

5.4 Diffusion Mobility of Urchin-like Nanoparticles

Brownian motion is a rapid and erratic motion of small particles in a liquid or gas phase due to collisions with surrounding molecules, and is characterized by the Brownian diffusivity D_B or the Brownian mobility μ_B, which are related by the Einstein

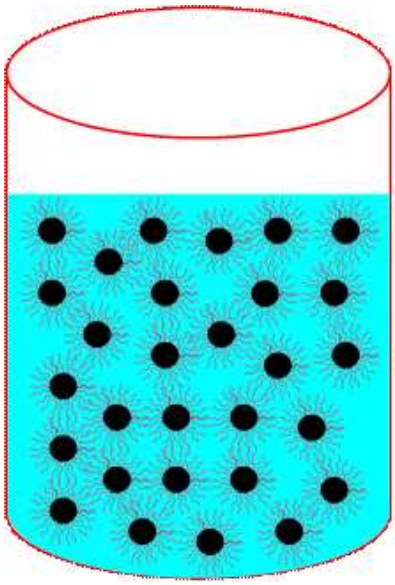

Figure 5-5 Illustration of well-dispersed urchin-like nanoparticles in PAO. This figure shows that nanoparticles are in Brownian motion and can easily get in touch with the help of extending-out carbon nanotubes

relationship, $D_B = k_B T \cdot \mu_B$, where k_B is the Boltzmann constant and T the temperature in Kelvin (Hunter 2001). Nanoparticles in motion may act as "heat boats" to directly transport energy or as "stirrers" to induce convection to promote heat transfer in fluids. The Brownian diffusivity of the urchin-like nanoparticles is measured in the prepared PAO-based nanofluids using a Photocor Complex-DLS instrument at room temperature (25^oC) (Hunter 2001). The autocorrelation function of the scattered light is plotted in Figure 5-6. The curve shows a typical exponential decay of the correlation function as a

function of the delay time. It can be used to deduce the Brownian diffusivity of nanoparticles in base fluids. The Brownian diffusivity of the urchin-like particles dispersed in PAO is found to be 1.74×10^{-9} cm^2/s at T=25°C. It is interesting to compare this value to the Brownian diffusivity of the bare, spherical nanoparticles with the same diameter as the urchin-like particles (about 150 nm), which is estimated to be about 3.01×10^{-9} cm^2/s based on the particle size and the viscosity of PAO. This comparison indicates that the attached CNTs do not significantly deteriorate the Brownian motion of the center particles in the urchin-like particles, possibly because of the flexibility of CNTs. On the other aspect, the CNTs with extremely high thermal conductivity and high aspect ration will benefit heat transfer in a great deal by providing long, rapid heat transport paths.

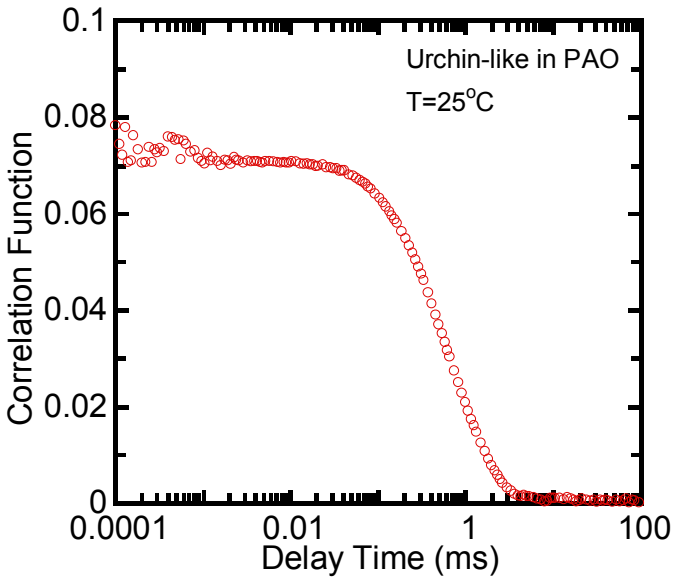

Figure 5-6 Correlation function of the scattered light vs. delay time for the nanofluid consisting of urchin-like particles and PAO. Measurements are taken with a Photocor-Complex DLS instrument

5.5 Thermal Conductivity Measurement of Nanofluids

The fluid thermal conductivity has been measured by the 3ω-wire method (Cahill 1990; Yang and Han 2006b). A miniaturized device is designed for the present measurement, requiring less than 1ml sample in volume. In this device, a metal wire (20 μm in diameter) is immersed into the liquid sample, acting as both a heater and a thermometer. To measure thermal conductivity at different temperatures, the test cell with the sample liquid is placed inside a circulating thermal bath and the testing temperature varies from 10 to 90^{o}C with an accuracy of ±0.01^{o}C. Calibration experiments were performed for hydrocarbon (oil), fluorocarbon and water at atmospheric pressure. Literature values were reproduced with an error of <1%.

The raw experimental data in the thermal conductivity measurement for the PAO oils, with and without urchin-like nanoparticles, are shown in Figure 5-7. The slope of the 2ω temperature oscillation curves will yield the thermal conductivity of the liquids. The less-steep curves representing the nanofluids containing urchin-like nanoparticles indicate they have higher thermal conductivity than the pure PAO oil. The measured thermal conductivity enhancement of nanofluids with urchin-like nanoparticles at 0.1 and 0.2 vol % is plotted over a temperature range of 10 ^{o}C to 90 ^{o}C. The thermal conductivity of the pure PAO is experimentally found to be 0.1434W/mK at 25 ^{o}C, which is in good agreement with literature data (Choi et al. 2001). The thermal conductivity enhancement of nanofluids is normalized to the base fluid conductivity at each specified temperature. As seen in the Figure 5-8, the nanofluid conductivity enhancement increases with increasing temperature, about 20.5% at 10 ^{o}C and 23.6% at 90 ^{o}C at the particle loading of 0.2 vol %, and also increases with increasing nanoparticle concentration. It is known

that the nanofluid conductivity enhancement will go as T^{α} (where $\alpha>1$) in the moderate temperature range if the particle Brownian motion is the key mechanism of thermal conductivity enhancement in nanofluids (Chon et al. 2005; Das et al. 2003a). The measured thermal conductivity enhancement of the nanofluids consisting of urchin-like nanoparticles dispersed in PAO, however, shows weaker temperature dependence, which is approximately linearly-proportional to temperature T. This implies that the diffusive heat conduction along highly-conductive CNTs in the nanofluids must play a significant role, which alone will lead to decreasing dependence with temperature (Hong et al. 2005).

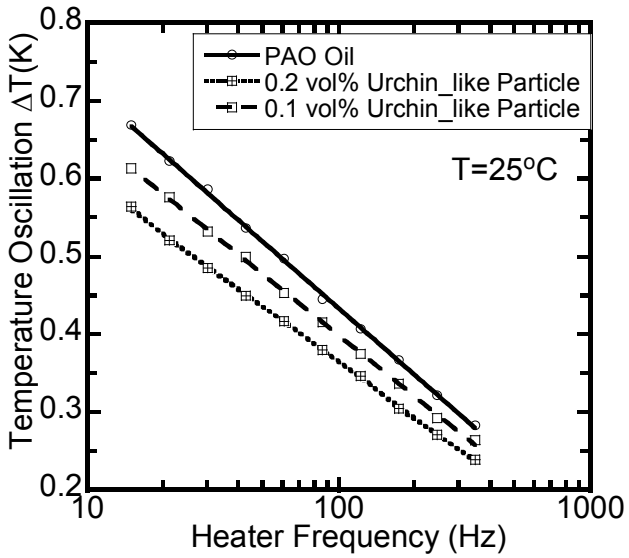

Figure 5-7 Measured amplitude of the temperature oscillation in the metal wire immersed in poly-alpha-olefin (PAO) with and without urchin-like particles as a function of frequency of the drive current. The test temperature is 25°C

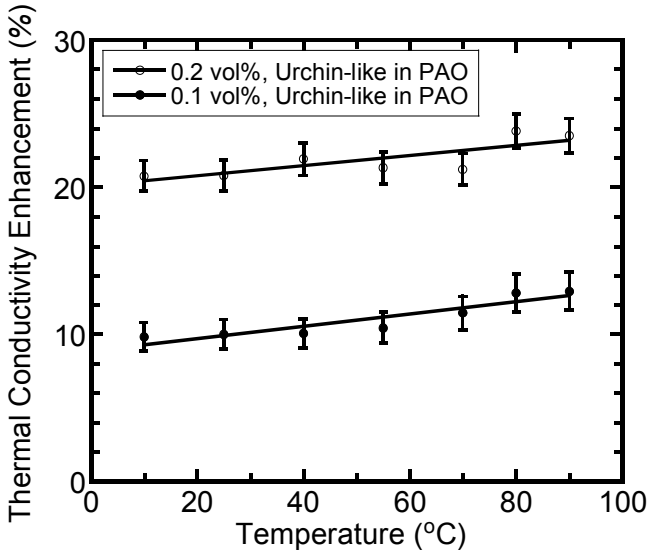

Figure 5-8 Temperature dependence of the thermal conductivity enhancement of nanofluids with urchin-like particles at 0.1 and 0.2 vol% concentrations. Thermal conductivity enhancement in the nanofluids is normalized by the thermal conductivity of the base fluids at each specified temperature. Linear fits to the data are shown as a guide to the eye

5.6 Discussion

It is worthwhile to compare the effectiveness of various particle morphologies, e.g. spheres, CNTs, and the urchin-like particles, on the thermal performance of nanofluids. Figure 5-9 lists the values of thermal conductivity enhancement in nanofluids such as alumina spheres (13nm diameter) in water (Masuda et al. 1993), CNTs in PAO (Choi et al. 2001), CNTs in decene (Xie et al. 2003), and our urchin-like particles in PAO. It can be found in this figure that the urchin-like nanoparticles can provide higher conductivity

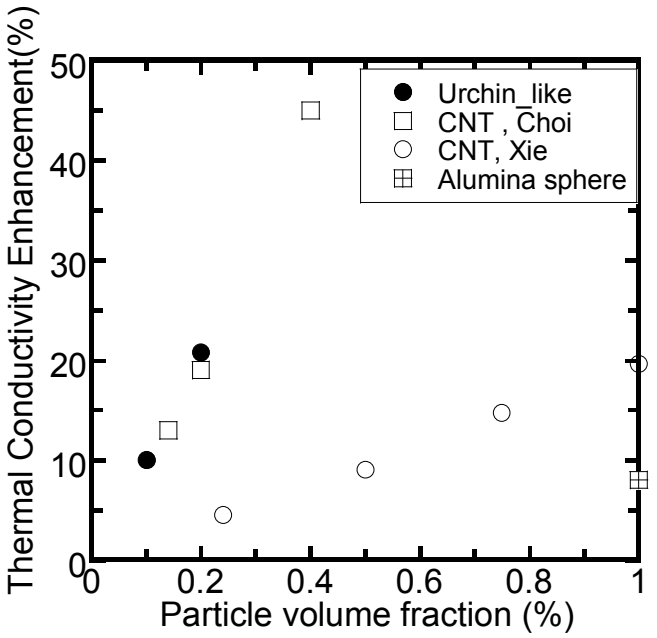

Figure 5-9 Performance comparison of particles with various morphologies, e.g., spheres, carbon nanotubes (CNT), and hybrid sphere-CNTs particles (urchin-like), in nanofluids. (Masuda et al. 1993) (Choi et al. 2001) (Xie et al. 2003)

enhancement in nanofluids relative to conventional spheres and CNTs if compared at the same particle loading. For example, it can be about 13 times higher than the value representing spherical alumina nanoparticles at 0.2 vol % that can be interpolated from the curve and please note that those alumina nanoparticles have smaller diameter, about 13nm in diameter. The Brownian motion of particles is the key mechanism of the thermal conductivity enhancement in nanofluids containing spherical nanoparticles while the diffusive heat conduction along the highly conductive tubes should be primarily responsible in nanofluids containing long fibers such CNTs. However, urchin-like particles could take advantages of both spheres and CNTs; in nanofluids containing urchin-like particles, heat can transport rapidly along highly conductive CNTs or from

one CNT to another through the center sphere while the central spheres are still considerably mobile (see DLS results in Figure 5-6). These coupling mechanisms are manifested in temperature dependence of thermal conductivity enhancement in nanofluids consisting of urchin-like nanoparticles, as shown in Figure 5-8. Optimizing the urchin-like structure could provide further improvements in heat transport in nanofluids.

5.7 Summary

In summary, a novel, hybrid CNTs-on-sphere structure, i.e. urchin-like nanoparticles, has been proposed for enhancing thermal transport in nanofluids, which is expected to take advantages of both nanosphere's mobility and CNTs' high thermal conductivity. Such urchin-like nanoparticles, synthesized by a spray pyrolysis method and then dispersed in PAO oil, have increased the thermal conductivity by about 20% at a 0.2% volume fraction of particles at room temperature. Moreover, the thermal conductivity enhancement is even larger at higher temperature, indicating a contribution of particle's Brownian motion to the thermal transport in nanofluids. The experimental results show that the urchin-like nanoparticles can provide higher thermal conductivity enhancement in nanofluids as compared to either CNTs or spheres at the same particle loading (0.2 vol %, shown in Figure 5-9). The enhanced thermal conductivity in nanofluids containing urchin-like nanoparticles is attributed to particle Brownian motion, high thermal conductivity and high-aspect-ratio of CNTs. Novel particle geometries, such as urchin-like nanoparticles, would open a new way to improve the performance of nanofluids.

6 Phase Change Water-in-FC72 Nanofluids

6.1 Introduction

Fluorocarbons as heat transfer fluids have inherently poor thermal conductivity compared to most solids. For example, FC72 is one of a line of FluorinertTM Electronic Liquids and is an important low-temperature heat transfer fluid due to its low pour points (-90 ^{o}C), excellent low temperature viscosity (absolute viscosity of FC72 is 0.64 cP at 25 ^{o}C, while for water, this value is 0.89), high dielectric constant, chemical inertness, compatibility with sensitive materials, nonflammability and nontoxicity. But the main drawback of FC72 as a heat transfer fluid is also outstanding – the thermal conductivity of FC72 is very low. At room temperature, the thermal conductivity of FC72 is 0.057 W/m.K, only one tenth of the thermal conductivity of water (0.58 W/m.K).

The utilization of liquid suspensions of solid nanoparticles has long been a most investigated way of increasing the thermal conductivity of heat transfer fluid. In fact, water has much higher thermal conductivity than many other heat transfer fluids, i.e., oils and fluorocarbons. It seems water nanodroplets may have potential to improve the thermal transport properties of oils and fluorocarbons. Therefore, a totally different design for thermal fluids that completely eliminates solid particles, and instead, uses liquid nanostructures has been proposed. Dispersions of liquid nanostructures (e.g., spherical droplets) in thermal fluids can be called "nanoemulsion fluids."

The idea of using encapsulated liquid nanodroplets for improving heat transfer in fluids was actually triggered by the studies on mechanisms of thermal conductivity enhancement in conventional nanofluids containing solid nanoparticles. Although various

possible mechanisms have been suggested, particle Brownian motion is now attracting more attention and considered to be the primary mechanism for the enhanced thermal conductivity in nanofluids. Based on this understanding, we could propose that if nanometer-sized liquid droplets could be dispersed into traditional heat transfer fluids, a new class of fluids with improved thermal conductivity would be produced. In such fluids, encapsulated liquid nanodroplets are in Brownian motion and are expected to enhance heat transport in base fluids, jus like what solid particles behave in conventional nanofluids. This strategy of enhancing thermal conductivity of fluids by encapsulated liquid nanodroplets has been demonstrated in FC72 containing nanometer-sized water droplets in our experiments. Such type of engineered fluids is named "nanoemulsion fluids" in order to be distinguished from conventional nanofluids containing solid nanoparticles. Compared with nanofluids made by dispersing nanoparticles in heat transfer fluids, nanoemulsions are much easier to make – adding water into FC72 after dissolving fluorinated surfactants and then mechanically shearing the mixture. In our experiment, a magnetic stirrer and an ultrasonic liquid processor are employed in sequence. Water-in-FC-72 nanoemulsions are then very convenient for large-volume industrial production. In addition, nanoemulsions are thermodynamically stable systems, which mean they do not have the agglomeration and the sedimentation problems existed in conventional nanofluids. Meanwhile, due to the low viscosity of the dispersed water phase, the fluid mobility of the continuous phase (i.e. FC-72) should not be impaired too much. In order to keep the high dielectric constant, DI water and nonionic fluorinated surfactant are preferred for the preparation of nanoemulsions.

This chapter will focus on synthesis and experimental study of thermophysical properties, i.e., thermal conductivity, viscosity, and specific heat, of water-in-FC72 nanoemulsion fluids. These as-prepared nanoemulsions are thermodynamically stable and transparent, while the encapsulated water nanodroplets are below 10nm in diameter. The phase change behavior of water nanodroplets dispersed in nanoemulsions is characterized by DSC. Water has a higher heat capacity than FC72 and a large heat of fusion, H_f = 39.78J/g. It seems that the addition of water will increase the heat capacity of FC72 and moreover, the large volume of latent heat absorbed by the encapsulated ice nanoparticles during the phase change process can be used to greatly improve the cooling performance of FC72.

6.2 Synthesis of Water-in-FC72 Nanofluids

In this chapter, nanoemulsion fluids are developed, which are suspensions of nanometer-sized, encapsulated liquid droplets emulsified in heat transfer fluids. The emulsified water droplets (<10nm in radius) are found to be able to increase the thermal conductivity of FC72 by up to 52%. Such nanoemulsion fluids can be scaled up to mass production and are thermodynamically stable systems.

Emulsions are dispersions of at least one liquid (disperse phase) in other liquids (continuous phase), which are part of a broad class of multiphase colloidal dispersions, and can be formed by shear-induced rupturing or self-assembly. Such fluids possess long-term stability and can be mass produced. Fluorocarbons are super-hydrophobic due to the weak Van der Waals forces between their molecules, while water is one of good solvents with strongest molecular interactions, which therefore makes the formation of water-in-

FC72 nanoemulsions thermodynamically unfavorable. In order to make the water-in-FC72 nanoemulsions stable, a proper surfactant must be used. The surfactant should be very fluorophilic and soluble in FC-72, that is, the surfactant is a fluorinated one (fluorinated amphiphiles). The resultant nanoemulsions are fluidic, transparent, thermodynamically stable and heterogeneous systems.

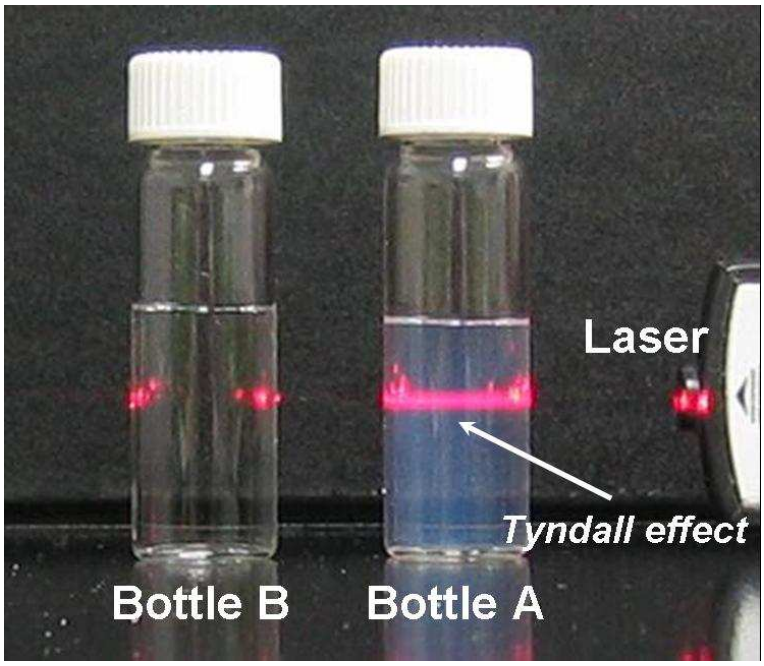

Figure 6-1 Water-in-FC72 nanoemulsion fluid (Bottle A) and pure FC72 (Bottle B). Liquids in both bottles are transparent. When a laser beam is passed through Bottles A and B, the Tyndall effect (i.e. a light beam can be seen when viewed from the side) is observed only in Bottle A. Pictures taken by a Canon PowerShot digital camera

By using high-intensity ultrasonic homogenizer (VCX 750, Sonics & Materials, Inc), DI water can be emulsified into FC72 with a small amount of fluorinated amphiphilic surfactant. In this study, nanoemulsions containing water nanodroplets up to

12 vol.% (7.1 wt.%) are produced and tested. Figure 6-1 shows the picture of the prepared water-in- FC72 nanoemulsion fluid and the pure FC72. The water-in-FC72 nanoemulsion fluids are transparent, but scatter incident light (i.e., the Tyndall effect). This indicates that FC72 and water are not molecularly dispersed but form a nanoemulsion. It is well known that nanoemulsions are thermodynamically stable, where the free energy is even lower than that in the unmixed system. In our experiment, the water-in-FC72 nanoemulsion fluids have been stable since being prepared six months ago. Moreover, such nanoemulsion fluids can be produced in large quantities to meet the industrial requirement.

6.3 Measurement of Diffusion Mobility of Water Nanodroplets

The Dynamic Light Scattering (DLS) technique is used to measure the size and Brownian diffusivity of the encapsulated water nanodroplets in nanoemulsions. The autocorrelation functions of the scattered light by the water-in-FC72 nanoemulsion fluids are shown in Figure 6-2. These curves show a typical exponential decay of the correlation functions and the slope can be used to deduce the particle size and diffusivity. The hydrodynamic radius and Brownian Diffusivity of the nanodroplets were found to be smaller than 10 nm and about 3.5×10^{-7} cm^2/s at T = 25 ^oC, respectively. A small change in nanodroplet radius was observed when the volume fraction of water in nanoemulsion fluid changes. The DSC measurement results are listed in Table 6-1. It can be seen that with increasing water concentration, the diameter of water nanodroplets decreases, and reason may lies in that more surfactant is needed in order to stabilize the nanoemulsions with higher water loadings. Usually R_h, the "hydrodynamic radius" of the interior

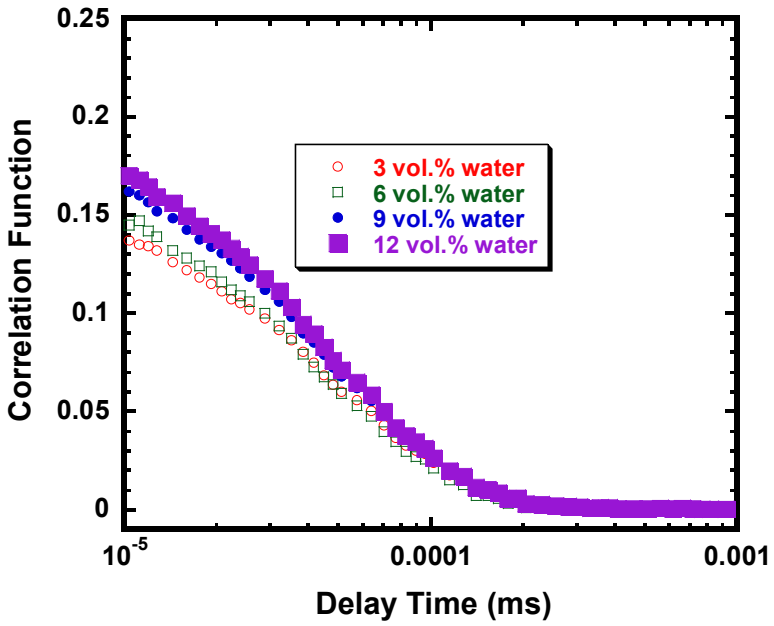

(a)

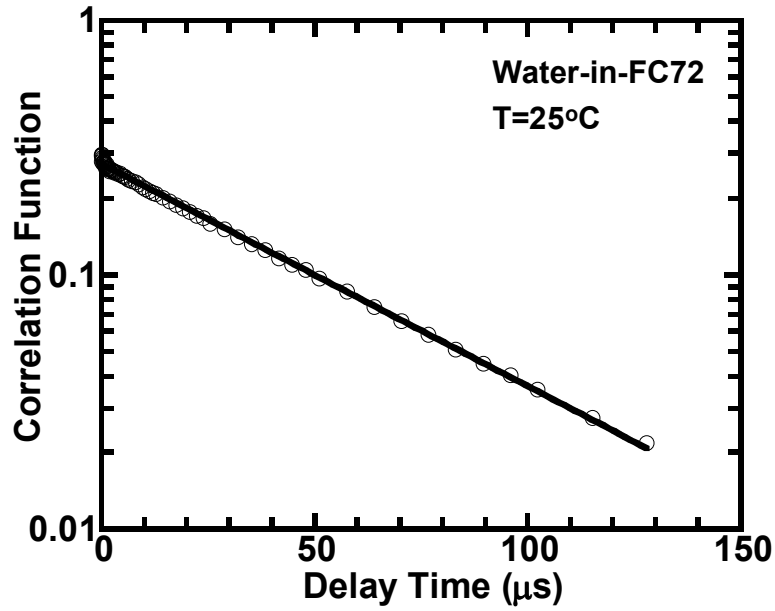

(b)

Figure 6-2 (a) Correlation function of the scattered light for the water-in-FC72 nanoemulsion fluids; (b) the curve for 6 vol% water-in-FC72 is fitted with the inelastic light scattering model. Measurements taken by a Photocor-Complex DLS instrument

water droplets, is a little bit larger than the real radius of the encapsulated nanodroplets due to the existence of the surfactant layers making the nanoemulsions a core-shell structure. The mobility of the interior droplets is simply related to their mobility through Stokes-Einstein equation,

$$D_B = k_B T \mu_B \tag{6-1}$$

where k_B is Boltzmann constant, T is the temperature and μ_B is the mobility, D_B is the diffusion coefficient.

Table 6-1 Diameters of encapsulated water nano-droplets in nanoemulsions of different volumetric fractions of water. The diameter of water droplets decreases with increasing water loading, the reason lies in that more surfactant are used for more concentrated nanoemulsions

Volumetric fraction of water (vol%)	**3**	**6**	**9**	**12**
Diameter (nm)	**10.053**	**9.7637**	**8.8991**	**8.0932**

6.4 Thermal Conductivity Measurements

The thermal conductivity of the water-in-FC72 nanoemulsion fluids has been measured by the 3ω-wire method. Because the thermal conductivity of the liquid, k_f, is inversely proportional to the slope of the 2ω temperature rise of the wire as a function of the driven frequency ω, the liquid thermal conductivity can be calculated by measuring the slope of the straight lines shown in Figure 6-3. Calibration experiments were performed in hydrocarbon (oil), fluorocarbon and water at atmospheric pressure. Literature values were reproduced within an error of <1%.

The raw experimental data for the FC72 with and without water nanodroplets are shown in Figure 6-3. The slope of the 2ω temperature oscillation curves will yield the thermal conductivity of the liquid. The less steep curve for the water-in-FC72 nanoemulsion fluid indicates it has a higher thermal conductivity as compared to the pure

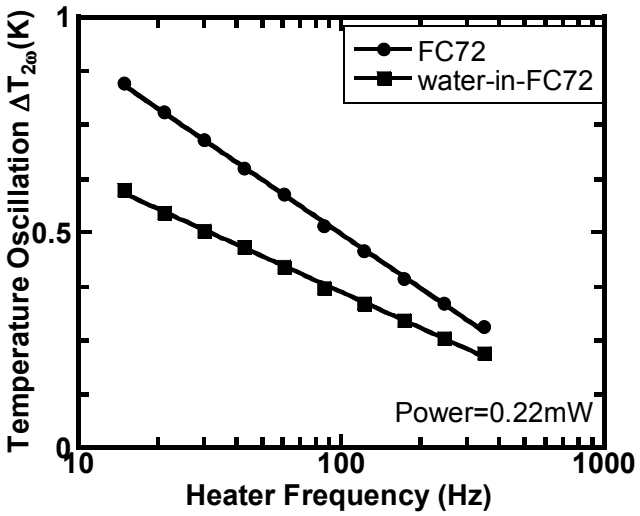

Figure 6-3 Measured amplitude of the temperature oscillation in the metal wire immersed in the FC72 with and without water nanodroplets as a function of frequency of the drive current. Volume fraction of the water nanodroplets is 12%

FC72. Figure 6-4 shows the thermal conductivity enhancement in water-in-FC72 nanoemulsion fluids as a function of the loading of water nanodroplets. Remarkably, very significant increase in thermal conductivity has been observed in water-in-FC72 nanoemulsion fluids. Thermal conductivity enhancements of up to 52% can be observed in nanoemulsion containing 12 vol.% (or 7.1 wt.%) of water nanodroplets. The observed enhancements in thermal conductivity are much larger than those predicted by the EMT.

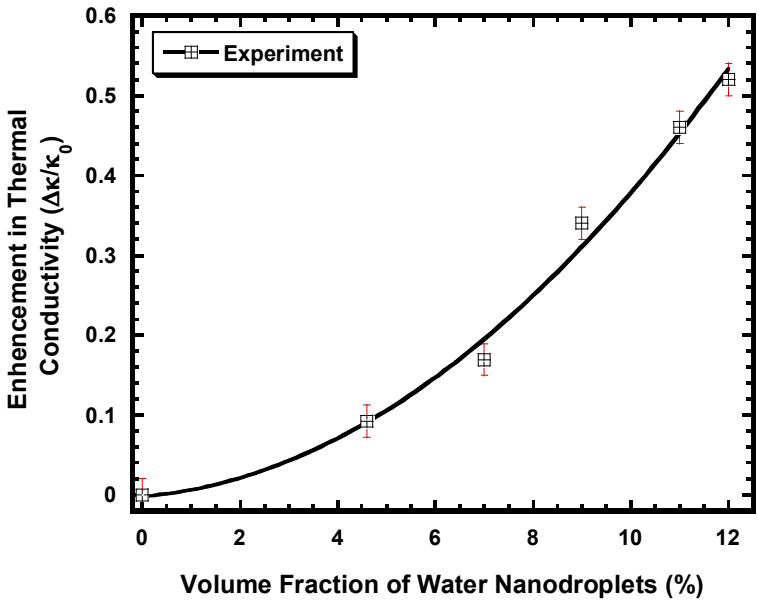

Figure 6-4 Thermal conductivity of FC72 is seen to be improved by up to 52% through emulsifying 12 vol% (or 7.1 wt%) water into FC72

In the EMT predictions, thermal resistance between the immiscible water and FC72 was taken into consideration. Since there is no report on thermal interfacial resistance between water and fluorocarbon, 65 MW/m^2 K (for the water-octane interface) is used to estimate the effective thermal conductivity of the water-in-FC72 nanoemulsion fluids based on the EMT. The larger-than-predicted conductivity enhancement indicates that thermal diffusion is not the only thermal conduction mechanism and the particle motion, which is not considered in the EMT, should play a key role in the thermal conductivity enhancement of the water-in-FC72 nanoemulsion fluids. This is also coincident with the high mobility or diffusivity of the water nanodroplets measured in the DLS experiment.

Another interesting phenomenon seen in Figure 6-4 is that the thermal conductivity enhancement of water-in-FC72 nanoemulsion fluids is nonlinear with volume or weight fraction of water nanodroplets, while theoretical predictions, such as EMT, clearly show

a linear relationship between the thermal conductivity enhancements and water fraction. This implies the existence of nonlinear droplet-droplet pair interactions. This nonlinear behavior is made possible at high concentration and extremely small size of water nanodroplets. In contrast, such nonlinear behavior is rarely observed in conventional solid nanoparticles-based nanofluids.

In order to show the significance of this work, we compared the thermal conductivity enhancement in our nanoemulsion fluids with the reported data on conventional nanofluids containing solid particles (fluids containing long fibers such as nanotubes not included), as shown in Figure 6-5. Although the strategy of adding particles to fluids for improving their thermal conductivity has been pursued for nearly a century, previous work is confined to millimeter-, micrometer- or nanometer-sized SOLID particles. Among those stable nanofluids, Cu nanoparticles dispersed in ethylene glycol have increased the thermal conductivity by 40%, which might be the highest enhancement reported to date. Without use of any solid particles, our nanoemulsion fluids remarkably exhibit very high thermal conductivity enhancement (about 52% enhancement), even higher than that of the Cu-nanoparticles based nanofluids. Most importantly, the development of nanoemulsion fluids could provide solutions to long-term-stability and mass-production problems that have long plagued the conventional nanofluids containing solid particles.

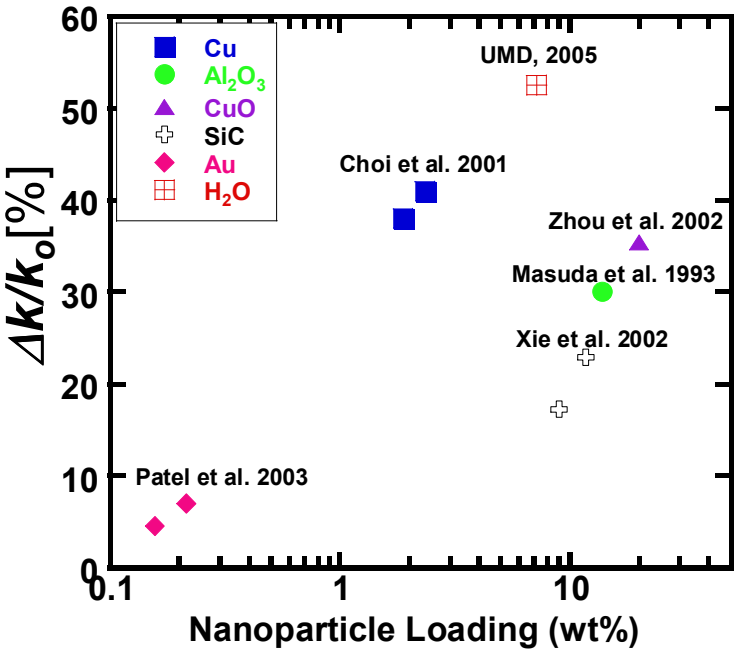

Figure 6-5 Brief summary of thermal conductivity enhancement in stable suspensions of nanoparticles in fluids. Early experimental studies are limited to solid nanoparticles, such as metal and oxide

6.5 Viscosity of Water-in-FC72 Nanofluids

Both thermal conductivity and viscosity of emulsions could be strongly and similarly associated with the microstructure and dynamics of the fluids. In order to comprehend the thermal conductivity of the nanoemulsion fluids, their dynamic viscosity is investigated experimentally. A commercial viscometer (Brookfield DV-I Prime) is used for the viscosity measurement. The dynamic viscosity is found to be 0.65 cP in the pure FC72, which matches very well with the literature values. Figure 6-6 shows the relative dynamic viscosity, μ_{nf} / μ_f, for the water-in-FC72 nanoemulsion fluids with varying water loading. A nonlinear relationship is observed between the viscosity

increase and the loading of water nanodroplets, a trend similar to thermal conductivity plotted in Figure 6-4. However, the relative viscosity is found to be about two times the relative conductivity if compared at the same water loading. It is worth noting that the fluid viscosity is measured at a range of shear rate or spindle rotational speed (50–100 RPM), and the viscosity is found to be independent of shear rate. This indicates that the nanoemulsion fluids in this experiment are Newtonian in nature.

The viscosity increase of dilute colloids has been predicted using the Einstein equation, $\mu_r = 1 + 2.5\phi$, where $\mu_r = \mu_{nf} / \mu_f$ is the relative viscosity and ϕ is the volume fraction of the dispersed phase. This equation, however, underpredicts significantly the viscosity increase in the water-in-FC72 nanoemulsion fluids at relatively high water loadings, as can be seen in Figure 6-6. This is because the Einstein equation is derived based on dilute systems (assuming volume fraction <0.01). For more highly concentrated systems where the hydrodynamic interaction and aggregation of nanoparticles become important, the Einstein equation must be augmented by higher order terms of the volume fraction as $\mu_r = 1 + 2.5\phi + B\phi^2 + \ldots..$ Although the coefficient for the first-order term, 2.5, can be strictly derived, it is not a simple task to theoretically determine those for the higher order terms because of the difficulty in accounting for the effects of increased concentrations. By fitting the experimental data in Figure 6-6, B is found to be about 117, indicating a strong nonlinear behavior. This nonlinear increase in viscosity is common in colloidal systems, and has been interpreted by the hydrodynamic interaction and/or aggregation of nanoparticles. These effects could also give an explanation for the deviation of the conductivity increase from the Hasselman-Johnson (HJ) model, as could

be inferred from the corresponding trends observed in viscosity (Figure 6-6) and thermal conductivity (Figure 6-4).

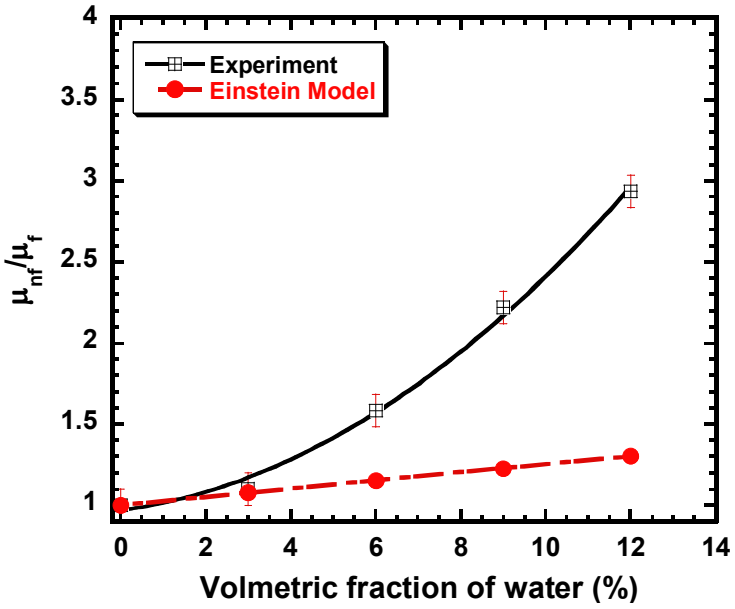

Figure 6-6 Viscosity of water-in-FC72 nanoemulsions measured at different volumetric fractions of water nanodroplets. The measurements were conducted at room temperature on a Brookfield viscometer

6.6 Heat Capacity of Water-in-FC72 Nanofluids

In addition to thermal conductivity and viscosity, heat capacity is also an important property in determining the thermal performance of heat transfer fluids. In this experiment, the heat capacity of the nanoemulsion fluids and the pure FC72 are measured using DSC (model TA-Q100). DSC measurements are taken at an ordinary cyclic ramp mode, and the scan rate is 10 °C/min. Figure 6-7 shows the cyclic DSC heating and cooling curves in the scanning temperature ranges of 0–50 °C for the water-in-FC72 nanoemulsion fluids. The volumetric specific heat can be directly extracted from these

curves with a given scanning rate. The volumetric specific heat of the pure FC72 is experimentally found to be 1.88 J/ml.K at room temperature, which is in good agreement with literature data.19 In the case of no phase transition of water nanodroplets, as shown in Figure 6-7, the volumetric specific heat of the nanoemulsion fluids at room temperature is found to be increased by 5.29%, 9.52%, 11.64%, and 17.90% for 3, 6, 9, and 12 vol. % of water loading, respectively. Little deviation is observed from the prediction of the simple mixing rule, i.e., $C_{p,nf} = \sum_i C_{p,i}\phi_i$, where $C_{p,nf}$ is the volumetric specific heat of nanofluids, $C_{p,i}$ is the heat capacity of the ith component, and ϕ_i is the volume fraction of the ith component of nanofluids. This enhancement in the effective heat capacity of nanofluids is simply because the specific heat of water is much higher than that of FC72.

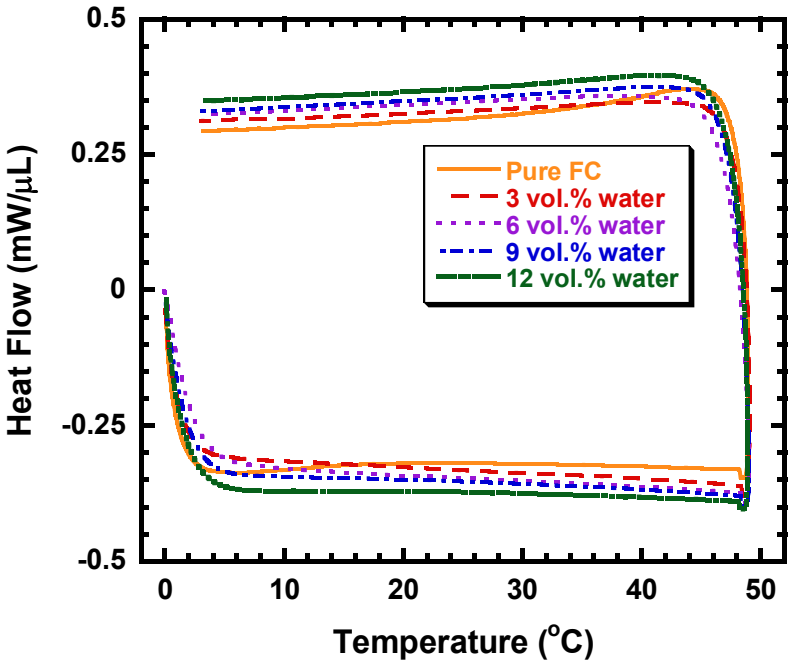

Figure 6-7 DSC cyclic curves of FC-72 and water-in-FC72 nanoemulsions. The heat capacity of fluids can be derived from these curves

Heat capacities of FC72 and nanoemulsions at a temperature of 25 ^{o}C were easily obtained from the DSC curves. At the same time, the heat capacities of nanoemulsions were calculated based on the volumetric fraction of water. The measured results match the calculated values well. Both measured and calculated heat capacities are shown in Figure 6-8. At a water volumetric fraction of 12%, over 15% increase in heat capacity is observed.

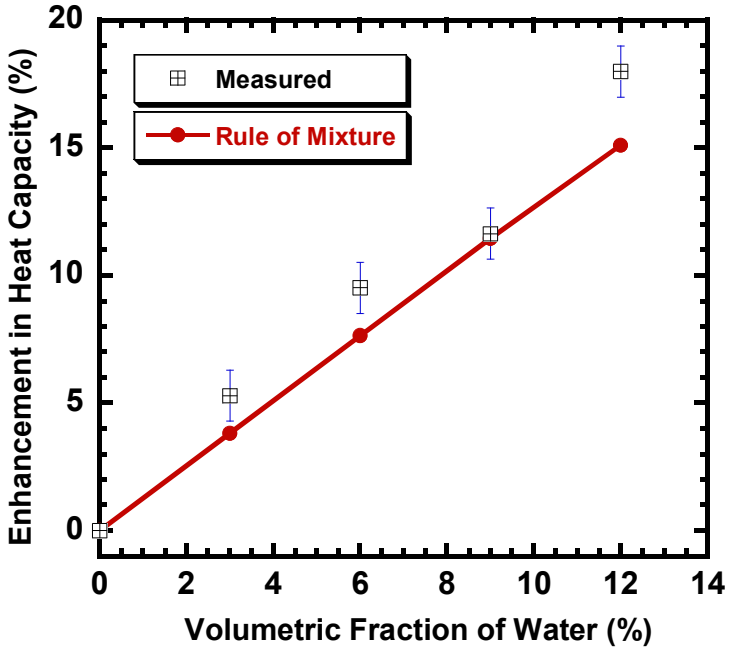

Figure 6-8 DSC measured and calculated heat capacities of water-in-FC72 nanoemulsions. The heat capacities of nanoemulsions are also calculated according to the rule of mixture (ROM)

6.7 Phase Change Behavior of Water-in-FC72 Nanofluids

A very interesting and useful behavior observed from Figure 6-9 is that, during the heating and cooling cycle, water nanodroplets undergo melting-freezing transition in the nanoemulsion fluids. The peak at about −20 °C is the exothermic crystallization (freezing)

peak for the water nanodroplets in the fluids. These water nanodroplets exhibit a relatively large melting-freezing hysteresis, about 20 °C, which is very likely caused by the change in the interface free energy of water nanodroplets relative to that of the bulk water. The nanodroplet size has a strong effect on the melting-freezing hysteresis, so the shape of the freezing peak provides information about the nanodroplet size and thus about the nanoemulsion stability. The presence of a single freezing peak in Figure 6-9 indicates that the nanoemulsion fluids are well dispersed and all water nanodroplets are nearly monodispersed in size. The impact of phase-changeable water nanodroplets on the fluid properties is obvious: the effective specific heat of the fluids can be significantly boosted. The effective specific heat can be defined as $C_{p,nf} = C_{p,f} + \phi H_{f,droplet} / \Delta T$, where ϕ is the volume fraction of the phase-changeable nanodroplets, $H_{f,droplet}$ is the latent heat of the phase-changeable nanodroplets per unit volume, and ΔT is the temperature difference between the heat transfer surface and the bulk fluid. In this experiment, if assuming ΔT =20 °C, the effective volumetric specific heat can be increased by up to 126% for the nanoemulsion fluid containing 12 vol % water nanodroplets when the water nanodroplets undergo phase transition. The use of phase-changeable nanodroplets is expected to provide a way to simultaneously increase the effective specific heat and thermal conductivity of conventional heat transfer fluids.

The heat of fusion H_f of pure water is 334 J/g, an outstanding value among those of phase change materials. The calculated H_f values of water-in-FC72 nanoemulsions for different water loading from 3 to 12 volumetric percent are 10, 20, 30, 40 J/ml, respectively, in good agreement of the measured results shown in Figure 6-9, which are 10.52, 15.44, 25.48, 39.78 J/ml, respectively. The volumetric heat capacity of water is

about 4.18 J/ml.K, and is over two times the heat capacity of FC-72. For a temperature increase from -20 to 0 ℃, 1 ml FC72 absorbs 110.4 joules heat. For the nanoemulsion containing 12 vol% water nanodroplets, the melting of ice nanoparticle absorbs 40 Joules heat, which means, upon the melting of ice nanoparticles in the nanoemulsion, the heat capacity of FC72 has been increased up by about 100%. Together with the enhancement in heat capacity caused only by the addition of water without phase change, totally a maximum heat capacity increase of 126% is obtained in the 12 vol.% water-in-FC72 nanoemulsions.

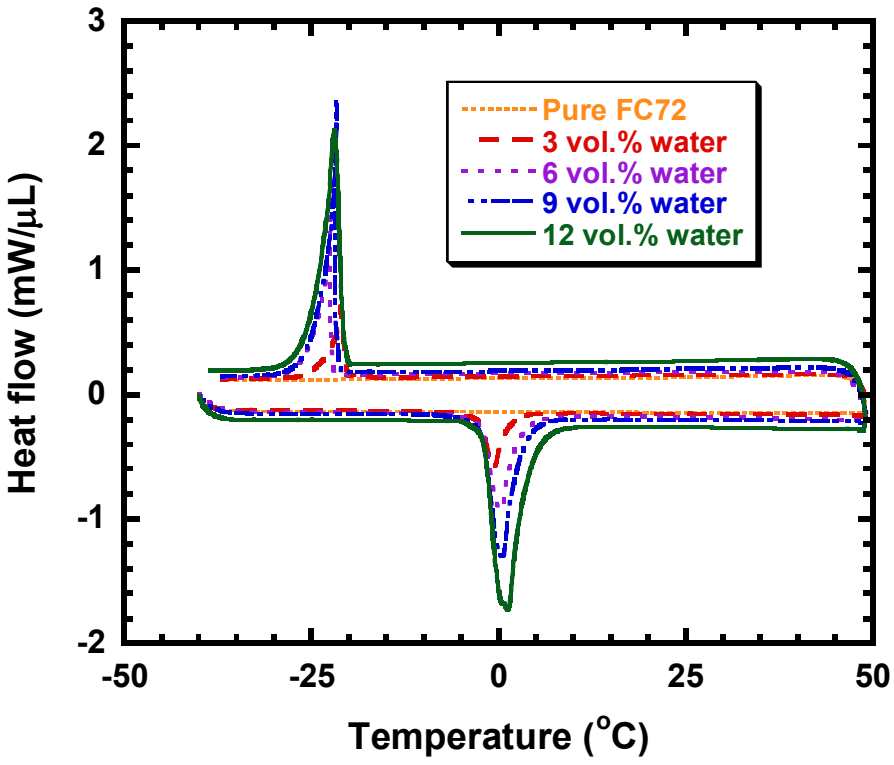

Figure 6-9 DSC cyclic curves of water-in-FC72 nanoemulsions for different water loading. Exothermal peaks are observed at -20 ℃, corresponding to the freezing of water nanodroplets, while endothermal peaks are observed at 0 ℃, corresponding to the melting of water nanoparticles

6.8 Natural Convective Heat Transfer in Nanofluids

To achieve a better understanding of transport mechanisms in the water-in-FC72 nanoemulsion fluids, natural convective heat transfer is investigated experimentally in these fluids. In this experiment, a 25 μm in diameter, 3 cm long platinum-iridium wire coated with 6 μm thick Teflon, is immersed in the fluids to serve as a test heater. This heater can be kept at constant temperature by a feedback circuit consisting of a Wheatstone bridge, as in hot-wire anemometry. This method is so-called temperature-controlled heating. The heat dissipated by the wire heater can be calculated directly from its electrical voltage and resistance. The measurement is taken under steady-state conditions. Due to facility constraints, this experiment is conducted at room temperature where the water nanodroplets do not undergo phase change.

The natural convective curves are plotted in Figure 6-10 for the pure FC72 and the nanoemulsion fluids containing from 3 to 12 vol % water nanodroplets. It is evident in this figure that the presence of water nanodroplets can systematically increase natural convective heat transfer in these nanoemulsion fluids. The heat transfer is enhanced further at 12 vol % than at 9 vol %. The increased heat transfer in the nanoemulsion fluids, could be explained using the classical correlation: $Nu_D = hD/k = mRa_D^{0.188}$, where *Nu* is the Nusselt number, *Ra* is the Rayleigh number, *h* is the heat transfer coefficient, D is the wire diameter, and m is an empirical constants. The natural convective heat transfer is predicted to be increased by 7.9% and 15%, in the water-in-FC72 nanoemulsion fluids containing 9 and 12vol.% water nanodroplets respectively, when the properties presented in the aforementioned sections are used. It can be found in Figure 6-10 that the

corresponding increases are 6.8% and 13%, respectively. The prediction and the experimental results are in reasonable agreement. Higher enhancement in natural convective heat transfer is expected in these fluids when the water nanodroplets undergo melting-freezing phase transition. Note that, in several conventional nanofluids containing solid nanoparticles, the rate of natural convective heat transfer has been experimentally found to be suppressed at large volume fractions of particles, but augmented for small volume fractions due to the drastic increase in viscosity.

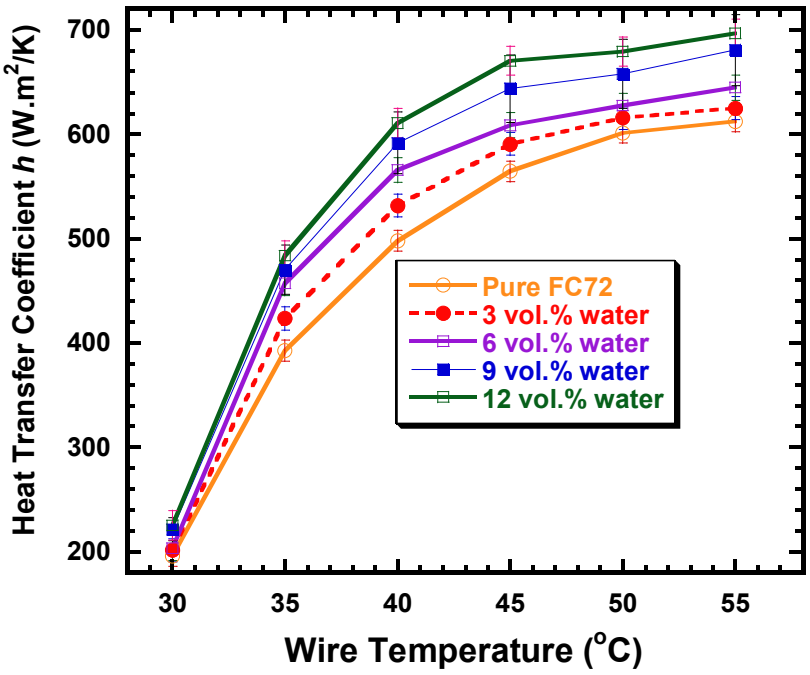

Figure 6-10 Natural convective heat transfer curves for pure FC72 and the water-in-FC72 nanoemulsion fluids. Note the bulk temperature of FC72 is 24 °C while the boiling point of FC 72 is 56 °C

6.9 Summary

In summary, the concept of nanoemulsion fluids — dispersions of liquid nanostructures in heat transfer fluids—has been demonstrated via the study of the water-in-FC72 nanoemulsion fluids. Thermophysical properties, including thermal conductivity, viscosity, and specific heat, have been investigated experimentally in these fluids. The viscosity increase appears to be nonlinear with the volume fraction of water nanodroplets, analogous to the trend observed in thermal conductivity. The nonlinear rise in conductivity and viscosity at high water loadings could be accounted for by hydrodynamic interaction and aggregation of water nanodroplets. These thermophysical properties along with the classical correlations could be used to explain the enhancement in natural convective heat transfer measured in these fluids. An interesting and very useful behavior observed is that water nanodroplets can undergo melting-freezing phase transition, which can lead to over 100% increase in effective specific heat of the fluids. The very promising development of nanoemulsion fluids with simultaneously enhanced thermal conductivity and specific heat could show a bright direction for thermal fluid studies. Nanoemulsion fluids consisting of water nanodroplets emulsified in FC72 have been developed and observed to exhibit significantly improved thermal conductivity enhancements compared to fluids containing no particles or conventional nanofluids containing solid particles. Moreover, such nanoemulsion fluids have long-term stability and can be produced in large quantities, holding great promise for becoming the next generation of heat transfer fluids needed for thermal management in the near future.

7 Phase-Change Indium-in-PAO Nanofluids

7.1 Introduction

Polyalphaolefins (PAOs) are synthetic oils made by polymerizing alpha-olefins as monomers. Now PAOS with low molecular weights have been used as lubricants and synthetic motor oils for vehicles in a wide temperature range. PAOs are a class of specially designed chemicals having many advantages over mineral oils, such as better oxidative stability, much smaller volatility, excellent low-temperature viscosities, extremely high viscosity index, excellent pour points and freedom from impurities. However, just like many other heat transfer fluids, the thermal conductivity of PAOs is relatively low, about 0.14 W/m. K at room temperature, only 24% of that of water. Besides thermal conductivity, the heat capacity of PAO is 1.736 J/ml.K, while the heat capacity of water is 4.18 J/ml.K. Thermophysical properties of some materials are shown in table 7-1 for comparison.

Table 7-1 Thermophysical properties of materials used for the synthesis of phase-change metallic nanoparticles-in-PAO nanofluids

Materials	Density (g/cm3)	Thermal conductivity (W/m.K)	Heat Capacity (J/ml.K)	Heat of fusion (J/ml)
PAO 2Cst	0.8	0.14	1.736	
Indium	7.31	81.8	1.7025	208.8884
Gallium	5.91	40.6	2.1920	473.8307
Wood's Metal	9.7	Low		371.0250
Fields' Metal	9.1	Low		
Amalloy117	9.16	Low		

The idea of adding solid nanoparticles to heat transfer fluids in order to enhance the thermal conductivity has been introduced somewhere else. As a new type of advanced heat transfer fluids, nanofluids have been attracting extensive research interest (Choi 1998; Das et al. 2006; Ding et al. 2006; Eastman et al. 2004; Han et al. 2007; Keblinski et al. 2005; Wen et al. 2005; Xie et al. 2001; Yang and Han 2006b). It has then been suggested to use nanofluids to improve the heat exchange efficiency instead of conventional heat transfer fluids.

In conventional nanofluids for heat transfer purpose, the high thermal conductivity of solid nanoparticles or carbon nanotubes is exploited and the nanofluids therefore obtain better thermal conduction. However, the heat capacity of nanofluids usually is not improved at all. The importance of enhancing heat capacity of nanofluids leads to the idea of using phase change nanoparticles instead of common solid nanoparticles to make nanofluids. Actually, slurries containing microencapsulated phase change materials (MCPCMs) have been investigated as heat transfer fluids in order to increase the thermal storage capacity (Farid et al. 2004; Yamagishi et al. 1996; Yamagishi et al. 1999). However, usually organic PCMs with very low thermal conductivity are used in these slurries, which may impair the thermal conductivity of fluids. Moreover, the diameter of the microcapsules is several micrometers, and these large particles could cause damage and corrosion problems to the channels and pipelines due to the high momentum and energy carried by large particles. In the previous chapter 6, water nanodroplets have already been used to boost both the thermal conductivity and the heat capacity of fluorocarbons. In this chapter, a concept of using metallic phase change nanoparticles as the dispersed phase to synthesize nanofluids instead of common solid metallic

nanoparticles is proposed. As an example, a phase change indium-in-PAO nanofluid is successfully synthesized and the thermal transport properties of the nanofluid are characterized. The phase transition behavior of the dispersed indium nanoparticles is also investigated.

7.2 Synthesis of Indium Nanoparticles

In this chapter, metallic phase change nanoparticles (low-melting point metals and eutectic alloys) are used to make nanofluids in attempt to simultaneously increase the thermal conductivity and the heat capacity of heat transfer fluids. This idea is demonstrated in this paper by the preparation and the characterization of indium-in-PAO nanofluids.

The conventional production methods of nanofluids are limited – nanofluids are usually produced by dispersing as-prepared nanoparticles or nanotubes into base fluids. In this chapter, one-step nanoemulsification method is used to synthesize the indium-in-PAO nanofluids, and this method has been introduced in Chapter 3. With this one-step method, nanofluids can be conveniently made by directly emulsifying low-melting-point liquid metals into PAOs with the presence of proper surfactants. After enough duration of being exposed to high-intensity ultrasonication, at a temperature above the melting points of metals, stable metallic nanodroplets-in-oil nanoemulsions are formed. By cooling off the nanoemulsions to below the freezing points of the nanodroplets, metallic nanoparticles are obtained which are stably suspended in the oil. The phase change is a reversible process and both nanodroplets and nanoparticles are stable in the oil.

The emulsifying of molten indium in PAO can be made with the addition of a proper amount of polymeric surfactant, e.g., polyolefin aminoester. This nanoemulsification technique for making nanofluids exploits the extremely high shear rates generated by the ultrasonic agitation and the relatively large viscosity of the continuous phase – PAO (Figure 7-1), to rupture the molten indium down to a diameter of below 100 nm. The indium nanoparticles in the nanofluids are about 20 ~ 40 nm in diameter according to the TEM observation. The nanofluids sustain stable and no precipitation was observed after the decreasing of temperatures to below the melting points of indium.

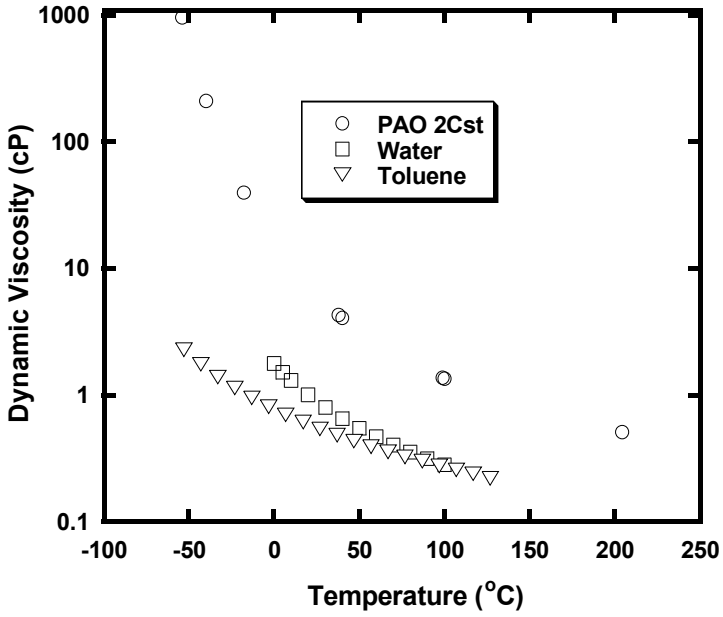

Figure 7-1 Dynamic viscosity of PAO, water and toluene as a function of temperature. Much higher viscosity index is found in PAO 2Cst than water and toluene

PAO has very high dynamic viscosity. According to Taylor's formula, the dimensions of the dispersed nanodroplets can be estimated as (Taylor 1934),

$$r \approx \sigma / (\mu_f \dot{\gamma}) \tag{7-1}$$

Where r is the radius of the ruptured nanodroplets; σ is the interfacial tension between the dispersed phase and continuous phase; μ_f is the viscosity of the continuous phase; $\dot{\gamma}$ is the shear rate. High viscosity of the continuous phase is conducive of obtaining nanodroplets. Comparison of the viscosity of PAO, water and toluene are made in Figure 7-1. In order to prepare indium-in-PAO nanofluids, bulk indium was added to PAO in the reaction vessel, and then the mixture was heated up to 20 ^{o}C above the melting temperature of indium by heating the vessel in a silicone oil thermal bath, whose temperature is digitally controllable. A thermocouple was immersed in the mixture to monitor the temperature. The experimental set-up is shown in Figure 7-2. After the metal was completely melted and the pre-set temperature was reached, polyalphaolefin aminoester as the surfactant was immediately injected into the reaction vessel. The significant excess amount of surfactant enabled new surface area of the ruptured droplets to be rapidly coated during emulsification, therefore limiting shear-induced coalescence (Mason et al. 2007). The molten metal was then dispersed in the PAO using a magnetic stirrer for 2 hours to create micro-scaled metal droplets. This premixed emulsion was then exposed to high-intensity ultrasound irradiation (VCX 750, Sonics & Materials, Inc) for more than 2 hours till stable nanoemulsion formed. A long time ultrasonic treatment is necessary in order that all droplets can experience the highest shear rate and their size has a reasonably uniform distribution. Once the nanoemulsion was cooled to room temperature, solidified indium nanoparticles were obtained and, these nanoparticles stay stable in the oil phase due to the existence of surfactant at their surface. It should be noted that nitrogen was used as purge gas to prevent oxidation during the ultrasonic treatment.

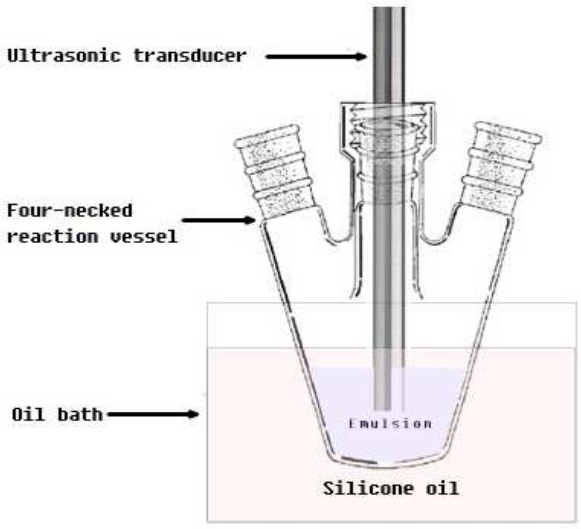

Figure 7-2 Experimental set-up of the nanoemulsion preparation

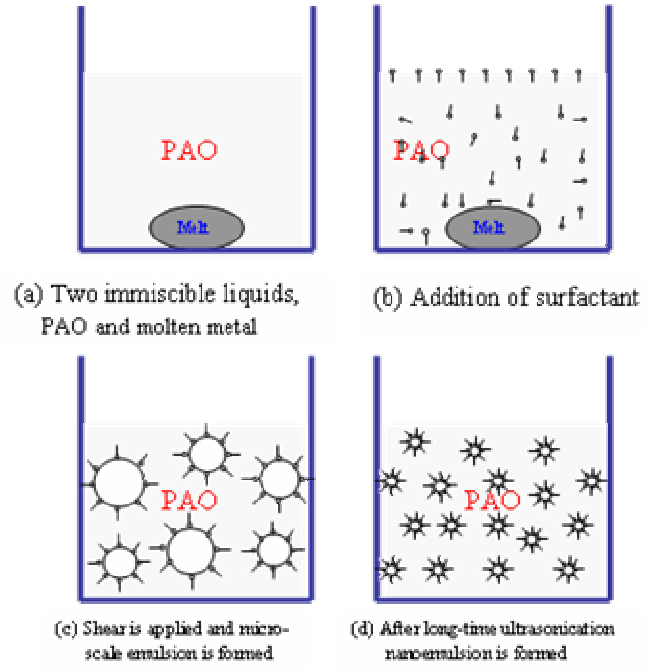

Figure 7-3 Schematic illustrating the formation of molten metal-in-oil nanoemulsion. (a) PAO and molten metals are in the reaction vessel. These two liquids are immiscible and phase separate; (b) Polymer surfactant is soluble in PAO and preferentially adsorbs at the interface. One end shows affinity to metallic liquids and the other end extends to the solvent to impart solubility; (c) The mixture is stirred using a magnetic stirrer and the bulk molten metal breaks into microscale droplets; (d) The microscale emulsion is exposed to high-intensity ultrasonication till nanoemulsion is formed

The process of nanoemulsion formation in this experiment is illustrated in Figure 7-3. Nanofluids can be centrifuged and indium nanoparticles can be gathered and re-dispersed into the solvent to make more concentrated nanofluids. The nanofluid used in this paper contains 8 vol.% indium nanoparticles.

The dimension and geometry of the indium nanoparticles are investigated under Field Emission Transmission Electron Microscope (FE-TEM, model JEOL 2100F). To prepare TEM samples, 5 μL nanofluid was transferred from the reaction vessel and dissolved in 5 ml toluene. One small drop of the toluene solution was placed on the carbon-coated copper grids. The toluene would evaporate rapidly and only nanoparticles were left atop the copper grids. TEM bright field (BF) images of indium nanoparticles are shown in Figure 7-4. The as-prepared nanoparticles are spherical, possibly because the liquid nanodroplets have a positive interfacial tension (i.e., surface energy) in the

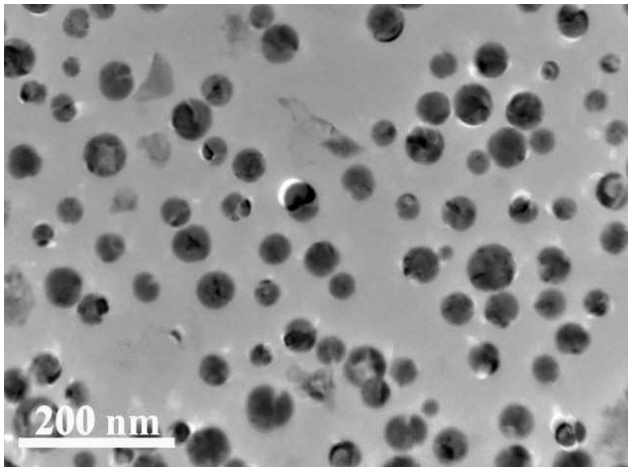

Figure 7-4 TEM BF image of indium nanoparticles

emulsification process and the solid nanoparticles inherited the shape of the liquid nanodroplets. The polymer surfactants appear to provide sufficient steric stabilization despite the strong cohesion forces among molten indium nanodroplets. Indium

nanoparticles are well dispersed and isolated from one another, rather than in the form of aggregates. The diameter of indium nanoparticle is found to be ~ 30 nm in average and in a range of distribution from 10 to 50 nm.

7.3 Thermal Conductivity Measurement

The thermal conductivity of the pure PAO and indium-in-PAO nanofluid (8 vol. %) were measured in the temperature range of 30 – 90^{o}C using a 3ω-wire technique (Cahill 1990; Yang and Han 2006a; Yang and Han 2006b). The thermal conductivity of the pure PAO and indium-in-PAO nanofluid, and as well as the relative thermal conductivity, are plotted against temperature in Figure 7-5. The relative thermal conductivity is defined as k_{nf}/k_f, where k_f and k_{nf} are thermal conductivities of the base fluid and nanofluid, respectively. The thermal conductivity of PAO is experimentally found to be 0.143 W/mK at room temperature, which compares well with the literature values (Choi et al. 2001).

It is evident in Figure 7-5 that the thermal conductivity enhancement increases slightly with increasing temperature in the In/PAO PCM nanofluid, about 10.7% at 30 ^{o}C and 12.9% at 90 ^{o}C. This temperature dependence is much weaker than that in some other nanofluids measured with the hot-wire technique. For example, the data of Das et al. showed a factor of about 3 increase in thermal conductivity enhancement for a temperature increase of about 30 ^{o}C (Das et al. 2003a). It seems the contribution of Brownian motion of indium nanoparticles to the thermal transport is not significant.

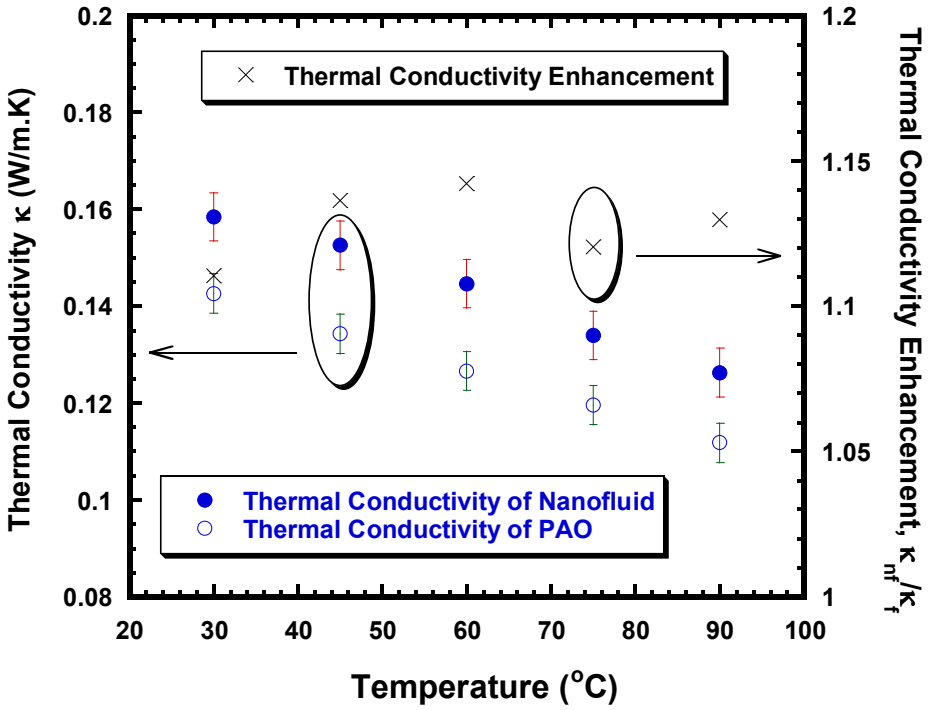

Figure 7-5 Thermal conductivity of the pure PAO and In/PAO nanofluid (left x-axis) and relative conductivity of the nanofluid (right x-axis) vs. temperature

7.4 Heat Capacity of Phase-Change Nanofluids

In addition to the thermal conductivity, heat capacity and rheological property are both important in determination of the thermal transport properties of nanofluids. Heat capacity of the nanofluid and the phase change behavior of included nanoparticles were investigated using a differential scanning calorimeter (DSC, model TA-Q100). The results are shown in Figure 7-6. Volumetric heat capacities of PAO and indium are 1.74 J/ml.K and 1.67 J/cm^3.K respectively at room temperature. In the case of no phase transition of indium nanoparticles, the heat capacity of nanofluid can be easily determined according to a simple rule of mixture (ROM) (Han and Yang 2008). The heat capacities of PAO and indium are so close, without phase change of nanoparticles, that

the addition of indium nanoparticles to PAO has minor influence on the heat capacity and, which has been verified by the DSC results, as shown in Figure 7-6.

7.5 Phase Change Behavior of indium-in-PAO nanofluids

An exciting and useful characteristic of phase-change-nanofluids is that those phase change nanoparticles included in nanofluids undergo a phase transition process, which is, melting and freezing, during heating and cooling cycles. The phase change behavior of the indium-in-PAO nanofluid is measured using a Differential Scanning Calorimeter (DSC, Model TA-Q100). DSC measurements were taken at an ordinary cyclic ramp mode, and the scan rate was 10 ^{o}C/min. The cyclic DSC curves are shown in Figure 7-6. On the DSC cyclic curves of the nanofluid and bulk indium, the endothermic peaks at around 158 ^{o}C corresponds to the melting of bulk indium and indium nanoparticles, while the exothermic peaks at 154 ^{o}C on the cyclic curve of bulk indium and 110 ^{o}C on the cyclic curve of the nanofluid correspond to the freezing of bulk indium and indium nanoparticles, respectively. Compared to that of bulk indium, a large hysteresis is found in the freezing process of indium nanoparticles, possibly due to the change in the interfacial energy of indium nanoparticles relative to that of bulk indium because indium nanoparticles are coated by polymeric surfactants, while the surface of bulk indium is exposed to air (Xu et al. 2006). The effects of the phase transition of included nanoparticles on the thermal transport properties of nanofluids are substantial. Through the addition of phase changeable indium nanoparticles, the effective heat capacity of the heat transfer fluids can be significantly improved. The effective specific heat can be defined as $C_{p,nf} = C_{p,f} + \phi H_{np} / \Delta T$, where ϕ is the volume fraction of the phase-

changeable nanoparticles, H_{np} is the latent heat of the phase-changeable nanoparticles per unit volume, and ΔT is the temperature difference between the heat transfer surface and the bulk fluid (Han and Yang 2008). In this experiment, if ΔT is assumed to be 45 °C, the effective volumetric specific heat can be increased by up to 20% for the nanofluid containing 8 vol. % indium nanoparticles due to the latent heat released and absorbed during phase transition. The application of phase-changeable nanoparticles in nanofluids is expected to provide a route to simultaneously increase the effective heat capacity and the thermal conductivity of conventional heat transfer fluids.

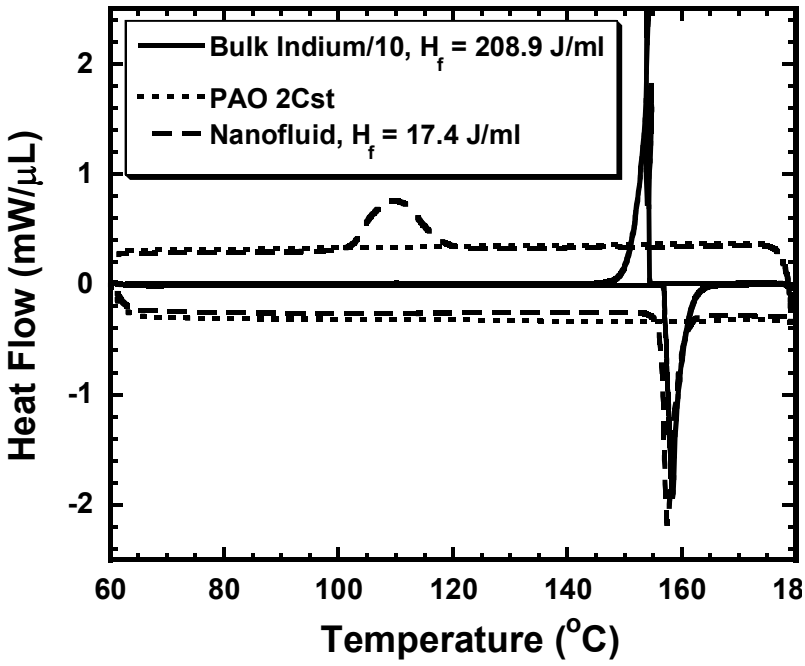

Figure 7-6 DSC curves of PAO, PAO-based nanofluid containing indium nanoparticles and bulk indium

Large hysteresis in the solidification temperature of the nanoparticles is observed in DSC heating-cooling cyclic curves. The hysteresis is about 40°C for indium nanoparticles. The melting phenomena of nanoparticles are being studied using either classical

thermodynamics or molecular simulation techniques. Several excellent theoretical models have been proposed to account for the size effect and successfully described or predicted the melting phenomena of nanoparticles, among which a theory based on the Laplace equation of the surface and the Gibbs-Duhem equation predicts a melting temperature depression in the form as(Peters et al. 1998),

$$T_{rm} = 1 - 2\alpha / (\rho_S H_f^b r) \quad 0 < T_{rm} \leq 1 \tag{7-2}$$

where T_{rm} is the reduced melting temperature, which equals to the ratio of melting temperatures of nanoparticles with radius r to that of bulk materials with radius of infinity, $T_{rm} = \frac{T_m(r)}{T_m(\infty)}$. ρ_S is the density of the solid, H_f^b is the latent heat of fusion of bulk materials and α is a value differing slightly in different models, for example, in a homogeneous melting model, α equals the difference between solid-vapor and liquid-vapor interfacial energies, $\alpha = \sigma_{SV} - \sigma_{LV}$. It can be derived from this model that the melting temperature of solid particles is strongly size dependent - the smaller nanoparticles possess lower melting temperatures. But actually, the depression of melting point of nanoparticles is not obvious till the particle size reduce to 10 nm. For the LMP metallic nanoparticles prepared by ultrasonication, the particle size is not small enough to have obvious depression in their melting points (Jiang et al. 2006). So apparently the hysteresis phenomenon of nanoparticle solidification is not only size dependent. Recent molecular dynamics studies have shown that the melting and freezing begin at the surface (Qi et al. 2001). The solidification temperature of nanoparticles is thus related to the interfacial energies between solids, liquids, and coating materials. If the interfacial energies of solid-liquid, solid-coating, and liquid-coating are denoted as between

Based on the classical nucleation theory, the melting and freezing of these nanoparticles are intimately tied to the interface energies between the solid metal and oil matrix, the liquid metal and oil matrix, and the solid and liquid metals (σ_{SM}, σ_{SL}, and σ_{LM}, respectively) (Vehkamaki 2006). The observed T_m slightly below the bulk value implies that $\sigma_{LM} < \sigma_{SM} + \sigma_{SL}$, where σ is the interfacial energy. Therefore, the solid nanoparticles will pre-melt or nucleate at the interfaces with the continuous oil phase. In contrast to melting, a relatively large freezing-point depression was found for indium nanoparticles dispersed in PAO oil. This is probably due to $\sigma_{SM} > \sigma_{SL} + \sigma_{LM}$. In this situation, the molten phase would not ‘‘pre-solidify’’ at the interfaces, and, instead, require critical nucleus inside these nanoparticles, i.e. homogeneous nucleation. So, these liquid nanoparticles could be subcooled to tens of degrees below the bulk melting temperature till critical nucleus associated with solidifying is reached. This characteristic might provide a way to tailor the phase transition behavior of nanoparticles via varying their interfacial energy or size for their different applications.

7.6 Viscosity of Indium-in-PAO Nanofluids

A Brookfield DV-I Prime viscometer is used for viscosity measurement of the base fluid and the nanofluid at different temperatures. Viscosities of PAO and the nanofluid are shown in Figure 7-7, along with the theoretical values obtained according to a modified Einstein equation. The dynamic viscosity of solid particle suspensions can be described by Einstein equation, $\mu_r = 1 + 2.5\phi$, where $\mu_r = \frac{\mu_{nf}}{\mu_f}$, is the ratio of the

viscosity of the nanofluid to that of the base fluid, and ϕ is the volume fraction of solid particles (Einstein 1906). The experimental results show that the viscosity of the nanofluid is from 22% to 30% higher than that of PAO depending on the temperature. The Einstein equation underestimates the viscosity increase in the indium-in-PAO nanofluid and the reason lies in that Einstein equation is derived based on dilute colloidal systems (assuming volumetric fraction of solids < 0.01). For more concentrated colloids in which the hydrodynamic interaction and aggregation become more important, a modified Einstein equation, $\mu_r = 1 + 2.5\phi + B\phi^2 + \cdots$, (Batchelor 1977) with higher order terms of the volume fraction is used. The coefficient of the linear term, 2.5 is strictly derived, however, the coefficient of the second-order term *B*, is not simple to theoretically determine due to the difficulty in accounting for the effects of concentrations. Herein *B* is obtained to be about 13.6 by fitting the experimental data using Least Square Method. The nonlinear viscosity increase in concentrated colloid is common, which is attributable to the hydrodynamic interaction and aggregation of the included nanoparticles (Batchelor 1977; Prasher et al. 2006c). In several EMT models, these effects have also been included to give a better explanation of the thermal conductivity enhancement of nanofluids than the Maxwell's model did.

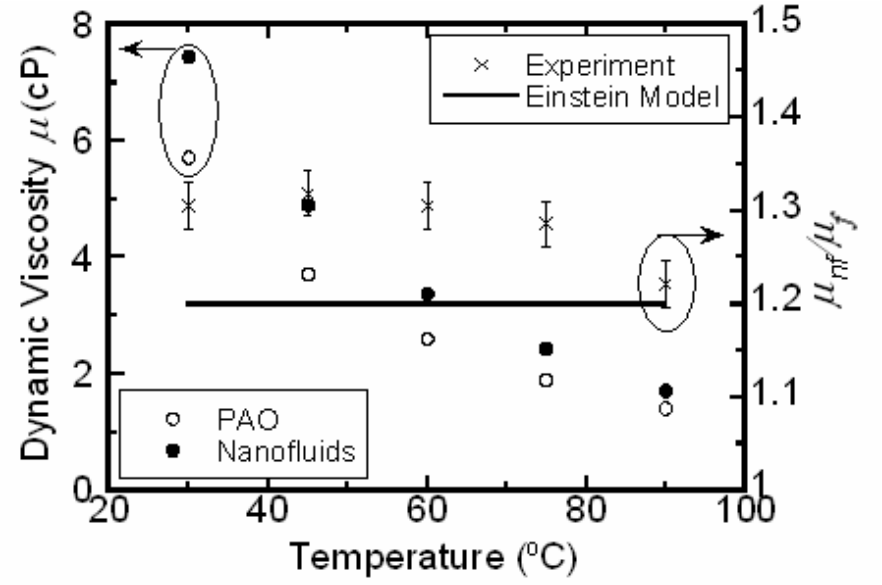

Figure 7-7 Dynamic viscosity of PAO and nanofluid at different temperatures. The coefficient *B* used in the modified Einstein equation is estimated with LSM as 13.6

7.7 Summary

To summarize, a novel concept of phase-change nanofluids by dispersing phase changeable nanoparticles into conventional heat transfer fluids has been demonstrated through the study of a PAO based nanofluid containing indium nanoparticles. Indium nanoparticles are produced by directly emulsifying molten indium in PAO at the presence of polymeric surfactant. The prepared indium nanoparticles sustain stable in the continuous PAO phase due to the polymeric surfactant impart solubility and steric stability to these nanoparticles. The average diameter of indium nanoparticles are about 30 nm. Thermophysical properties, including the thermal conductivity, the heat capacity and the viscosity have been investigated experimentally. Up to 12.9% enhancement in thermal conductivity has been found at different measurement temperatures. The viscosity increase of nanofluids appears to obey the prediction of Einstein's equation.

The phase transition behavior of the nanofluid is examined using DSC. It is found that the indium nanoparticles undergoes a reversible phase transition while staying stable in PAO and exhibit a relatively large hysteresis in the melting-freezing process compared to that of bulk indium. Up to 20% increase in heat capacity of the nanofluid can be obtained by adding 8 vol.% of phase changeable indium nanoparticles. The development of phase-change nanofluids with simultaneously enhanced thermal conductivity and specific heat shows the potential of this new type advanced heat transfer fluids.

8 Modeling Thermal Transport in Nanofluids

8.1 Introduction

In this chapter, thermal transport properties, including the density, the heat capacity, the viscosity, and the thermal conductivity of nanofluids are theoretically modeled to give an in-depth understanding of the properties of nanofluids.

Investigation of the transport properties of heterogeneous composites had been carried out since Maxwell's pioneer work. For the simplicity of modeling, nanofluids are assumed to be composed of a continuous phase, that is, the base heat transfer fluid, and one or more discontinuous phases, that is, dispersed solid nanoparticles and/or liquid nanodroplets. Obviously, the properties of nanofluids are dependent on intrinsic properties of base fluids and nanoparticles and/or nanodroplets. In addition, the details of the microstructures of nanofluids, including the geometry, the dimensions, the volumetric fraction, the distribution and the motion of nanoparticles or nanodroplets, the properties of interfaces between base fluids and nanoparticles, etc.

8.2 Density, Heat Capacity and Dynamic Viscosity of Nanofluids

The density and the heat capacity of nanofluids can be simply estimated according to the Rule of Mixture (ROM) (details can be found in **Appendix**). The dynamic viscosity of nanofluids is usually calculated by using Stokes-Einstein equation (when $\varphi < 0.03$) or a more accurate Eistein-Batechelor equation (for $\phi < 0.1$) (**Appendix**).

8.3 Thermal Conductivity Enhancement

8.3.1 Effective Medium Theory

Conventionally, the calculations of the thermal conductivity of nanofluids are carried out without taking into consideration of the size, the geometry, the distribution and the motion of dispersed particles, while only thermal conductivities of base fluids and particles, and the volumetric fraction of particles count. These models are termed "Effective Medium Theory" and are used to describe the thermal conductivity of suspensions of large particles. Details of EMT models are shown in **Appendix**.

Maxwell (Maxwell 1873) was the first to investigate the thermal conduction of liquid suspensions analytically by considering a very dilute suspension containing spherical particles and ignoring the interactions among particles. Herein, effective thermal conductivity of nanofluids, $\boldsymbol{k_{EMT}}$, are thus depends only on thermal conductivity of matrices/base fluids, $\boldsymbol{k_f}$ **,** thermal conductivity of dispersed particles, $\boldsymbol{k_p}$, and the volumetric fraction of particles, ϕ.

The Maxwell's model was then adopted and modified by Hamilton and Crosser (HC model) (Hamilton and Crosser 1962a; Hamilton and Crosser 1962b) after taking into consideration of the particle geometry, and their model has been used for the description of the thermal conductivity enhancement of a dilute suspension of spherical/non-spherical particles in a liquid or a solid.

In addition to the shape factor, the interfaces between two materials, i.e., liquid base fluids and solid particles, acts as a thermal barrier to the heat flow because of the poor chemical bonding between atoms and/or molecules at the interfaces, and the difference in

thermal expansion properties of the different materials. It usually can be neglected for macroscopic objects; however, this is not the case for particles with reduced size. It is therefore important that the interfacial resistance, or Kapitza resistance, R_k, should be included in the calculations in order to more accurately predict the temperature distribution, heat flux, and the thermal conductivity of the liquid suspensions. Interfacial resistance R_k arises from the differences in phonon spectra of the two materials, and subsequently from the scattering of the phonons at the interfaces. Hasselman and Johnson modified Maxwell's model in order to include a term of the interfacial thermal resistance (Hasselman and Johnson 1987). The resulting theoretical prediction for the effective thermal conductivity enhancement of the particle-in-liquid colloidal suspensions is given by,

$$k_{EMT} = \frac{k_p(1+2\Gamma) + 2k_f + 2\left[k_p(1-\Gamma) - k_f\right]\phi}{k_p(1+2\Gamma) + 2k_f - \left[k_p\left(1-\Gamma\right) - k_f\right]\phi} k_f \qquad (8\text{-}1)$$

In this equation, $\Gamma = 2R_{bd}k_f / d_p$, where d_p is the average particle diameter, R_{bd} is the interfacial thermal resistance (or Kapitza resistance), and d is the diameter of spherical particles. In the absence of thermal boundary resistance ($R_{bd} = 0$), the above equation reduces to Maxwell's model.

The Hasselman and Johnson model has been used to describe the thermal conductivity enhancement in water-in-FC72 nanoemulsion nanofluids. The diameter of water nanodroplets is d_p = ~ 10 nm; the thermal conductivity of water is 0.58 W/m.K; the thermal conductivity of FC72 is estimated by [0.060 – 0.00011T (^{o}C)] W/m.K, i.e., at 25 ^{o}C, thermal conductivity of FC72 is 0.057 W/m.K. The interfacial thermal conductance,

G = 65 MW/m^2.K is used in the calculations and the modeling result have been shown in Figure 8-1. Obviously the experimentally measured values of thermal conductivity are much higher than those predicted by EMT theory. The larger-than-predicted conductivity enhancement indicates that there are other mechanisms contribute to the thermal conductivity enhancement in nanofluids.

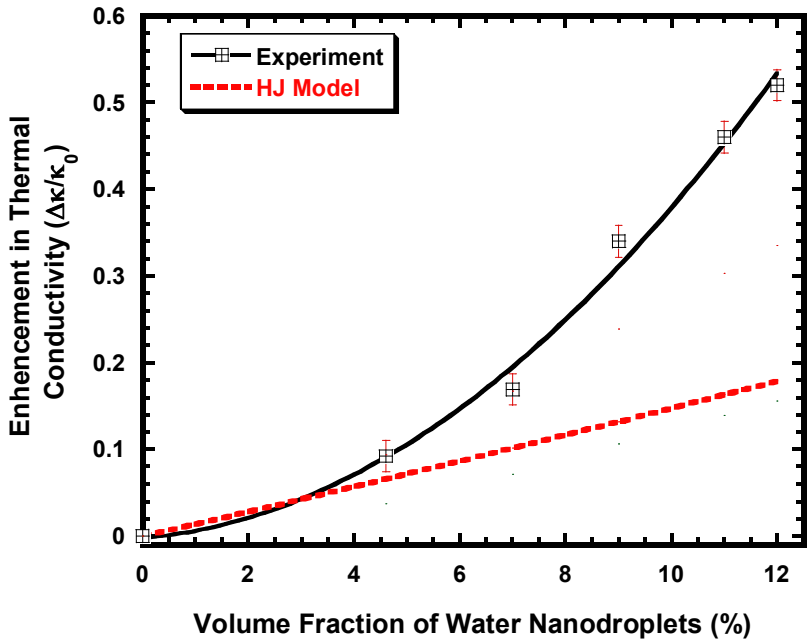

Figure 8-1 Experimental data and EMT values of the thermal conductivity enhancement in water-in-FC72 nanofluids

As for indium-in-PAO nanofluids, the average diameter of nanoparticles is d_p = ~30 nm; the interfacial resistance is estimated as $R_{bd} = 3.22 \times 10^{-8}$ m^2.K/W; the thermal conductivity of PAO 2 Cst is a function of temperature and decreases with increasing temperature; the thermal conductivity of indium is 81.8 W/m.K. The Hasselman-Johnson model is also used to describe the thermal conductivity enhancement in nanofluids and

results are shown in Figure 8-2. It can be observed that the thermal conductivity enhancements predicted by HJ model match the experimental results well.

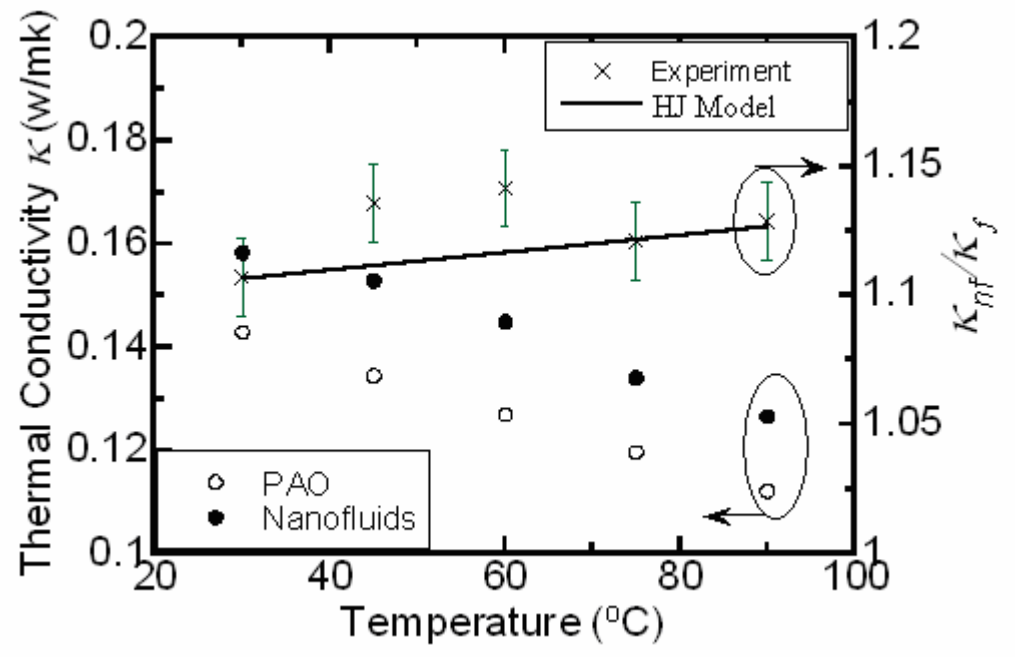

Figure 8-2 Thermal conductivity of the pure PAO and indium-in-PAO nanofluid (left x-axis) and relative conductivity of the nanofluid (right x-axis) vs. temperature. The relative thermal conductivity estimated from the HJ Model (solid line) is also shown for comparison. A temperature-independent interfacial resistivity $R_{bd} = 3.22 \times 10^{-8}\ m^2\ K/W$ is used in this calculation

8.3.2 Brownian motion of Nanoparticles

In order to explain the anomalous enhancement in thermal conductivity of nanofluids, Keblinski proposed four possible mechanisms (Keblinski et al. 2005; Keblinski et al. 2002): (1) Brownian Motion of nanoparticles; (2) liquid layering at liquid/particle interface; (3) ballistic nature of heat transport in nanoparticles; (4) nanoparticle clustering in nanofluids (Details are provided in **Appendix**). It is believed

that micro-convection induced by the Brownian motion of nanoparticles may be one of the main reasons responsible for the increase of nanofluid thermal conductivity. When a particle immersed in a fluid, it moves randomly due to the interaction between the particle and its surrounding fluid molecules and this random motion is called “Brownian motion”. The Brownian motion of large particles is negligibly small and it is not considered in the traditional particulate flow. However, when the size of particle is as small as nanoparticles, the Brownian motion becomes significant. It has been reported that the thermal conductivity enhancement in nanofluids increase substantially with increasing temperature and decreasing particle size, which indicates the contribution of Brownian motion to the thermal conduction in nanofluids. This is also consistent with the high mobility or diffusivity of the water nanodroplets measured in the DLS experiment.

However, conventional EMT models on thermal conductivity of nanofluids are based on an assumption that the heat transports in each phase and between phases are only governed by the diffusion. These models successfully explain the effective thermal conductivity of liquid suspensions containing millimeter or even micrometer sized solid particles. The higher-than-predicted, temperature and size dependent thermal conductivity of nanofluids needs the discovery of new thermal transport mechanisms of nanofluids.

Nanofluids are homogeneous and well dispersed system. Due to the tininess of nanoparticles in nanofluids, additional energy transport may arise from the Brownian motions induced by stochastic and inter-particle interacting forces.

It is already known that the velocity of nanoparticles is inversely proportional to the square of the particle diameter, and with reducing particle size, the drift velocity of

nanoparticles increases rapidly. For example, for nanoparticles with diameters ranging from 100 ~ 10 nm which are suspended in water at room temperature (25 ^{o}C), the velocity increases from about 3×10^{-4} m/s to about 3×10^{-2} m/s. A model has been derived by Jang and Choi (Jang and Choi 2004) based on conduction, Kapitza resistance at the interfaces and convection by taking into consideration of four modes of energy transport: thermal conductance of fluid, thermal diffusion in nanoparticles, interactions & collisions between nanoparticles, and micro-convection effects caused by Brownian motion. As the particle size is reduced to tens of nanometer, the Brownian motion of nanoparticles becomes drastic, and micro-convection effects become dominant.

In their model, Jang and Choi introduced a completely new idea that the Brownian motion of nanoparticles would produce a convection-like effect at nanoscale in nanofluids. The contribution of micro-convection to the thermal conductivity of nanofluids is estimated as,

$$k_{convec} \propto C\frac{d_{mol,f}}{d_p}k_f \,\mathrm{Re}_{d_p}^2 \,\mathrm{Pr}\,\phi \tag{8-2}$$

In this equation, C is a proportional constant, $d_{mol,f}$ is the diameter of the base fluid molecule, and Re_{d_p} is the Reynolds number defined by,

$$\mathrm{Re}_{d_p} = \frac{U_p d_p}{\mu_f}$$

in which U_p and μ_f are the random motion velocity of nanoparticles and dynamic viscosity of the base fluid. U_p has been defined as (Bhattacharya et al. 2004),

$$U_P = \frac{2k_B T}{\pi \mu_f d_p^2}$$

Translational diffusivity, D_B is given in the Stokes equation,

$$D_B = \frac{k_B T}{3\pi \mu_f d_p}$$

where k_B is the Boltzmann constant, μ_f is the viscosity of the base fluid and T is the temperature.

The advantage of this advanced model is that both the temperature and the size dependences of the thermal conductivity enhancement have been taken into consideration, and the predictions made by this model are in excellent agreement with the experimental data. Conventional EMT models fail to explain these dependences and the reason lies in that in those models, nanoparticles are considered to be motionless, which holds only for large particles. The new dynamic model, by including the micro-convection mechanism due to the Brownian motion of nanoparticles, not only explains the particle loading and the temperature dependence, but also successfully explains the strong particle size dependence for the first time. This model has shown that the localized micro-convection caused by Brownian motion of nanoparticles plays a key role in enhanced thermal conductivity of nanofluids.

The thermal conductivity enhancement in water-in-FC72 nanofluids are then described by using the dynamic model, starting from the HJ model (Hasselman and

Johnson 1987) and taking into consideration of the contribution of the Brownian motion effects of water nanodroplets. The length of C-C bond is about 154 pm, and so the diameter of FC72 molecules is estimated as ~ 0.7 nm. Base on this molecular diameter, the mean free path of FC72 molecules can be estimated,

$$l_{mol,f} = \frac{1}{\sqrt{2}\pi {d_{mol}}^2 n}$$

where n is the density of FC72 molecules, which can be estimated as $n = 2.9825 \times 10^{27} / m^3$.

The enhancement of thermal conductivity in nanofluids then comes from two contributions: static thermal conduction and thermal convection caused by Brownian motion of nanoparticles, as shown in the following equation,

$$k_{nf} = \frac{k_p(1+2\Gamma) + 2k_f + 2\left[k_p(1-\Gamma) - k_f\right]\phi}{k_p(1+2\Gamma) + 2k_f - \left[k_p(1-\Gamma) - k_f\right]\phi} k_f + C\left(\frac{d_{m,f}}{d_p}\right)\left(\frac{k_B T}{3\pi\mu_f \nu_f l_f}\right)^2 \Pr \phi k_f \tag{8-3}$$

This model is used to describe the thermal conductivity of water-in-FC72 nanofluids and the results are shown in Figure 8-3. It can be found that this model still underestimates the thermal conductivity enhancement at high concentrations of water nanodroplets even the contribution of the Brownian motion has been considered. The reason lies in that with increasing water concentration, the pair interactions between

water nanodroplets become significant, so that the contribution of particle interaction can not be neglected. However, particle interactions are neglected in this new dynamic model.

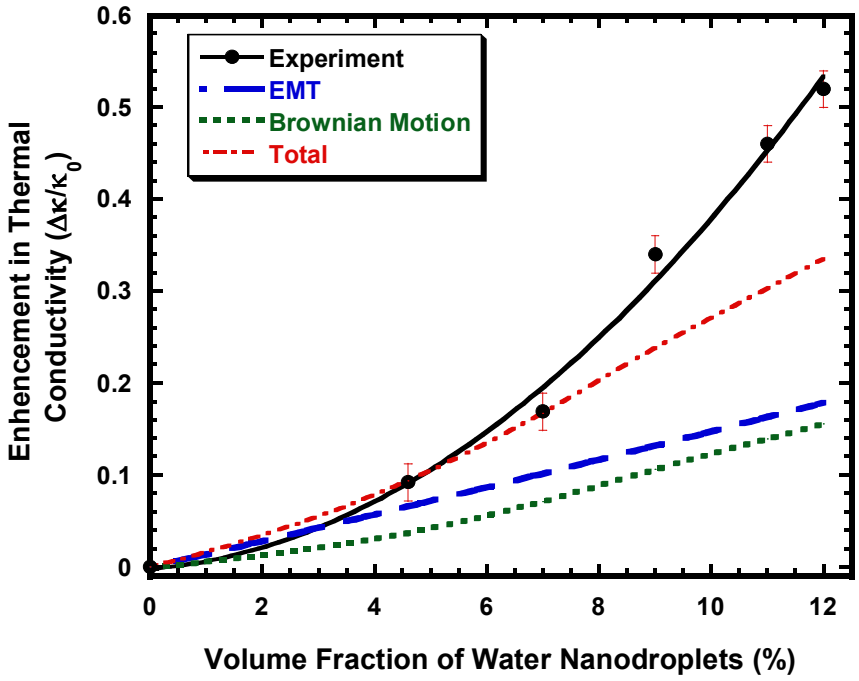

Figure 8-3 Comparison of the thermal conductivity enhancement predicted by a theoretical model and the experimental data. The theoretical models include the contributions from both thermal conduction and Brownian motion

No anomalous enhancement of thermal conductivity has been found in indium-in-PAO nanofluids. Since HJ model well describes the thermal conductivity, it seems that the contribution of Brownian motion of indium nanoparticles to the thermal transport is less important compared to water nanodroplets in FC72. There are several reasons, which can be used to explain this phenomenon. The first reason is that the dynamic viscosity of FC72 is much lower than that of PAO (0.64 cP vs. 5.7 cP). Secondly, water nanodroplets are only 10 nm in diameter, while indium nanoparticles are 30 nm. So the Brownian

diffusivity and the velocity of indium nanoparticles in PAO are much smaller than those of water nanodroplets in FC72 according to the Stokes-Einstein equation. Another reason is the addition of long-chain polymeric surfactants during synthesizing indium nanoparticles. Polymeric surfactants with high molecular weight attach onto the surface of indium nanoparticles, cause increase in the effective diameter of particles and produce a drage force, which make the nanoparticles behave like a large particles in base fluids. Moreover, the thermal conductivity of polymeric surfactant is relatively low, so the polymer surfactants at the surface of nanoparticles may increase the Kapitza resistance.

8.3.3 Other Mechanisms

Other mechanisms for the thermal conductivity enhancement in nanofluids include the ordered layering formation of liquid molecules at the surface of nanoparticles and the effects of nanoparticle clusters/aggregates.

Liquid molecules in contact with solids show more structural ordering than molecules in the bulk liquid. Experiments and simulations have shown that an ordered layer of liquid molecules forms at the liquid-solid interfaces and the width of the ordered interfacial layer is on the order of several atomic distances (Yu et al. 1999a; Yu et al. 1999b). The magnitude of the ordered layers of liquid molecules increases with increasing solid–liquid bonding strength, and usually the ordered layer extend into the liquid over several atomic or molecular distances. These ordered layers show crystalline-like structures and have higher thermal conductivity than disordered bulk liquids. For example, the thermal conductivity of water is 0.56 W/m.K at 0 ℃, while the thermal conductivity of ice is 2.2 W/m.K.

The molecular diameter of conventional heat transfer fluids, for example, water, is about 3 Å, which means the interfacial liquid layering is about 5~15 Å. The liquid layering around the particle may give a path for rapid heat transfer. The effect of the liquid layering is insignificant when the particle is large, however, with decreasing particle size, the volume of ordered liquid molecules increases drastically.

Based on the effective medium theory, the equivalent thermal conductivity of the "composite nanoparticle" composed of the nanoparticle and the ordered layer of liquid molecules, k_{cp} can be obtained. At the same time, the effective volume fraction of nanoparticles, ϕ_{eff}, also increases due to the formation of nanolayers. By plugging k_{cp} and ϕ_{eff} into the Maxwell's model, the thermal conductivity enhancement due to the formation of highly conductive ordered-liquid structure can then be simply calculated according to the Effective Medium Theory, and the results are shown in Figure 8-5 (Details in **Appendix**).

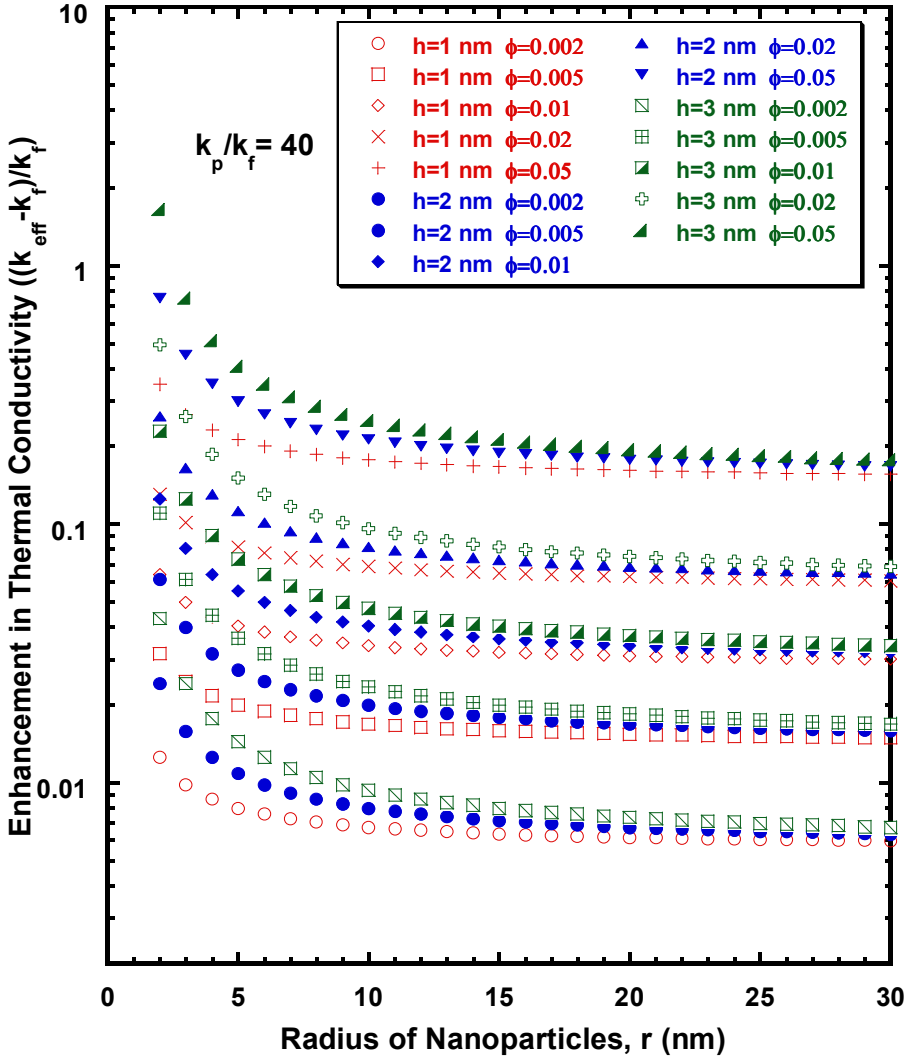

Figure 8-4 Thermal conductivity enhancements as a function of nanoparticle radius with consideration of the effect of ordered layers of liquid molecule on the surface of nanoparticles

Another mechanism for the thermal conductivity enhancement in nanofluids is the formation of clusters/aggregates of nanoparticles. Nanoparticles could cluster into percolating networks, create fast paths with much lower (than that of base fluids) thermal resistance and thus have a major effect on the effective thermal conductivity. It has been postulated that the anomalous enhancement in thermal conductivity of nanofluids at least

partly be due to nanoparticles clustering and the consequential percolating networks. A hypothesis is proposed depending upon the formation of loose clusters of nanoparticles due to the attractive forces between them. The size of the cluster/aggregate structure is larger than the individual particles, and hence, the volumetric fraction of the clusters is larger than that of the collection of particles. The effective thermal conductivity based on the volume fraction of the clusters would be more than that predicted based on particle volume fraction. While this proposition has the correct trend, it implicitly assumes that conductivity of the trapped fluid molecules is higher than that of the fluid. The detailed discussion of the contribution of nanoparticle aggregates to the thermal conductivity enhancement is given in **Appendix**.

9 Conclusions, Major Contributions and Future Directions

9.1 Conclusions of Experimental and Modeling Work

In this study, new nanofluids based on Hexadecane, FC72 and PAO are synthesized by adding semiconductor nanorods, urchin-like nanoparticles, phase-change nanodroplets and phase-change nanoparticles as the dispersed phases. A one-step nano-emulsification technique has been developed and used to synthesize these nanofluids. The thermal transport properties of nanofluids, including thermal conductivity, viscosity, heat capacity and heat transfer coefficient in convective environment were characterized and modeled. A reliable 3ω-wire method has been established to precisely measure the thermal conductivity enhancement of nanofluids. Obvious thermal conductivity increase from 6% to 52% has been observed in these nanofluid systems.

Bi_2Te_3 nanorods were successfully prepared with a sonochemical method, which are 20 nm in diameter and 170 nm in length. These nanorods were dispersed into hexadecane using ultrasonication and oleic acid was used as the surfactant. Stable nanorods-in-oil nanofluids were made, and their temperature-dependent thermal conductivity has been investigated in a temperature range from 20 to 50 ^{o}C. The thermal conductivity of Bi_2Te_3 nanorods apparently decreases with increasing temperature, and consequently the thermal conductivity enhancement in nanofluids also decreases when operating temperature rises, 6.1% at 20 ^{o}C and 3.9% at 50 ^{o}C; however, the thermal conductivity of nanofluids is still slightly higher than theoretical values predicted by EMT due to the Brownian motion of nanorods. The experimental and analytical results show that the dominant mechanism in thermal conductivity enhancement in nanofluids is

determined by the particle aspect ratio. The effects of the Brownian motion are predominant in nanofluids containing spherical nanoparticle or nanoparticles with low aspect ratios, while the diffusive heat conduction mechanism will gradually take over the dominance as the aspect ratio of nanoparticles increases.

A hybrid tubes-on-spheres nanostructure, i.e., urchin-like nanoparticles, has been designed for enhancing thermal transport in nanofluids, which is expected to take advantages of both nanosphere's diffusive mobility and CNTs' high-conductivity. Such urchin-like nanoparticles, synthesized by a spray pyrolysis method and then dispersed in PAO oil, have increased the thermal conductivity by about 20% for volume fractions of 0.2% at room temperature. The experimental results indicate that the urchin-like nanoparticles can provide higher thermal conductivity enhancement in nanofluids as compared to either CNTs or oxide spheres at the same particle loading. The enhanced thermal conductivity in nanofluids containing urchin-like nanoparticles is attributed to the high thermal conductivity of CNTs, the high-aspect-ratio of CNTs, the Brownian motion of nanoparticles, as well as the fast heat transfer path through the central oxide nanoparticles. A conclusion can be drawn from this research that novel particle morphologies, such as urchin-like nanoparticles, would provide a new opportunity for nanofluid research.

The concept of nanoemulsion fluids -- dispersions of liquid nanostructures in heat transfer fluids -- has been demonstrated via the study of the water-in-FC72 nanoemulsion fluids. Thermophysical properties, including thermal conductivity, viscosity, and specific heat, have been investigated experimentally in these fluids. Up to 52% enhancement in thermal conductivity has been observed in these nanofluids. It has also been observed that

the viscosity increase is nonlinear with increasing volume fraction of water nanodroplets, analogous to the trend observed in thermal conductivity. The nonlinear rise in thermal conductivity and viscosity at high water loadings could be accounted for by the hydrodynamic and thermodynamic interaction between nanodroplets, as well as aggregation and clustering effects. The thermophysical properties along with the classical correlations could be used to explain the 15% enhancement in natural convective heat transfer measured in these fluids. An interesting and very useful behavior observed is that water nanodroplets can undergo melting-freezing phase transition, which can lead to over 120% increase in the effective heat capacity of fluids. The very promising development of nanoemulsion fluids with simultaneously enhanced thermal conductivity and heat capacity could show a bright direction for thermal fluid studies. These water nanodroplets –in-FC72 fluids have exhibited significantly improved thermal conductivity enhancements compared to fluids containing no particles or conventional nanofluids containing solid particles. Moreover, such nanoemulsion fluids have long-term stability and can be produced in large quantities, holding great promise for becoming the next generation of heat transfer fluids needed for thermal management in the near future.

Another phase-change nanofluids by dispersing phase changeable metallic nanoparticles into conventional heat transfer fluids has been demonstrated through the study of a PAO based nanofluid containing indium nanoparticles. Indium nanoparticles are produced by directly emulsifying molten indium in PAO at the presence of polymeric surfactant. The as-prepared indium nanoparticles sustain stable in the continuous PAO phase due to the polymeric surfactant impart solubility and steric stability to these nanoparticles. The average diameter of indium nanoparticles are about 30 nm.

Thermophysical properties, including the thermal conductivity, the heat capacity and the viscosity have been investigated experimentally. Up to 12.9% enhancement in thermal conductivity has been found at different measurement temperatures. The viscosity increase of nanofluids obeys the prediction of Einstein's equation. The phase transition behavior of the nanofluid is examined using a differential scanning calorimeter (DSC). It is found that the indium nanoparticles undergoes a reversible phase transition while staying stable in PAO and exhibit a relatively large hysteresis in the melting-freezing process compared to that of bulk indium. Up to 20% increase in heat capacity of the nanofluid can be obtained by adding 8 vol.% of indium nanoparticles. The development of phase-change nanofluids with simultaneously enhanced thermal conductivity and specific heat have provided us a new opportunity of research on advanced heat transfer fluids with improved thermal transport properties.

Hasselman and Johnson model has been used to describe the thermal conductivity enhancement in water-in-FC 72 nanoemulsion nanofluids. The interfacial thermal conductance, G = 65 MW/m^2.K is used in the calculations. Obviously the experimentally measured values of thermal conductivity are much higher than those predicted by this EMT model. The larger-than-predicted conductivity enhancement indicates that the particle motion, which is not considered in the EMT plays a key role in the thermal conductivity enhancement of the water-in-FC72 nanoemulsion fluid. This is also consistent with the high mobility or diffusivity of the water nanodroplets measured in DLS experiments. In general, for smaller particles and less-viscous base liquids, the particles are more mobile and better enhancement in thermal transport can be achieved in the fluids.

The thermal conductivity enhancement in water-in-FC72 nanofluids are then described by using a modified dynamic model, starting from the HJ model (Hasselman and Johnson 1987) and taking into consideration of the contribution of Brownian motion effects of water nanodroplets. This model take into account of the contributions from both the thermal conduction (EMT theory) and the Brownian motion of nanoparticles (the second term on the right side of the equation). The results show that this model still underestimates the thermal conductivity enhancement at high concentrations of water nanodroplets even the contribution of the Brownian motion has been considered. The reason lies in that with increasing water concentration, the pair interaction between water nanodroplets becomes significant, so that the contribution of particle interaction can not be neglected. However, particle interaction effect is neglected in HJ model.

For indium-in-PAO nanofluids, the average diameter of nanoparticles is ~30 nm; the interfacial resistance is estimated as $R_{bd} = 3.22 \times 10^{-8}$ m^2.K/W. Hasselman and Johnson model is used to describe the thermal conductivity enhancement in nanofluids. The result shows that the thermal conductivity enhancements predicted by HJ model match the experimental results well. The reason is due to the addition of long-chain polymeric surfactants during synthesizing indium nanoparticles. Though the average diameter of indium nanoparticles is only ~30 nm, polymeric coatings with high molecular weight attached onto the surface of nanoparticles cause increase in the effective diameter of particles and make the nanoparticles behave like a large particles in base fluids, and the effect of particle motions can be neglected. Moreover, the thermal conductivity of polymer is relatively low, so the polymer surfactants at the surface of nanoparticles increase the Kapitza resistance.

A trade-off phenomenon of increase in viscosity of nanofluids was observed upon the addition of nanodroplets or nanoparticles to enhance thermal conductivity and heat capacity. Einstein-Batchelor correlation was used to predict the viscosity of nanofluids and good agreement was found with the experimental results. The natural convective heat transfer of water-in-FC72 nanoemulsion fluids was also investigated. It is evident that the presence of water nanodroplets can systematically increase the natural convective heat transfer in these nanoemulsion fluids and up to 15% increase in convective heat transfer rate was obtained.

9.2 Major Contributions

This study provides important and comprehensive information for the design, the synthesis, the characterization and the modeling of nanofluids, which have been regarded as potential advanced heat transfer fluids with improved thermal transport properties. The major contributions and accomplishments of this research are as follows:

1. A one-step nanoemulsification method has been developed for mass producing nanofluids. Water-in-FC72 and indium-in-PAO (synthetic oils) nanofluids were successfully synthesized by directly emulsifying water and low-melting point metals in FC72 and PAO respectively, with the presence of appropriate amphiphilic surfactants; the as-prepared water-in-FC72 and indium-in-PAO nanofluids are stable. The diameter of water nanodroplets is around 9 to 10 nm, whilst the diameter of indium nanoparticles ranges from 10 to 50 nm;

2. A reliable 3ω-wire method is established and used to precisely measure the thermal conductivity enhancement in nanofluids. The main advantage of this 3ω-wire method is that the temperature difference between the metal wire and the bulk liquid can be as small as ~ 1 ^{o}C, while this temperature difference for the conventional hot-wire transient method is about ~ 5 ^{o}C; thus the effect of natural convection on the thermal conductivity measurement is greatly reduced;

3. Bi_2Te_3 nanorods were prepared using sonochemical method and dispersed into Hexadecane. The thermal conductivity of Bi_2Te_3 apparently decreases as the temperature increases and thus the contributions of thermal conduction and Brownian motion to the thermal conductivity of nanofluids can be decoupled. The temperature dependence of thermal conductivity in Bi_2Te_3 nanorods-Hexadecane nanofluids was investigated and the analysis of the experimental data suggests that the dominant mechanism in thermal conductivity enhancement in nanofluids strongly depends on the nanoparticle aspect ratio. The effect of the Brownian motion is predominant in nanofluids containing spherical nanoparticle, while the diffusive thermal conduction mechanism will gradually take over the dominance as the aspect ratio increases;

4. A hybrid tubes-on-spheres nanostructure has been designed and used to increase the thermal conductivity of PAO. It has been experimentally shown that this hybrid structure can combine the advantages of CNTs and oxide nanospheres: CNTs have high thermal conductivity and large aspect ratio, and thus are very effective to increase the thermal conductivity of heat transfer fluids, while the oxide spheres act as Brownian motion centers, maintain the stability of the

nanofluid system and provide a fast heat transfer path among carbon nanotubes; The performance of nanofluids containing this hybrid nanoparticles is much better than nanofluids containing only CNTs or oxide nanoparticles and this would open a new direction to improve the performance of nanofluids;

5. Phase Change water-in-FC72 nanofluids are synthesized and characterized. The thermal conductivity is enhanced by 52% by adding 12 vol.% water nanodroplets. Meanwhile, the thermal conductivity enhancement and the viscosity increase are found to be nonlinear with the increasing volume fraction of water. Meanwhile, 15% enhancement of heat transfer rate in a naturally convective environment has been observed. Furthermore, water nanodroplets can undergo melting-freezing phase transition, which leads to 126% increase in effective specific heat of the fluids. The very promising development of nanoemulsion fluids with simultaneously enhanced thermal conductivity and specific heat could show a bright direction for thermal fluid studies. Water-in-FC72 nanofluids have long-term stability and can be produced in large quantities, showing potential for becoming advanced heat transfer fluids for thermal management;

6. Phase Change Indium-in-PAO nanofluids are synthesized with the one-step nanoemulsification method. Phase changeable and thermally conductive indium nanoparticles are expected to simultaneously improve the thermal conductivity and the heat capacity of conventional HTFs. The as-prepared indium nanoparticles sustain stable in the continuous PAO phase due to the polymeric surfactant impart solubility and steric stability to these nanoparticles. The

average diameter of indium nanoparticles is 30 nm. Thermophysical properties, including the thermal conductivity, the heat capacity and the viscosity have been investigated experimentally. 13% enhancement in thermal conductivity has been observed in these nanofluids at 90 ^{o}C. It has found that the indium nanoparticles undergo a reversible phase transition while staying stable in PAO. Up to 20% increase in heat capacity of the nanofluid can be obtained with a 8 vol.% loading of phase changeable indium nanoparticles.

9.3 Future Directions

The objective of the nanofluid research is to develop new nanofluids synthesis methods, build reliable thermophysical measurement equipments, synthesize novel nanofluids with outstanding thermal transport properties, obtain comprehensive experimental data and appropriate theoretical models, and then these data and models can be used to guide the production of nanofluids for different applications, that is, if requirements of nanofluids for different applications are proposed, a specific nanofluid can be designed to meet such requirements by dispersing particles with specific properties, size and geometry, choosing base fluids, setting proper volume fraction of nanoparticles and using appropriate synthesis techniques.

A multidisciplinary center for nanofluids research has been founded in MIT for nuclear energy industry. Researchers in this center are evaluating the potential impact of using nanofluids in nuclear energy industry on the safety, neutron and economic issues. The exciting results are just demonstrating the potential of applications of nanofluids. Static measurements of thermal conductivity as well as other dynamic measurements

yield encouraging results. Although the use of nanofluids in a wide variety of thermal management applications has a brilliant future, the main blockade that hindering the development of nanofluid research and application is that a detailed atomic-leveled understanding of all the mechanisms which are responsible for the observed change of properties is unclear. However, there are still several important clues indicating the mechanisms of heat transfer in nanofluids, which can be drawn from numerous research papers on nanofluid properties:

1. Size of dispersed nanoparticles seems to be important. With reducing nanoparticle size, the dispersion behavior improves and the surface-to-volume ratio increases. Thermal transport in nanofluids involves the heat transfer in the vicinity of the nanoparticle-fluid interfaces, so the increased surface area will improve the heat transfer rate between nanoparticles and fluids. However, based on today's synthetic and processing techniques, the size of nanoparticles is hard to control or can only be controlled over a rather narrow range of sizes. Thus it is difficult in the nanofluid research to uncouple the effect of particle size on heat transfer from other factors. A challenge is to develop new synthetic and dispersion techniques to enable a systematic study of a series of nanofluids which are only different in the size of the dispersed nanoparticles.
2. Particle agglomeration and coagulation is undesirable. If the nanoparticles can be prevented from agglomerating and coagulating, the dispersion behavior of them improves substantially. Other than the nanofluids containing carbon nanotubes, larger enhancements in thermal conductivity have been obtained in nanofluids with less agglomeration. On the other hand, studies have shown the thermal

transport of nanofluids is strongly affected by the presence of surfactants or dispersants which attach to the surface or nanoparticles. These chemicals improve the dispersion of nanoparticles; however, the Kapitza resistance of the nanoparticle-fluid interface may also be strongly affected by these chemicals.

3. The temperature dependence of thermal conductivity enhancement may be exploited. Quite a few studies have reported that the thermal conductivity enhancement of nanofluids show a strong temperature dependence. This temperature effect not only provides a clue that the nanoparticle motion in nanofluids plays an important role, but also indicates that nanofluids are suitable to be used as a type of advanced coolants at elevated temperatures.
4. Surface properties of nanoparticle surface are an important factor. Previous studies have indicated that thermal transport in nanofluids would be affected by the surfactant molecules attached to nanoparticle surfaces. Surfactants improve the dispersion, impart solubility to nanoparticles, and provide long-term stability of nanofluids. However, the thermal resistance of the nanoparticle-fluid interface is also affected by surfactants attached to the surface. Surfactants could impact particle mobility and the ordered layering of liquid molecules. Sometimes, surface treatment of nanoparticles is a better way to improve the dispersion in fluids instead of using surfactants.
5. Nanoparticle geometry has influence on the effectiveness. At the current stage, spherical nanoparticles and long carbon nanotubes are the most used nanostructures for nanofluids. Other nanostructures, such as nanorods, nanowires, nanoplates and complex-shaped nanoparticles are less investigated. It has been

shown that nanorods with moderate aspect ratio are effective to increase the thermal conductivity of fluids, while they are still in Brownian Motion and keep stability of nanofluids.

6. Phase change nanoparticles are useful to simultaneously improve the thermal conductivity and heat storage capacity of nanofluids and further increase the heat transfer efficiency. Two phase-change nanofluids have been developed and characterized in this research and very promising results were observed. Other combinations of phase change nanoparticles and base fluids are going to be explored.

9.4 Relevant Publications and Patents

1. **Z.H. Han,** B. Yang. *Synthesis and thermal characterization of phase-changeable indium/polyalphaolefin nanofluids.* Applied Physics Letters, 92(24), 243104 (2008).
2. **Z.H. Han,** B. Yang, Y. Qi, Y, J. Cumings. *Synthesis of Low-Melting-Point Metallic Nanoparticles with a Nanoemulsion Method.* Ultrasonics, submitted.
3. **Z.H. Han,** B. Yang. *Thermophysical characteristics of water-in-FC72 nanoemulsion fluids.* Applied Physics Letters, 92 (1), 013118 (2008).
4. **Z.H. Han,** B. Yang, S.H. Kim, M.R. Zachariah. *Application of hybrid sphere/carbon nanotube particles in nanofluids.* Nanotechnology 18(10), 105701 (2007).
5. B. Yang, **Z.H. Han**. *Temperature-dependent thermal conductivity of nanorod-based nanofluids.* Applied Physics Letters, 89 (8), 083111 (2006).

6. B. Yang, **Z.H. Han**. *Thermal conductivity enhancement in water-in-FC72 nanoemulsion fluids.* Applied Physics Letters, 88 (26), 261914 (2006).
7. B. Yang and **Z.H. Han**, "Suspensions of Metallic Nanoparticles with Low-melting Temperature for Heat Transfer Applications," Invention Disclosure, PS-2006-078, 2006.
8. B. Yang and **Z.H. Han**, "Emulsions of heat transfer fluids including nanodroplets to enhance thermal conductivities of the fluids," United States Patent Pending, Application No. 11/549169, Oct. 13, 2006.

Appendix

Density of Nanofluids:

The density of nanofluids, ρ_{nf} can be simply estimated as,

$$\rho_{nf} = \frac{m_{nf}}{Vol_{nf}} = \frac{m_f + m_p}{Vol_f + Vol_p} = \frac{\rho_f Vol_f + \rho_p Vol_p}{Vol_f + Vol_p} = (1-\phi)\rho_f + \phi\rho_p \qquad (1)$$

where ϕ is the volume fraction of dispersed phase, ρ_f is the density of the base fluid material and ρ_p the density of nanoparticle material.

Specific Heat Capacity of Nanofluids:

By using the same rule, the specific volumetric heat capacity of a nanofluid, $C_{p,nf}$ can be calculated by a similar equation,

$$\rho_{nf} C_{p,nf} = (1-\phi)\rho_f C_{p,f} + \phi\rho_p C_{p,p} \qquad (2)$$

where $C_{p,f}$ is the heat capacity of the base fluid material and $C_{p,p}$ is the heat capacity of nanoparticle material. According to this equation, basically it is expected that decrease in heat capacity may occur with addition of solid nanoparticles. Some experimental results of specific heat measurements of nanofluids have shown no difference, however, modifications may be needed on these simple equations in case nanoparticles or nanodroplets show size-dependent specific heat.

Viscosity of Nanofluids:

Stokes-Einstein formula is a good approximation for the dynamic viscosity, μ_{nf} of nanofluids,

$$\mu_{nf} = \mu_f (1 + 2.5\phi) \tag{3}$$

where μ_f is the viscosity of the base fluid. Stokes-Einstein is valid only when is small, i.e. $\phi < 0.05$. This equation, however, usually underestimates significantly the viscosity increase in nanofluids at relatively high nanoparticle loadings. For more highly concentrated systems where the hydrodynamic interaction and aggregation of nanoparticles become important, the Einstein equation must be augmented by higher order terms of the volume fraction as,

$$\mu_{nf} = \mu_f (1 + 2.5\phi + B\phi^2 + ...) \tag{4}$$

This equation is called Eistein-Batechelor equation (Batchelor 1976; Batchelor 1977). Although the coefficient for the first-order term, 2.5, and the one for the second term, 6.2, can be strictly derived, it is not a simple task to theoretically determine those for the higher order terms because of the difficulty in accounting for the effects of increased concentrations.

Thermal Conductivity of Nanofluids:

1. Effective Medium Theory (EMT)

Effective thermal conductivity of composites or nanofluids, $\boldsymbol{k_{EMT}}$, are dependent only on the thermal conductivity of base fluids, $\boldsymbol{k_f}$, the thermal conductivity of dispersed particles, $\boldsymbol{k_p}$, and the volumetric fraction of particles, ϕ , and can be expressed as,

$$k_{EMT} = f(k_f, k_p, \phi) \tag{5}$$

An empirical equation called the mixture rule (Lawrence 1973) is given as,

$$k_{EMT}^n = (1-\phi)k_f^n + \phi k_p^n, \ -1 \le n \le 1 \tag{6}$$

For n =1, the empirical equation turns into the parallel mixture rule,

$$k_{EMT} = (1-\phi)k_f + \phi k_p \tag{7}$$

While for n = -1, the equation becomes the series mixture rule,

$$k_{EMT} = \frac{1}{(1-\phi)k_f^{-1} + \phi k_p^{-1}} = k_f + \phi \frac{k_p - k_f}{k_p - \phi(k_p - k_f)} \tag{8}$$

Maxwell (Maxwell 1873) investigated the conduction of liquid suspensions analytically by considering a very dilute suspension containing spherical particles and ignoring the interactions among particles. If the radius of spherical particles are identical, and can be denoted as r_p, in a temperature field T and temperature gradient $\boldsymbol{G_T}$, the governing equation for the steady-state condition is the Laplace equation,

$$\nabla^2 T(\mathbf{r}) = 0 \tag{9}$$

By introducing a large sphere of radius R_0, within which all the solid spherical particles are included in this large sphere, so that from a point $r>>R_0$, the sphere with radius R_0 is considered as a system with an effective thermal conductivity $\boldsymbol{k_{EMT}}$ embedded in a matrix (base fluid) with a thermal conductivity of $\boldsymbol{k_f}$, so the temperature field outside the sphere R_0 can then be expressed as,

$$T(r)=\left(-1+\frac{k_{EMT}-k_f}{2k_f+k_{EMT}}\frac{r_0^3}{r^3}\right)\mathbf{G}_T\cdot\mathbf{r} \tag{10}$$

The above equation is obtained by solving the Laplace equation with the following boundary conditions,

$$T(r)\big|_{r\to\infty}=-\mathbf{G}_T\cdot\mathbf{r}\ ,\ T(r)\big|_{r\to R_0^-}=T(r)\big|_{r\to R_0^+} \tag{11}$$

$$k_{EMT}\left.\frac{\partial T(r)}{\partial r}\right|_{r\to R_0^-}=k_f\left.\frac{\partial T(r)}{\partial r}\right|_{r\to R_0^+} \tag{12}$$

At the same time, the temperature field *T(r)* can also be viewed as all the spherical solid particles with radius r_p being embedded in the matrix with a thermal conductivity of k_f. Using the superposition principle, the following equation can be derived,

$$T(r)=\left(-1+\frac{k_p-k_f}{2k_f+k_p}\frac{\phi r_0^3}{r^3}\right)\mathbf{G}_T\cdot\mathbf{r} \tag{13}$$

By equating the above two equations (8-10) and (8-13), the effective thermal conductivity k_{EMT} can be obtained as,

$$k_{EMT}=\frac{k_p+2k_f+2(k_p-k_f)\phi}{k_p+2k_f-(k_p-k_f)\phi}k_f \tag{14}$$

where k_{EMT} is the effective thermal conductivity of the suspension; k_p is the thermal conductivity of the solid particles; k_f is the thermal conductivity of the base fluids; ϕ is the volumetric fraction of the solid particles.

The Maxwell's model was then adopted and modified by Hamilton and Crosser (HC model) (Hamilton and Crosser 1962a; Hamilton and Crosser 1962b) after taking into the consideration of the particle shape, and their model has been used for the description of the thermal conductivity enhancement of a dilute suspension of spherical/non-spherical particles in a liquid or a solid. The Hamilton-Crosser model can be written as,

$$k_{EMT} = \frac{\alpha + (n-1) - (n-1)(1-\alpha)\phi}{\alpha + (n-1) + (1-\alpha)\phi} k_f \qquad (15)$$

where $\alpha = k_p / k_f$ is thermal conductivity ratio; n is the empirical shape factor, which equals,

$$n = \frac{3}{\Psi}$$

Ψ is the sphericity of the particle, which is defined as the ratio of the surface area of a hypothetical sphere whose volume equals to that of the particle, to the surface area of the particle. For examples, n = 3 for spheres and n = 6 for cylinders.

In addition to the shape factor, the interfaces between two materials, i.e., liquid base fluids and solid particles, acts as a thermal barrier to the heat flow because of the poor chemical bonding between atoms and/or molecules at the interfaces, and the difference in thermal expansion properties of the different materials. It usually can be neglected for macroscopic objects; however, this is not the case for particles with reduced size. It is therefore important that the interfacial resistance, or Kapitza resistance, R_k, should be included in the calculations in order to more accurately predict the temperature distribution, heat flux, and the thermal conductivity of the

suspensions/composites. Interfacial resistance R_k arises from the differences in phonon spectra of the two materials, and subsequently from the scattering of the phonons at the interfaces. Hasselman and Johnson had modified Maxwell's model in order to include a term of the interfacial thermal resistance (Hasselman and Johnson 1987). The resulting theoretical prediction for the effective thermal conductivity enhancement of the particle-in-liquid colloidal suspensions is given by,

$$k_{EMT} = \frac{k_p(1+2\Gamma) + 2k_f + 2\left[k_p(1-\Gamma) - k_f\right]\phi}{k_p(1+2\Gamma) + 2k_f - \left[k_p\left(1-\Gamma\right) - k_f\right]\phi} k_f \qquad (16)$$

In this equation, $\Gamma = 2R_{bd}k_f / d_p$, where d_p is the average particle diameter, R_{bd} is the interfacial thermal resistance (or Kapitza resistance). In the absence of thermal boundary resistance ($R_{bd} = 0$), the above equation reduces to Maxwell's model.

All the above models do not include the pair interactions between the solid particles. Jeffrey (Jeffrey 1973) modified the Hamilton-Crosser model by taking into consideration of the pair interactions of randomly dispersed spheres, which can be expressed as,

$$k_{EMT} = \left[1 + 3b\phi + \left(3b^2 + \frac{3b^2}{4} + \frac{9b^3}{16}\frac{\alpha+2}{2\alpha+3} + \frac{3b^4}{2^6} + ...\right)\phi^2\right] k_f \qquad (17)$$

where $b = (\alpha - 1)/(\alpha + 2)$, $\alpha = k_p / k_f$ is thermal conductivity ratio. Jeffrey's model is accurate to order of ϕ^2, in which the high-order terms represent pair interactions of randomly dispersed spheres.

There are several other models used to describe the effective thermal conductivities of liquids suspensions, such as Davis's model and Lu-Lin's model, which are shown as follows,

Davis's Model (Davis 1986):

$$k_{EMT} = \left[1 + \frac{3(\alpha - 1)}{(\alpha + 2) - (\alpha - 1)\phi}\left(\phi + f(\alpha)\phi^2 + 0\left(\phi^3\right)\right)\right] k_f \tag{18}$$

where $\alpha = k_p / k_f$ is thermal conductivity ratio; $f(\alpha) = 2.5$ for $\alpha = 10$; $f(\alpha) = 0.5$ for $\alpha = \infty$. This model is accurate to order ϕ^2. High-order terms represent pair interactions of randomly dispersed spheres.

Lu-Lin's model (Lu and Lin 1996):

$$k_{EMT} = \left(1 + a\phi + b\phi^2\right) k_f \tag{19}$$

This model can be used for liquid suspensions containing spherical and non-spherical particles. For spherical particles, a=2.25, b=2.27 for $\alpha = 10$; a=300, b=4.51 for $\alpha = \infty$.

2. Modern models

2.1. Interfacial Liquid layering

According to the Maxwell's model, which has been introduced in the foregoing text, the effective thermal conductivity of a homogeneous suspension can be described as,

$$k_{EMT} = \frac{k_p + 2k_f + 2\left(k_p - k_f\right)\phi}{k_p + 2k_f - \left(k_p - k_f\right)\phi} k_f \tag{20}$$

where k_{EMT} is the effective thermal conductivity of the suspension; k_p is the thermal conductivity of the solid particles; k_f is the thermal conductivity of the base fluids; ϕ is the volumetric fraction of the solid particles.

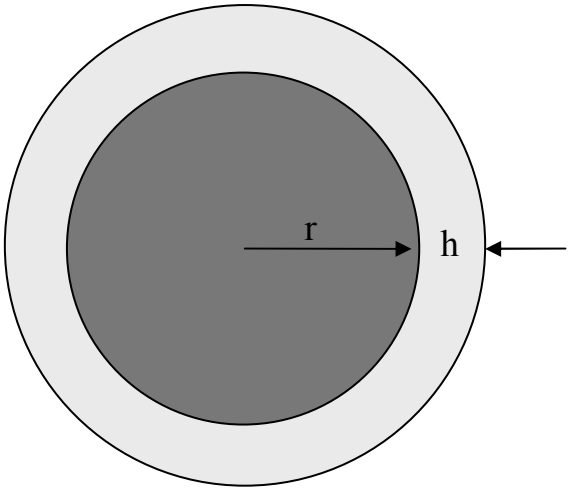

Figure A-1 Schematic cross-sectional structure of a nanoparticle and the interfacial nanolayer of liquid molecules

Based on the effective medium theory, the equivalent thermal conductivity of the "composite nanoparticles", k_{cp}, can be expressed as (Schwartz et al. 1995),

$$k_{cp} = \frac{[2(1-\alpha)+(1+\xi)^3(1+2\alpha)]\alpha}{-(1-\alpha)+(1+\xi)^3(1+2\alpha)} k_p \tag{21}$$

where $\alpha = k_{layer} / k_p$, is the ratio of nanolayer's and particle's thermal conductivities; $\xi = h / r$ is the ratio of the ordered layer thickness to the radius of the nanoparticle, as shown in Figure A-1.

The effective volume of nanoparticles increases due to the formation of nanolayers,

$$\phi_{eff} = n_p . \frac{4}{3}\pi(r+h)^3 = n_p . \frac{4}{3}\pi r^3 (1+h/r)^3 = n_p . \frac{4}{3}\pi r^3 (1+\xi)^3 = \phi(1+\xi)^3 \quad (22)$$

in which n_p is the number of particles.

Plug k_{cp} and ϕ_{eff} into the Maxwell's model, the Maxwell equation can be updated as,

$$k_{EMT} = \frac{k_{cp} + 2k_f + 2\left(k_{cp} - k_f\right)\phi_{eff}}{k_{cp} + 2k_f - \left(k_{cp} - k_f\right)\phi_{eff}} k_f \quad (23)$$

2.2. Brownian motion of nanoparticles

When they are well dispersed in fluids (air or liquids), tiny particles are in random Brownian motion. If only the diffusion of nanoparticles in one dimension is considered, the force balance on a particle in Brownian motion takes the form of (Friedlander 2000),

$$m\frac{du}{dt} = -fu + F(t) \quad (24)$$

where m is the particle mass, u is the velocity, f is the coefficient of friction, and t is the time. From this equation, it can be seen that the force acting on a particle can be divided into two parts. The first term on the right of the equation is the frictional resistance of the fluid, which is assumed to be proportional to the velocity of the particle. In the case of spherical particles, whose size is much

larger than the mean free path of fluid molecules, based on Stokes equation, the friction coefficient *f* can be expressed as,

$$f = 3\pi\mu_f d_p \tag{25}$$

$F(t)$ represents a fluctuating force due to the thermal motion of molecules of the ambient fluid. This force can be assumed to be independent of the velocity of particles, and its mean value, $\overline{F}(t)$ vanishes over a larger number independent particles (interactions between these particles is neglected). Moreover, $F(t)$ is assumed to fluctuate much more rapidly with time than the velocity. Over some interval, Δt , u will be practically unchanged while there will be practically no correlation between the values of $F(t)$ at the beginning and end of the interval.

Now a group of small particles are taken into consideration, which are originally located near the plane $x = 0$ at $t = 0$. At a later time $t > 0$, particles move around as a result of Brownian motion to form a cloud, which is symmetric around $x = 0$.

By setting $A(t) = F(t)/m$, $\beta = f/m$ and multiplying both sides by x, the displacement from the plane x = 0, the result of a single particle becomes,

$$x\frac{du}{dt} + \beta ux = xA \tag{26}$$

Rearranging,

$$\frac{dux}{dt} + \beta ux = u^2 + xA \tag{27}$$

Integrating between t = 0 and t, the result is (Friedlander 2000),

$$ux = e^{-\beta t}\int_0^t u^2 e^{\beta t'} dt' + e^{-\beta t}\int_0^t Axe^{\beta t'} dt' \tag{28}$$

where t' is dummy number of time t for integration. By using the initial condition, $ux = 0$ at $t = 0$, and averaging over all the particles,

$$\overline{ux} = \frac{\overline{u^2}}{\beta}\left(1 - e^{-\beta t}\right) \tag{29}$$

Because $\overline{u^2}$ is assumed to be a constant and $\overline{Ax} = 0$ due to no correlation between the instantaneous force and the particle displacement. The following relationships also hold,

$$\overline{ux} = \frac{\overline{xdx}}{dt} = \frac{\overline{dx^2}}{2dt} = \frac{1}{2}\frac{d[\overline{x^2}]}{dt} \tag{30}$$

Because that the derivative of mean with respect to time in the above equation particles is equal to the mean of the derivative with respect to time. By equating the last two equations and integrating once from t = 0,

$$\frac{\overline{x^2}}{2} = \frac{\overline{u^2}t}{\beta} + \frac{\overline{u^2}}{\beta^2}\left(e^{-\beta t} - 1\right) \tag{31}$$

For $t >> \beta^{-1}$,

$$\frac{\overline{x^2}}{2} = \frac{\overline{u^2}t}{\beta} \tag{32}$$

Because the particles share the molecular thermal motion of the fluid, the principle of equipartition of energy is assumed to apply to the translational energy of the particles,

$$\frac{m\overline{u^2}}{2} = \frac{k_B T}{2} \tag{33}$$

So,

$$\frac{\overline{x^2}}{2} = \frac{k_B T t}{f} \tag{34}$$

Setting

$$D_B = \frac{\overline{x^2}}{2t} = \frac{k_B T}{f} \tag{35}$$

$$\overline{x^2} = 2D_B t \tag{36}$$

where D_B is defined as the coefficient of diffusion. This is the Stokes-Einstein expression for Brownian motion.

For three dimension,

$$\overline{R^2} = \overline{x^2} + \overline{y^2} + \overline{z^2} = 6D_B t \tag{37}$$

For the translational diffusion of the Brownian motion, according to the Stokes-Einstein relationship (Chandler 1974),

$$D_B = \frac{k_B T}{n\pi\mu_f d_p} \tag{38}$$

where n = 6 for non-slip and n = 4 for slip boundary conditions, μ_f is the viscosity of the solvent.

The instantaneous velocity of the Brownian nanoparticles can be estimated as (Bhattacharya et al. 2004):

$$U_P = \frac{2k_B T}{\pi\mu_f d_p^2} \tag{39}$$

While d_p is the diameter of the nanoparticles.

It can be seen from the above equation that the velocity is inversely proportional to the square of the particle diameter, and with reducing particle size, the drift velocity of nanoparticles increases rapidly. A model has been derived by Jang and Choi (Jang and Choi 2004) based on conduction, Kapitza resistance at the interfaces and convection by taking consideration of four modes of energy transport: thermal conductance of fluid; thermal diffusion in nanoparticles; interactions, collisions between nanoparticles and convection-like effects at nano-scale due to the Brownian motion. As the particle size is reduced, the Brownian motion of nanoparticles becomes larger, and convection-like effects become dominant. Microscopic motions of nanoparticles causing micro-convections are believed to may enhance heat transfer, and this mechanism is not taken into account in conventional EMT theories which apply in liquid suspensions containing large particles, the particles are assumed to be stationary and this

assumption holds when the particle is large. For nanoparticles in nanofluids, microscopic forces including the Van der Waals force, the electrostatic force resulting from the electric double layer, the stochastic force, and the hydrodynamic force, are significant compared to their inertia and enough to cause the nanoparticles to move around. However, it should be advised that the stochastic force and the electrostatic force are significant only for tiny particles, while the Van der Waals force becomes large at small distances between particles. Therefore, there exists a relation between the effective thermal conductivity and the particle size, as has been observed in experiments.

The enhancement in thermal conductivity due to the Brownian motion can be estimated at given temperature of the base fluid containing nanoparticles with known size and geometry. The contribution to enhancement in effective thermal conductivity of the rotational motion of spherical particles can be estimated as (Leal 1973),

$$\Delta k_{rot} = k_f \cdot \phi \cdot \left[\frac{1.176(k_p - k_f)^2}{\left(k_p + 2k_f\right)^2} + 5 \times \left(0.6 - 0.028 \frac{k_p - k_f}{k_p + 2k_f} \right) \right] Pe_r^{3/2} \qquad (40)$$

where Pe_r is the Peclet number, and $Pe_r = \left(r^2 \gamma \rho c_{p,f} / k_f\right)$, in which r is the radius of nanoparticles, γ is the velocity gradient calculated from the mean Brownian motion velocity and the average distance between nanoparticles, ρ is the density, and $c_{p,f}$ is the specific heat of the base fluid. The contribution of the translational motion of nanoparticles to the thermal conductivity enhancement has been given by Gupta et al as (Gupte et al. 1995),

$$\Delta k_{eff,trans} = k_f \cdot \left(0.0556 Pe_t + 0.1649 Pe_t^2 - 0.0391 Pe_t^3 + 0.0034 Pe_t^4\right) \quad (41)$$

where Pe_t is the modified Peclet number and defined as $Pe_t = \left(U_p L \Pi \rho_f c_{p,f} / k_f\right) \phi^{3/4}$, in which U_p is the velocity of the nanoparticles relative to the bulk liquid, while Π is defined as $\Pi = (r_p / \phi^{1/3}) \cdot (4\pi / 3)^{1/3}$.

The thermal conductivity increase due to Brownian motion of nanoparticles includes both the contributions of rotational and translational motions. However, it can be estimated from the above two equations that the increase in thermal conductivity is small due to the small Peclet number, which means that heat transfer by advection of the nanoparticles is less than that transferred by fluid molecules diffusion. In other words, when the particles move in liquid, the temperature of the particles quickly equilibrate with that of the surrounding fluids due to the small size of the particles. The Brownian motion of nanoparticles in nanofluids has been considered as the most probable mechanism when developing theoretical models to explain the anomalous thermal conductivity enhancement of nanofluids. Though it has been pointed out that the direct Brownian motion contribution to heat transfer in nanofluids is negligible, reported experimental data have indicated that Brownian motion should be responsible to for two important thermal transport phenomena in nanofluids: strong temperature- and particle-size dependent thermal conductivity enhancement. Xie et al. (Xie et al. 2003) measured the thermal conductivity of aqueous alumina nanofluids with varying nanoparticle sizes and showed that the thermal conductivity enhancement of nanofluids strongly depends on particles size. In 2004, two ANL researchers,

Dr. Jang and Dr. Choi (Jang and Choi 2004) developed a dynamic model by taking into consideration of the Brownian motion induced convection.

In this model, they introduced a completely new idea that the Brownian motion of nanoparticles would produce a convection-like effect at nanoscale in nanofluids. The effective thermal conductivity of nanofluids is given by,

$$k_{nf} = k_f(1-\phi) + k_p\phi + C\frac{d_f}{d_p}k_f \,\mathrm{Re}_{d_p}^2 \,\mathrm{Pr}\,\phi \tag{42}$$

In this equation, C is a proportional constant, and Re_{d_p} is the Reynolds number defined by,

$$\mathrm{Re}_{d_p} = \frac{U_p d_p}{\nu_f}$$

in which U_p and ν_f are the random motion velocity of nanoparticles and kinematic viscosity of the base fluid. U_p has been defined as,

$$U_p = \frac{D_B}{l_{mol,f}}$$

where D_B is the nanoparticle diffusion coefficient and $l_{mol,f}$ is the mean free path of the molecules of the base fluid. D_B is given in the Stokes equation,

$$D_B = \frac{k_B T}{3\pi\mu_f d_p}$$

where k_B is the Boltzmann constant, μ_f is the viscosity of the base fluid and T is the temperature.

2.3. Cluster Formation

Interfacial layering may play an important role when nanoparticles are extremely small and the ordered layers of liquid molecules are relatively thick. For example, in order to double the effective volume of a particle with a diameter of 10nm, the layered-liquid thickness is required to be about 2.5 nm. It has been concluded that a 3 nm thick layered liquid molecules are necessary to explain the experimental results of the thermal conductivity enhancement for nanofluids of alumina in water (Xue 2003). However, experiments and theoretical simulations have already shown that a typical ordered layer of liquid molecules at the surface of a solid is only on the order of a few atomic distances, that is, about 1 nm (Yu et al. 1999a; Yu et al. 1999b). And doubts rise on this mechanism when there is surfactant or dispersant coating the surface of nanoparticles.

Eastman et al. have already discussed this mechanism in detail (Eastman et al. 2004). However, in both the hypotheses it is not clear that there exists a basis for the assumed properties.

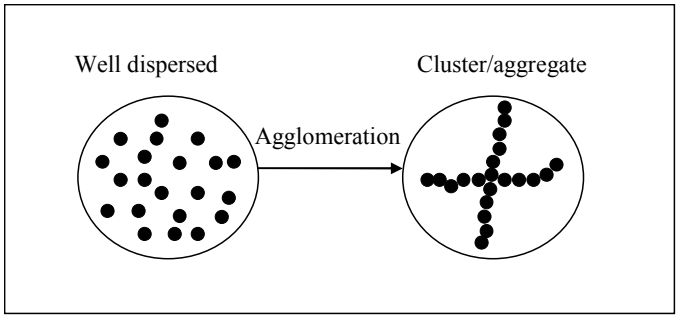

Figure A-2 Formation of nanoparticle clusters/aggregates

As shown in Figure A-2, nanostructured materials usually form loose clusters or aggregates trying to minimize the surface energy caused by the large specific surface area of nanostructures. Even in well-dispersed nanofluid, these clusters or aggregates in nanofluids form and behave like percolating structures, and thermal conduction paths can arise through these amorphous-like structures. Therefore, the effective thermal conductivity enhancement of nanofluids goes up beyond the Maxwell's limit of 3ϕ, with ϕ being the volumetric fraction of the nanoparticles. This cluster or aggregate effect has been taken into account to calculate the effective thermal conductivity by introducing a cluster radius distribution function *n(r)*, and the modified Maxwell equation is,

$$k_{nf} = k_f + \frac{3\phi\int_0^\infty \frac{k_p - k_f}{k_p + 2k_f} n(r)dr}{(1-\phi) + 3\phi\int_0^\infty \frac{k_f}{k_p + 2k_f} n(r)dr} k_f \tag{43}$$

in which the cluster radius distribution function *n(r)* is estimated by a log-normal distribution,

$$n(r) = \frac{1}{\sqrt{2\pi}(\ln\delta)r} e^{-\left[\frac{\ln(r/r_p)}{\sqrt{2\pi}(\ln\delta)}\right]^2} \tag{44}$$

The standard deviation δ can take a value of 1.5 (Wang et al. 2003a).

Prasher et al. (Prasher et al. 2006b) also argued that effective thermal conductivity of nanofluids based on solely thermal conduction would be

significantly enhanced resulting from aggregation of the nanoparticles. The following equation was then used to include the cluster effect of nanoparticles,

$$k_{nf} = k_f + 3\left(r_a / r_p\right)^{3-d_f} \phi \frac{k_a - k_f}{2k_f + k_a - 3\left(r_a / r_p\right)^{3-d_f} \phi\left(k_a - k_f\right)} k_f \tag{45}$$

where r_a is the radius of gyration of aggregates, d_f is the fractal dimension of the aggregates. Previous studies have indicated that d_f ranges from 1.75 to 2.5.

The Bruggeman equation has been suggested to estimate the thermal conductivity of nanoparticle aggregates, $k_{a,}$

$$\left[1 - \left(r_p / r_a\right)^{3-d_f}\right] \frac{k_f - k_a}{k_f + 2k_a} + \left(r_p / r_a\right)^{3-d_f} \frac{k_p - k_a}{k_p + 2k_a} = 0 \tag{46}$$

Xuan (Xuan et al. 2003) even developed a comprehensive dynamic model which takes into account not only the convection effects but also the cluster effect through the introduction of a cluster gyration radius $r_{c,}$ which needs to be determined empirically,

$$k_{nf} = k_f + 3\phi \frac{k_p - k_f}{2k_f + k_p - \phi(k_p - k_f)} k_f + \frac{1}{2} \rho_p C_{p,p} U_p \sqrt{\frac{k_B T}{3\pi \mu_f r_c}} \tag{47}$$

According to these equations, clusters and aggregates of nanostructured materials contribute to the effective thermal conductivity. However, large clusters and aggregates tend to settle out from the base fluids and then may cause drop in

thermal conductivity. Therefore, the size of nanoparticle clusters and aggregates is a critical factor to the enhancement in thermal conductivity of nanofluids.

Bibliography

Agostiano, A., Catalano, M., Curri, M. L., Della Monica, M., Manna, L., and Vasanelli, L. (2000). "Synthesis and structural characterisation of CdS nanoparticles prepared in a four-components "water-in-oil" microemulsion." *Micron*, 31(3), 253-258.

Ahmadi, T. S., Wang, Z. L., Green, T. C., Henglein, A., and El-Sayed, M. A. (1996). "Shape-Controlled Synthesis of Colloidal Platinum Nanoparticles." *Science*, 272(5270), 1924-1925.

Andersson, P., and Backstrom, G. (1976). "Thermal conductivity of solids under pressure by the transient hot wire method." *Review of Scientific Instruments*, 47(2), 205-209.

Arik, M., Bar-Cohen, A., and You, S. M. (2007). "Enhancement of pool boiling critical heat flux in dielectric liquids by microporous coatings." *International Journal of Heat and Mass Transfer*, 50(5-6), 997-1009.

Assael, M. J., Chen, C. F., Metaxa, I., and Wakeham, W. A. (2004). "Thermal Conductivity of Suspensions of Carbon Nanotubes in Water." *International Journal of Thermophysics*, 25(4), 971-985.

Assael, M. J., Metaxa, I. N., Arvanitidis, J., Christofilos, D., and Lioutas, C. (2005). "Thermal Conductivity Enhancement in Aqueous Suspensions of Carbon Multi-Walled and Double-Walled Nanotubes in the Presence of Two Different Dispersants." *International Journal of Thermophysics*, 26(3), 647-664.

Asua, J. M. (2002). "Miniemulsion polymerization." *Progress in Polymer Science*, 27(7), 1283-1346.

Bai, F., and Lu, W. Q. (2003). "Numerical Analysis of Laminar Forced Convection Heat Transfer in Microencapsulated Phase Change Material Suspensions." *Journal of Enhanced Heat Transfer*, 10(3), 311-322.

Bang, I. C., Chang, S. H., and Baek, W.-P. (2005a). "Direct observation of a liquid film under a vapor environment in a pool boiling using a nanofluid." *Applied Physics Letters*, 86(13), 134107-1341.

Bang, I. C., Chang, S. H., and Baek, W.-P. (2005b). "Visualization of a principle mechanism of critical heat flux in pool boiling." *International Journal of Heat and Mass Transfer*, 48(25-26), 5371-5385.

Bang, I. C., and Heung Chang, S. (2005). "Boiling heat transfer performance and phenomena of Al2O3-water nano-fluids from a plain surface in a pool." *International Journal of Heat and Mass Transfer*, 48(12), 2407-2419.

Bar-Cohen, A. "Thermal management of microelectronics in the 21st century." *Electronic Packaging Technology Conference*, Singapore, 1997.

Batchelor, G. K. (1976). "Brownian diffusion of particles with hydrodynamic interaction." *Journal of Fluid Mechanics*, 74, 1-29.

Batchelor, G. K. (1977). "Effect of Brownian-motion on bulk stress in a suspension of spherical-particles." *Journal of Fluid Mechanics*, 83, 97-117.

Berber, S., Kwon, Y. K., and David, T. (2000). "Unusually High Thermal Conductivity of Carbon Nanotubes." *Physical Review Letters*, 84(20), 4613 - 4616.

Bhattacharya, P., Saha, S. K., Yadav, A., Phelan, P. E., and Prasher, R. S. (2004). "Brownian dynamics simulation to determine the effective thermal conductivity of nanofluids." *Journal of Applied Physics*, 95(11), 6492-6494.

Biercuk, M. J., Llaguno, M. C., Radosavljevic, M., Hyun, J. K., Johnson, A. T., and Fischer, J. E. (2002). "Carbon nanotube composites for thermal management." *Applied Physics Letters*, 80(15), 2767-2769.

Borca-Tasciuc, T. (2000). "Thermoelectric Transport Properties of Superlattices," Ph.D. Thesis, University of California, Los Angeles.

Bourlinos, A., Giannelis, E., Zhang, Q., Archer, L., Floudas, G., and Fytas, G. (2006). "Surface-functionalized nanoparticles with liquid-like behavior: The role of the constituent components." *The European Physical Journal E - Soft Matter*, 20(1), 109 - 117.

Buongiorno, J. (2006). "Convective Transport in Nanofluids." *Journal of Heat Transfer*, 128(3), 240-250.

Cahill, D. G. (1990). "Thermal conductivity measurement from 30 to 750 K: the 3 omega method." *Review of Scientific Instruments*, 61(2), 802-808.

Chandler, D. (1974). "Translational and rotational diffusion in liquids. II. Orientational single-particle correlation functions." *The Journal of Chemical Physics*, 60(9), 3508-3512.

Chang, H., Tsung, T. T., Chen, L. C., Jwo, C. S., Tsung, J. W., and Lu, Y. C. (2005). "The electrochemical properties of SiC nanoparticle suspension." *Journal of Materials Engineering and Performance*, 14(2), 158-162.

Chang, H., Tsung, T. T., Chen, L. C., Yang, Y. C., Lin, H. M., Han, L. L., and Lin, C. K. (2004). "TiO_2 nanoparticle suspension preparation using ultrasonic vibration-assisted Arc-Submerged Nanoparticle Synthesis System (ASNSS)." *Materials Transactions*, 45(3), 806-811.

Che, J., Cagin, T., and Goddard III, W. A. (2000). "Thermal conductivity of carbon nanotubes." *Nanotechnology*(2), 65-69.

Chein, R., and Huang, G. (2005). "Analysis of microchannel heat sink performance using nanofluids." *Applied Thermal Engineering*, 25(17), 3104-3114.

Chen, B., Wang, X., Zhang, Y., Xu, H., and Yang, R. (2006). "Experimental research on laminar flow performance of phase change emulsion." *Applied Thermal Engineering*, 26(11-12), 1238-1245.

Chen, G. (1996). "Non local and non equilibrium heat conduction in the vicinity of nanoparticules." *Journal of Heat Transfer*, 118, 539-545.

Chen, G., Borca-Tasciuc, D., and Yang, R. G. (2004). "Nanoscale Heat Transfer." *Encyclopedia of Nanoscience and Nanotechnology*, 7, 429-459.

Choi, S. U. S. "Nanofluid technology : current status and future research." *Korea-U.S. Technical Conference on Strategic Technologies*, Vienna, VA, 1998.

Choi, S. U. S., and Eastman, J. A. "Enhancing thermal conductivity of fluids with nanoparticles." *International mechanical engineering congress and exhibition*, San Francisco, CA, 1995.

Choi, S. U. S., Zhang, Z. G., Yu, W., Lockwood, F. E., and Grulke, E. A. (2001). "Anomalous thermal conductivity enhancement in nanotube suspensions." *Applied Physics Letters*, 79(14), 2252-2254.

Chon, C. H., Kihm, K. D., Lee, S. P., and Choi, S. U. S. (2005). "Empirical correlation finding the role of temperature and particle size for nanofluid (Al/sub 2/O/sub 3/) thermal conductivity enhancement." *Applied Physics Letters*, 87(15), 153107-1531.

Chon, C. H., Paik, S. W., Tipton, J. B., and Kihm, K. D. (2006). "Evaporation and Dryout of Nanofluid Droplets on a Microheater Array." *Journal of Heat Transfer*, 128(8), 735.

Das, S. K., Choi, S. U. S., and Patel, H. E. (2006). "Heat transfer in Nanofluids - A review." *Heat Transfer Engineering*, 27(10), 3-19.

Das, S. K., Putra, N., and Roetzel, W. (2003a). "Pool boiling characteristics of nano-fluids." *International Journal of Heat and Mass Transfer*, 46(5), 851-862.

Das, S. K., Putra, N., and Roetzel, W. (2003b). "Pool boiling of nano-fluids on horizontal narrow tubes." *International Journal of Multiphase Flow*, 29(8), 1237-1247.

Das, S. K., Putra, N., Thiesen, P., and Roetzel, W. (2003c). "Temperature dependence of thermal conductivity enhancement for nanofluids." *Transactions of the ASME. Journal of Heat Transfer*, 125(4), 567-574.

Davis, R. H. (1986). "The effective thermal conductivity of a composite material with spherical inclusions." *International Journal of Thermophysics*, 7(3), 609-620.

Davis, V. A., Ericson, L. M., Parra-Vasquez, A. N. G., and Fan, H. (2004). "Phase Behavior and Rheology of SWNTs in Superacids." *Macromolecules*, 37(1), 154-160.

Ding, Y., Alias, H., Wen, D., and Williams, R. A. (2006). "Heat transfer of aqueous suspensions of carbon nanotubes (CNT nanofluids)." *International Journal of Heat and Mass Transfer*, 49(1), 240-250.

Duncan, A. B., and Peterson, G. P. (1994). "Review of microscale heat transfer." *Journal of Applied Mechanics Review*, 47(9), 397-428.

Eastman, J. A. "Novel thermal properties of nanostructured materials." *International Symposium on Metastable Mechanically Alloyed, and Nanocrystalline Materials*, Wollongong, Australia, 1998.

Eastman, J. A., Choi, S. U. S., Li, S., Thompson, L. J., and Lee, S. "Enhanced thermal conductivity through the development of nanofluids." *Fall Meeting of the Materials Research Society (MRS)*, Boston, USA, 1996.

Eastman, J. A., Choi, S. U. S., Li, S., Yu, W., and Thompson, L. J. (2001). "Anomalously increased effective thermal conductivities of ethylene glycol-based nanofluids containing copper nanoparticles." *Applied Physics Letters*, 78(6), 718-720.

Eastman, J. A., Choi, U. S., Li, S., Soyez, G., Thompson, L. J., and DiMelfi, R. J. "Novel thermal properties of nanostructured materials." *Materials Science Forum*, Switzerland, 629-634, 1999.

Eastman, J. A., Phillpot, S. R., Choi, S. U. S., and Keblinski, P. (2004). "Thermal Transport in Nanofluids." *Annual Review of Materials Research*, 34(1), 219-246.

Einstein, A. (1906). "A new determination of the molecular dimensions." *Annalen Der Physik*, 19, 289-306.

Etemad, S. G., Heris, S. Z., and Esfahany, M. N. (2006). "Experimental investigation of oxide nanofluids laminar flow convective heat transfer." *International Communications in Heat and Mass Transfer*, 33(4), 529-535.

Evans, W., Fish, J., and Keblinski, P. (2006). "Role of Brownian motion hydrodynamics on nanofluid thermal conductivity." *Applied Physics Letters*, 88(9), 093116.

Farid, M. M., Khudhair, A. M., Razack, S. A. K., and Al-Hallaj, S. (2004). "A review on phase change energy storage: materials and applications." *Energy Conversion and Management*, 45(9-10), 1597-1615.

Fleitman, A. H., and Weeks, J. R. (1971). "Mercury as a Nuclear Coolant." *Nuclear Engineering and Design*, 16(3), 266-278.

Friedlander, S. K. (2000). *Smoke, Dust, and Haze: Fundamentals of Aerosol Dynamics*, Oxford Press, New York.

Gesenhues, U. (1999). "Substructure of Titanium Dioxide Agglomerates from Dry Ball-milling Experiments." *Journal of Nanoparticle Research*, 1(2), 223-234.

Goldburg, W. I. (1999). "Dynamic Light Scattering." *American Journal of Physics*, 67(12), 1152-1160.

Golobiac, I., and Ferjancic, K. (2000). "The role of enhanced coated surface in pool boiling CHF in FC-72." *Heat and Mass Transfer*, 36(6), 525-531.

Gosselin, L., and Silva, A. K. d. (2004). "Combined ``heat transfer and power dissipation" optimization of nanofluid flows." *Applied Physics Letters*, 85(18), 4160-4162.

Granqvist, C. G., and Hunderi, O. (1978). "Conductivity of inhomogeneous materials: Effective-medium theory with dipole-dipole interaction." *Physical Review B*, 18(4), 1554 -1561.

Gross, U., and Song, Y. W. (1996). "Thermal conductivities of new refrigerants R125 and R32 measured by the transient hot-wire method." *International Journal of Thermophysics*, 17(3), 607-619.

Guo, L., Yang, S., Yang, C., Yu, P., Wang, J., Ge, W., and Wong, G. K. L. (2000). "Highly monodisperse polymer-capped ZnO nanoparticles: Preparation and optical properties." *Applied Physics Letters*, 76(20), 2901-2903.

Gupte, S. K., Advani, S. G., and Huq, P. (1995). "Role of Micro-Convection Due to Non Affine Motion of Particles in a Mono-Disperse Suspension." *International Journal of Heat and Mass Transfer*, 38(15), 2945-2958.

Hamilton, R. L., and Crosser, O. K. (1962a). *I and EC Fundamentals*.

Hamilton, R. L., and Crosser, O. K. (1962b). "Thermal Conductivity of Heterogeneous Two Component Systems." *Industrial and Engineering Chemistry Fundamentals*, 1(3), 187-191.

Han, Z. H., and Yang, B. (2008). "Thermophysical characteristics of water-in-FC72 nanoemulsion fluids." *Applied Physics Letters*, 92(1), 013118.

Han, Z. H., Yang, B., Kim, S. H., and Zachariah, M. R. (2007). "Application of hybrid sphere/carbon nanotube particles in nanofluids." *Nanotechnology*, 18, 105701.

Hasselman, D. P. H., and Johnson, L. F. (1987). "Effective Thermal Conductivity of Composites with Interfacial Thermal Barrier Resistance." *Journal of Composite Materials*, 21(6), 508-515.

Hong, K. S., Hong, T.-K., and Yang, H.-S. (2006). "Thermal conductivity of Fe nanofluids depending on the cluster size of nanoparticles." *Applied Physics Letters*, 88(3), 31901-311.

Hong, T. K., Yang, H. S., and Choi, C. J. (2005). "Study of the enhanced thermal conductivity of Fe nanofluids." *Journal of Applied Physics*, 97(6), 64311-641.

Hunter, R. J. (2001). *Foundations of colloid science*, Oxford University Press, Oxford.

Hwang, Y., Lee, J. K., Lee, J. K., Jeong, Y. M., Cheong, S. I., Ahn, Y. C., and Kim, S. H. (2008). "Production and dispersion stability of nanoparticles in nanofluids." *Powder Technology*, In Press, Corrected Proof.

Hwang, Y., Park, H. S., Lee, J. K., and Jung, W. H. (2006). "Thermal conductivity and lubrication characteristics of nanofluids." *Current Applied Physics, Nano Korea 2005 Symposium*, 6(Supplement 1), e67-e71.

Inaba, H. (2000). "New challenge in advanced thermal energy transportation using functionally thermal fluids." *International Journal of Thermal Sciences*, 39(9-11), 991-1003.

Inaba, H., Zhang, Y., Horibe, A., and Haruki, N. (2007). "Numerical simulation of natural convection of latent heat phase-change-material microcapsulate slurry packed in a horizontal rectangular enclosure heated from below and cooled from above." *Heat and Mass Transfer*, 43(5), 459-470.

Jang, S. P., and Choi, S. U. S. (2004). "Role of Brownian motion in the enhanced thermal conductivity of nanofluids." *Applied Physics Letters*, 84(21), 4316-4318.

Jeffrey, D. J. (1973). "Conduction Through a Random Suspension of Spheres." *Proceedings of the Royal Society of London. Series A, Mathematical and Physical Sciences*, 335(1602), 355-367.

Jiang, H., Moon, K.-s., Dong, H., Hua, F., and Wong, C. P. (2006). "Size-dependent melting properties of tin nanoparticles." *Chemical Physics Letters*, 429(4-6), 492-496.

Jiang, J. S., Gao, L., Yang, X. L., Guo, J. K., and Shen, H. L. (1999). "Nanocrystalline NiZn ferrite synthesized by high energy ball milling." *Journal of Materials Science Letters*, 18(21), 1781-1783.

Jiang, L., Gao, L., and Sun, J. (2003). "Production of aqueous colloidal dispersions of carbon nanotubes." *Journal of Colloid and Interface Science*, 260(1), 89-94.

Keblinski, P., Eastman, J. A., and Cahill, D. G. (2005). "Nanofluids for thermal transport." *Materials Today*, 8(6), 36-44.

Keblinski, P., Phillpot, S. R., Choi, S. U. S., and Eastman, J. A. (2002). "Mechanisms of heat flow in suspensions of nano-sized particles (nanofluids)." *International Journal of Heat and Mass Transfer*, 45(4), 855-863.

Khanafer, K., Vafai, K., and Lightstone, M. (2003). "Buoyancy-driven heat transfer enhancement in a two-dimensional enclosure utilizing nanofluids." *International Journal of Heat and Mass Transfer*, 46(19), 3639-3653.

Kim, J., Choi, C. K., Kang, Y. T., and Kim, M. G. (2006a). "Effects of Thermodiffusion and Nanoparticles on Convective Instabilities in Binary Nanofluids." *Nanoscale and Microscale Thermophysical Engineering*, 10(1), 29 - 39.

Kim, J., Kang, Y. T., and Choi, C. K. (2004a). "Analysis of convective instability and heat transfer characteristics of nanofluids." *Physics of Fluids*, 16(7), 2395-2401.

Kim, J. S., Cha, W. H., Rainey, K. N., Lee, S., and You, S. M. "Liquid cooling module using FC-72 for electronics cooling." *Thermal and Thermomechanical Phenomena in Electronics Systems, 604-611, 2006.*

Kim, S. H., Liu, B. Y. H., and Zachariah, M. R. (2002). "Synthesis of Nanoporous Metal Oxide Particles by a New Inorganic Matrix Spray Pyrolysis Method." *Chem. Mater.*, 14(7), 2889-2899.

Kim, S. H., Liu, B. Y. H., and Zachariah, M. R. (2004b). "Ultrahigh Surface Area Nanoporous Silica Particles via an Aero-Sol-Gel Process." *Langmuir*, 20(7), 2523-2526.

Kim, S. H., Woo, K. S., Liu, B. Y. H., and Zachariah, M. R. (2005). "Method of measuring charge distribution of nanosized aerosols." *Journal of Colloid and Interface Science*, 282(1), 46-57.

Koo, J., and Kleinstreuer, C. (2005). "Laminar nanofluid flow in microheat-sinks." *International Journal of Heat and Mass Transfer*, 48(13), 2652-2661.

Krishnamurthy, S., Bhattacharya, P., Phelan, P. E., and Prasher, R. S. (2006). "Enhanced Mass Transport in Nanofluids." *Nano Letters*, 6(3), 419-423.

Kulkarni, D. P., Das, D. K., and Chukwu, G. A. (2006). "Temperature dependent rheological property of copper oxide nanoparticles suspension (nanofluid)." *Journal of Nanoscience and Nanotechnology*, 6(4), 1150-1154.

Kumar, D. H., Patel, H. E., Kumar, V. R. R., Sundararajan, T., Pradeep, T., and Das, S. K. (2004). "Model for Heat Conduction in Nanofluids." *Physical Review Letters*, 93(14), 144301.

Kwak, K., and Kim, C. (2005). "Viscosity and thermal conductivity of copper oxide nanofluid dispersed in ethylene glycol." *Korea-Australia Rheology Journal*, 17(2), 35-40.

Lawrence, E. N. (1973). "Thermal conductivity of particulate-filled polymers." *Journal of Applied Polymer Science*, 17(12), 3819-3820.

Leal, L. G. (1973). "On the Effective Conductivity of a Dilute Suspension of Spherical Drops in the Limit of Low Particle Peclet Number." *Chemical Engineering Communications*, 1(1), 21 - 31.

Lee, S., Choi, S. U. S., Li, S., and Eastman, J. A. (1999). "Measuring thermal conductivity of fluids containing oxide nanoparticles." *Transactions of the ASME. Journal of Heat Transfer*, 121(2), 280-289.

Li, C. H., and Peterson, G. P. (2006). "Experimental investigation of temperature and volume fraction variations on the effective thermal conductivity of nanoparticle suspensions (nanofluids)." *Journal of Applied Physics*, 99(8), 084314.

Li, X. F., Zhu, D. S., Wang, X. J., Wang, N., Gao, J. W., and Li, H. (2008). "Thermal conductivity enhancement dependent pH and chemical surfactant for Cu-H2O nanofluids." *Thermochimica Acta*, 469(1-2), 98-103.

Liu, M. S., Lin, C. C., Huang, I. T., and Wang, C. C. (2006). "Enhancement of thermal conductivity with CuO for nanofluids." *Chemical engineering and technology*, 29(1), 72-77.

Liu, M. S., Lin, M. C., Huang, I. T., and Wang, C. C. (2005). "Enhancement of thermal conductivity with carbon nanotube for nanofluids." *International communications in heat and mass transfer*, 32(9), 1202-1210.

Liu, Z. W., Lin, W. W., Lee, D. J., and Peng, X. F. (2001). "Pool Boiling of FC-72 and HFE-7100." *Journal of Heat Transfer*, 123(2), 399-400.

Lu, S.-Y., and Lin, H.-C. (1996). "Effective conductivity of composites containing aligned spheroidal inclusions of finite conductivity." *Journal of Applied Physics*, 79(9), 6761-6769.

Ma, H. B., Wilson, C., Borgmeyer, B., Park, K., Yu, Q., Choi, S. U. S., and Tirumala, M. (2006). "Effect of nanofluid on the heat transport capability in an oscillating heat pipe." *Applied Physics Letters*, 88(14), 143116.

Maiga, S. E. B., Nguyen, C. T., Galanis, N., and Roy, G. (2004). "Heat transfer behaviours of nanofluids in a uniformly heated tube." *Superlattices and Microstructures*, 35(3-6), 543-557.

Marquis, F. D. S., and Chibante, L. P. F. (2005). "Improving the heat transfer of nanofluids and nanolubricants with carbon nanotubes." *JOM*, 57(12), 32-43.

Mason, T. G., Wilking, J. N., Meleson, K., Chang, C. B., and Graves, S. M. (2007). "Nanoemulsions: Formation, Structure, and Physical Properties." *Journal of Physics: Condensed Matter*, 19, 079001.

Masuda, H., Ebata, A., Teramae, K., and Hishinuma, N. (1993). "Alteration of Thermal conductivity and Viscosity of Liquid by Dispersing Ultra-fine Particles." *Netsu Bussei (Japan)*, 7(4), 227-233.

Maxwell, J. C. (1873). *A treatise on electricity and magnetism*, Dover Publications.

Miner, A., and Ghoshal, G. (2004). "Cooling of high-power-density microdevices using liquid metal coolants." *Applied Physics Letters*, 85(3), 506-508.

Mohseni, K., and Baird, E. S. (2007). "Digitized Heat Transfer Using Electrowetting on Dielectric." *Nanoscale and Microscale Thermophysical Engineering*, 11(1), 99 -108.

Mudawar, I. "Direct-immersion cooling for high power electronic chips." *Thermal Phenomena in Electronic Systems,* 74-84, 1992.

Murshed, S. M. S., Leong, K. C., and Yang, C. (2005). "Enhanced thermal conductivity of TiO_2-water based nanofluids." *International Journal of Thermal Sciences*, 44(4), 367-373.

Nagasaka, Y., and Nagashima, A. (1981). "Simultaneous measurement of the thermal conductivity and the thermal diffusivity of liquids by the transient hot-wire method." *Review of Scientific Instruments*, 52(2), 229-232.

Nolas, G. S., Sharp, J., and Goldsmid, H. J. (2001). *Thermoelectrics: Basic Principles and New Materials Development*, Springer Verlag, Berlin.

Pak, B. C., and Cho, Y. I. (1998). "Hyrdrodynamic and Heat Transfer Study of Dispersed Fluids with Submicron Metallic Oxide Particles." *Experimental Heat Transfer*, 11(2), 151-170.

Patel, H. E., Das, S. K., Sundararajan, T., Sreekumaran Nair, A., George, B., and Pradeep, T. (2003). "Thermal conductivities of naked and monolayer protected metal nanoparticle based nanofluids: manifestation of anomalous enhancement and chemical effects." *Applied Physics Letters*, 83(14), 2931-2933.

Peters, K. F., Cohen, J. B., and Chung, Y.-W. (1998). "Melting of Pb nanocrystals." *Physical Review B*, 57(21), 13430 - 13438.

Phelan, P. E., Bhattacharya, P., and Prasher, R. S. (2005). "Nanofluids for Heat Transfer Applications." *Annual Reviews of Heat Transfer*, 14, 255-275.

Prasher, R., Bhattacharya, P., and Phelan, P. E. (2005). "Thermal Conductivity of Nanoscale Colloidal Solutions (Nanofluids)." *Physical Review Letters*, 94(2), 025901.

Prasher, R., Bhattacharya, P., and Phelan, P. E. (2006a). "Brownian-Motion-Based Convective-Conductive Model for the Effective Thermal Conductivity of Nanofluids." *Journal of Heat Transfer*, 128(6), 588-595.

Prasher, R., Phelan, P. E., and Bhattacharya, P. (2006b). "Effect of Aggregation Kinetics on the Thermal Conductivity of Nanoscale Colloidal Solutions (Nanofluid)." *Nano Letters*, 6(7), 1529-1534.

Prasher, R., Song, D., Wang, J., and Phelan, P. (2006c). "Measurements of nanofluid viscosity and its implications for thermal applications." *Applied Physics Letters*, 89(13), 133108.

Putra, N., Roetzel, W., and Das, S. (2003). "Natural convection of nano-fluids." *Heat and Mass Transfer*, 39(8-9), 775-784.

Qi, Y., Cagin, T., Johnson, W. L., and Goddard III, W. A. (2001). "Melting and crystallization in Ni nanoclusters: The mesoscale regime." *The Journal of Chemical Physics*, 115(1), 385-394.

Rainey, K. N., and You, S. M. (2000). "Pool Boiling Heat Transfer From Plain and Microporous, Square Pin-Finned Surfaces in Saturated FC-72." *Journal of Heat Transfer*, 122(3), 509-516.

Rayleigh, L. (1892). "On the influence of obstacles arranged in rectangular order upon the properties of a medium." *Philos. Mag.*, 34, 481-502.

Ren, Y., Xie, H., and Cai, A. (2005). "Effective thermal conductivity of nanofluids containing spherical nanoparticles." *Journal of Physics D (Applied Physics)*, 38(21), 3958-3961.

Ruoff, R. S., and Lorents, D. C. (1995). "Mechanical and thermal properties of carbon nanotubes." *Carbon Nanotubes*, 33(7), 925-930.

Said, M. A. M., and Agarwal, R. K. "Numerical Simulation of Natural Convection Heat Transfer in Nanofluids." *38th AIAA Thermophysics Conference*, Toronto, Ontario, Canada, 1-14, 2005.

Sanchez-Ramirez, J. R., Jimenez Perez, J. L., Cruz Orea, A., Gutierrez Fuentes, R., Bautista-Hernandez, A., and Pal, U. (2006). "Thermal diffusivity of nanofluids containing Au/Pd bimetallic nanoparticles of different compositions." *Journal of Nanoscience and Nanotechnology*, 6(3), 685-690.

Schwartz, L. M., Garboczi, E. J., and Bentz, D. P. (1995). "Interfacial transport in porous media: Application to dc electrical conductivity of mortars." *Journal of Applied Physics*, 78(10), 5898-5908.

Suenaga, K., Colliex, C., Demoncy, N., Loiseau, A., Pascard, H., and Willaime, F. (1997). "Synthesis of Nanoparticles and Nanotubes with Well-Separated Layers of Boron Nitride and Carbon." *Science*, 278(5338), 653-655.

Suslick, K. S. (1991). "The sonochemical hot spot." *The Journal of the Acoustical Society of America*, 89(4B), 1885-1886.

Suslick, K. S., Choe, S. B., Cichowlas, A. A., and Grinstaff, M. W. (1991). "Sonochemical synthesis of amorphous iron." *Nature*, 353(6343), 414 - 416.

Suslick, K. S., Fang, M., and Hyeon, T. (1996). "Sonochemical synthesis of iron colloids." *Journal of the American Chemical Society*, 118(47), 11960-11961.

Suslick, K. S., and Nyborg, W. L. (1990). "Ultrasound: Its Chemical, Physical and Biological Effects." *The Journal of Acoustical Society of America*, 87(2), 919-920.

Suslick, K. S., and Price, G. J. (1999). "Applications of ultrasound to materials chemistry." *Annual Review of Materials Science*, 29, 295-326.

Talapin, D. V., Rogach, A. L., Mekis, I., Haubold, S., Kornowski, A., Haase, M., and Weller, H. (2002). "Synthesis and surface modification of amino-stabilized CdSe, CdTe and InP nanocrystals." *Colloids and Surfaces A: Physicochemical and Engineering Aspects*, 202(2-3), 145-154.

Taylor, G. I. (1934). "The Formation of Emulsions in Definable Fields of Flow." *Proceedings of the Royal Society of London. Series A, Containing Papers of a Mathematical and Physical Character*, 146(858), 501-523.

Tiarks, F., Willert, M., Landfester, K., and Antonietti, M. (2001). "The controlled generation of nanosized structures in miniemulsions." Adsorption and Nanostructures, 110-112.

Tran, P. X., and Soong, Y. "Preparation of nanofluids using laser ablation in liquid technique." *ASME Applied Mechanics and Materials Conference*, Austin, TX, 2007.

Tsai, C. Y., Chien, H. T., Ding, P. P., Chan, B., Luh, T. Y., and Chen, P. H. (2004). "Effect of structural character of gold nanoparticles in nanofluid on heat pipe thermal performance." *Materials Letters*, 58(9), 1461-1465.

Tzeng, S., Lin, C., and Huang, K. (2005). "Heat transfer enhancement of nanofluids in rotary blade coupling of four-wheel-drive vehicles." *Acta Mechanica*, 179(1), 11-23.

Vassallo, P., Kumar, R., and D'Amico, S. (2004). "Pool boiling heat transfer experiments in silica-water nano-fluids." *International Journal of Heat and Mass Transfer*, 47(2), 407-411.

Vehkamaki, H. (2006). *Classical Nucleation Theory in Multicomponent Systems*, Springer, New York.

Vissers, D. R., Holmes, J. T., Bartholme, L. G., and Nelson, P. A. (1974). "Hydrogen-activity meter for liquid sodium and its application to hydrogen solubility measurements." *Nuclear Technology*, 21(3), 235-244.

Wagener, M., and Gunther, B. (1999). "Sputtering on liquids - a versatile process for the production of magnetic suspensions." *Journal of Magnetism and Magnetic Materials*, 201, 41-44.

Wang, B. X., Zhou, L. P., and Peng, X. F. (2003a). "A fractal model for predicting the effective thermal conductivity of liquid with suspension of nanoparticles." *International Journal of Heat and Mass Transfer*, 46(14), 2665-2672.

Wang, B. X., Zhou, L. P., Peng, X. F., and Zhang, X. X. "Enhancing the effective thermal conductivity of liquid with dilute suspensions of nano particles." *15th Symposium on Thermophysical Properties*, Boulder, USA, 2003.

Wang, X., Xu, X., and Choi, S. U. S. (1999). "Thermal Conductivity of Nanoparticle - Fluid Mixture." *Journal of Thermophysics and Heat Transfer*, 13(4), 474-480.

Wasp, E. J., Kenny, J. P., and Gandhi, R. L. (1977). *Solid-Liquid Flow Slurry Pipeline Transportation*, Transaction Technology Publications, Berlin.

Wegner, K., Walker, B., Tsantilis, S., and Pratsinis, S. E. (2002). "Design of metal nanoparticle synthesis by vapor flow condensation." *Chemical Engineering Science*, 57(10), 1753-1762.

Wen, D., and Ding, Y. (2004a). "Experimental investigation into convective heat transfer of nanofluids at the entrance region under laminar flow conditions." *International Journal of Heat and Mass Transfer*, 47(24), 5181-5188.

Wen, D., and Ding, Y. (2005a). "Effect of particle migration on heat transfer in suspensions of nanoparticles flowing through minichannels." *Microfluidics and Nanofluidics*, 1(2), 183 - 189.

Wen, D., and Ding, Y. (2005b). "Experimental investigation into the pool boiling heat transfer of aqueous based alumina nanofluids." *Journal of Nanoparticle Research*, 7(2), 265-274.

Wen, D., Ding, Y., and Williams, R. (2005). "Nanofluids turn up the heat." *Chemical Engineer*(771), 32-34.

Wen, D. S., and Ding, Y. L. (2004b). "Effective Thermal Conductivity of Aqueous Suspensions of Carbon Nanotubes (Carbon Nanotube Nanofluids)." *Journal of Thermophysics and heat transfer*, 18(4), 481-485.

White, F. M. (1991). *Viscous Fluid Flow*, McGraw-Hill Higher Education, New York.

Wu, J., Bai, G. R., Eastman, J. A., Zhou, G., and Vasudevan, V. K. "Synthesis of TiO_2 Nanoparticles Using Chemical Vapor Condensation." *MRS Proceedings, Symposium Z: Chemistry of Nanomaterial Synthesis and Processing*, San Francisco, 2005.

Xie, H., Lee, H., Youn, W., and Choi, M. (2003). "Nanofluids containing multiwalled carbon nanotubes and their enhanced thermal conductivities." *Journal of Applied Physics*, 94(8), 4967-4971.

Xie, H., Wang, J., Xi, T., and Liu, Y. (2001). "Study on the thermal conductivity of SiC nanofluids." *Journal of the Chinese Ceramic Society*, 29(4), 361-364.

Xie, H., Wang, J., Xi, T., and Liu, Y. (2002). "Thermal Conductivity of Suspensions Containing Nanosized SiC Particles." *International Journal of Thermophysics*, 23(2), 571-580.

Xie, H. W., J.; Xi, T.; Liu, Y.; Ai, F.; Wu, Q. (2002). "Thermal conductivity enhancement of suspensions containing nanosized alumina particles." *Journal of Applied Physics*, 91(7), 4568-4572.

Xu, Q., Sharp, I. D., Yuan, C. W., Yi, D. O., Liao, C. Y., Glaeser, A. M., Minor, A. M., Beeman, J. W., Ridgway, M. C., Kluth, P., III, J. W. A., Chrzan, D. C., and Haller, E. E. (2006). "Large Melting-Point Hysteresis of Ge Nanocrystals Embedded in SiO_2." *Physical Review Letters*, 97(15), 155701.

Xu, Z. Z., Wang, C. C., Yang, W. L., Deng, Y. H., and Fu, S. K. (2004). "Encapsulation of nanosized magnetic iron oxide by polyacrylamide via inverse miniemulsion polymerization." *Journal of Magnetism and Magnetic Materials*, 277(1-2), 136-143.

Xuan, Y., and Li, Q. (2000). "Heat transfer enhancement of nanofluids." *International Journal of Heat and Fluid Flow*, 21(1), 58-64.

Xuan, Y., and Li, Q. (2003). "Investigation on Convective Heat Transfer and Flow Features of Nanofluids." *Journal of Heat Transfer*, 125(1), 151-155.

Xuan, Y., Li, Q., and Hu, W. (2003). "Aggregation structure and thermal conductivity of nanofluids." *AIChE Journal*, 49(4), 1038-1043.

Xuan, Y., and Roetzel, W. (2000). "Conceptions for heat transfer correlation of nanofluids." *International Journal of Heat and Mass Transfer*, 43(19), 3701-3707.

Xue, Q. (2000). "Effective-medium theory for two-phase random composite with an interfacial shell." *Journal of Materials Science and Technology*, 16(4), 367-369.

Xue, Q.-Z. (2003). "Model for effective thermal conductivity of nanofluids." P*hysics Letters A,* 307(5), 313-317.

Yamagishi, Y., Sugeno, T., Ishige, T., Takeuchi, H., and Pyatenko, A. T. "An evaluation of microencapsulated PCM for use in cold energy transportation medium." E*nergy Conversion Engineering Conference, 1996. IECEC 96. Proceedings of the 31st Intersociety,* 2077-2083.

Yamagishi, Y., Takeuchi, H., Pyatenko, A. T., and Kayukawa, N. (1999). "Characteristics of microencapsulated PCM slurry as a heat-transfer fluid." A*IChE Journal,* 45(4), 696-707.

Yang, B., and Han, Z. H. (2006a). "Temperature-dependent thermal conductivity of nanorod-based nanofluids." A*pplied Physics Letters,* 89(8), 083111.

Yang, B., and Han, Z. H. (2006b). "Thermal conductivity enhancement in water-in-FC72 nanoemulsion fluids." A*pplied Physics Letters,* 88(26), 261914.

Yang, Y., Grulke, E. A., Zhang, Z. G., and Wu, G. (2006). "Thermal and rheological properties of carbon nanotube-in-oil dispersions." J*ournal of Applied Physics,* 99(11), 114307.

Yatsuya, S., Tsukasaki, Y., Mihama, K., and Uyeda, R. (1978). "Preparation of Extremely Fine Particles by Vacuum Evaporation onto a Running Oil Substrate." J*ournal of Crystal Growth,* 45(1), 490-494.

You, S. M., Kim, J. H., and Kim, K. H. (2003). "Effect of nanoparticles on critical heat flux of water in pool boiling heat transfer." A*pplied Physics Letters,* 83(16), 3374-3376.

Yu, C.-J., Richter, A. G., Datta, A., Durbin, M. K., and Dutta, P. (1999a). "Observation of Molecular Layering in Thin Liquid Films Using X-Ray Reflectivity." P*hysical Review Letters,* 82(11), 2326 - 2329.

Yu, C. J., Richter, A. G., Kmetko, J., Datta, A., and Dutta, P. (1999b). "X-ray diffraction evidence of ordering in a normal liquid near the solid-liquid interface." E*urophysical Letters,* 50(4), 487-491.

Yu, W., and Choi, S. U. S. (2003). "The Role of Interfacial Layers in the Enhanced Thermal Conductivity of Nanofluids: A Renovated Maxwell Model." J*ournal of Nanoparticle Research,* 5(1-2), 167-171.

Yu, W., and Choi, S. U. S. (2004). "The role of interfacial layers in the enhanced thermal conductivity of nanofluids: A renovated Hamilton and Crosser model." J*ournal of Nanoparticle Research,* 6(4), 355-361.

Yudin, I. K., Nikolaenko, G. L., Kosov, V. I., Agayan, V. A., and Anisimov, M. A. (1997). "A compact Photo- Correlation Spectromoter for Research and Education." I*nternational Journal of Thermophysics,* 18(5), 1237-1248.

Zhao, C. Y., and Lu, T. J. (2002). "Analysis of Microchannel Heat Sinks for Electronics Cooling." I*nternational Journal of Heat and Mass Transfer,* 45(24), 4857?869.

Zhu, H., Lin, Y., and Yin, Y. (2004). "A novel one-step chemical method for preparation of copper nanofluids." Jo*urnal of Colloid and Interface Science,* 277(1), 100-103.

Zhu, J., Koltypin, Y., and Gedanken, A. (2000). "General Sonochemical Method for the Preparation of Nanophasic Selenides: Synthesis of ZnSe Nanoparticles." Ch*emistry of Materials,* 12(1), 73-78.